Potential Methods for Heart Rate Monitoring During Neonatal Resuscitation in The Delivery Room



Shiemaa Sidahmed

Department of Electrical and Electronic Engineering

The University of Nottingham

A thesis submitted for the degree of

Doctor of Philosophy

May 2019

Dedication

To my precious angel, Lana, who came to us during the writing of this thesis. You have made me stronger and more fulfilled than I could have ever imagined.

To my wonderful editing services and soulmate, Mazin, who encouraged me to achieve my dreams despite of all the struggles.

To my parents, Prof. Zeinab Kassab and Dr Sidahmed Awad, for their endless love, support and encouragement. No words can express my love and gratitude.

To my sister, Asmaa, and my brothers, Mohamad and Abubakr, the journey would not be easy without your support.

I love you all to the moon and back.

Acknowledgements

I would like to express my gratitude to my supervisors for their valuable support and motivating spirit during the Ph.D. journey: Prof. John Crowe, Prof. Barrie Hayes-Gill and Dr Roger Light.

I am very grateful to the Dean of Engineering Scholarship panel (2014), who awarded me the opportunity to carry out my doctoral research at the University of Nottingham.

I would like to thank SurePulse Company for funding this project and providing the required support throughout the whole period of my research, and I am especially thankful to Dr James Carpenter and Dr Son Nguyen for their valuable help.

I would like also to thank my mentor during the first year of the doctoral studies, Dr Matthew Butler, for his valuable help and enriching discussions.

I am grateful to all my friends and colleagues in the University of Nottingham, my office mates in the tower building – room 1003, and my friends in the Sudanese Nile Society who were really supportive and made the journey joyful and easier.

Abstract

This thesis aims to investigate the use of dry and capacitive ECG sensors for newborns' heart rate monitoring in the delivery room. The main limitations of the standard wet ECG sensors for this application are the need for skin preparation and possible skin scarring caused by the conductive gel.

The Initial proposal was to use capacitive ECG sensors to couple the ECG signal from the babies backs through the cotton towels and plastic bags used in the delivery room to wrap the newborns. EPIC capacitive sensors made by Plessey were tested for this application on baby and adult volunteers. The sensors were unable to couple a detectable ECG signal through the delivery room materials from the baby volunteers. On the other hand, the sensors were able to collect an ECG signal through thin cotton sheets, which makes them of interest for neonatal intensive care applications where the babies are kept with minimal clothing.

The conductive fabric sensors were tested as a potential method for ECG recordings using dry skin contact, where no skin preparation is needed. Three types of fabric sensors were tested on adult and baby volunteers to record ECG signals from the forehead and left arm. Two of the materials enabled the collection of good quality signals when they were connected to a clinically approved ECG monitor. The advantages of the fabric materials as ECG sensors are their flexibility, which enables them to bend around the body. Besides, they can be easily attached to existent ECG monitors using the ECG standard leads with press studs. The fabric sensors are recommended for further clinical trials.

Keywords: Newborns Heart Rate Monitoring; Dry ECG; Capacitive ECG; Fabric Sensors; NICU Monitoring; Forehead ECG

Contents

1 Introduction **1**

1.1 Overview 1
1.2 Objective 2
1.3 Research Impact 3
1.4 Thesis Layout 4

2 Literature Review **5**

2.1 Overview 5
2.2 Introduction to Neonatal Resuscitation Guidelines 7
2.3 Neonatal Heart Rate Detection Methods 10
2.3.1 PPG and Pulse Oximetry 10
2.3.2 Doppler Ultrasound 10
2.3.3 Electrocardiogram (ECG) 11
2.4 ECG Electrodes 13
2.4.1 Overview 13
2.4.2 Limitations of Wet Electrodes 14
2.4.3 Dry/Capacitive ECG Electrodes 15
2.4.3.1 Definitions 15
2.4.3.2 The Electrical Model of Skin Interface 15
2.4.4 Limitations of Dry/Capacitive Electrodes 20
2.5 The Applications of Dry/Capacitive ECG in Neonatal Care 22
2.5.1 Delivery Room Monitoring 22
2.5.2 NICU Monitoring 25
2.6 ECG from Head 27
2.7 ECG Noise and Interference 30
2.8 Conclusions 31

3 Materials and Methods **32**
3.1 Overview . . . 32
3.2 Capacitive Sensors Materials and Systems . . . 32
3.2.1 EPIC Sensor Overview . . . 32
3.2.2 EPIC Sensors Placement . . . 34
3.2.3 ECG Acquisition Systems . . . 36
3.2.3.1 Pilot System . . . 36
3.2.3.2 Array System . . . 37
3.3 Fabric Sensors Materials and Systems . . . 39
3.3.1 Overview . . . 39
3.3.2 Fabric Sensors Placement . . . 40
3.3.3 Fabric Sensors Materials . . . 40
3.3.4 Wireless ECG Recorder . . . 41
3.3.5 GE B450 Monitor . . . 44
3.4 Skin Interface Impedance Measurement . . . 44
3.4.1 Electrode Impedance . . . 44
3.4.2 Impedance Measurements Setups . . . 45
3.5 Heart Rate Detection Algorithm . . . 48

4 Capacitive Sensors: Results and Discussion **51**
4.1 Introduction . . . 51
4.2 The Experimental Setup of Dry/Capacitive Contact . . . 53
4.3 The Dry Contact Coupling . . . 56
4.3.1 Adult Volunteers Results . . . 56
4.3.2 Baby Volunteers Results . . . 59
4.3.3 Summary . . . 61
4.4 The Capacitive Coupling Through The Delivery Room Materials . . . 62
4.4.1 Adult Volunteers Results . . . 63
4.4.2 Baby Volunteers Results . . . 66
4.4.3 Summary . . . 68
4.5 Capacitive Coupling Through Cotton Sheets . . . 70
4.5.1 Adult Volunteers Results . . . 70
4.5.2 Baby Volunteers Results . . . 73
4.5.3 Summary . . . 76
4.6 Capacitive Coupling Through Cotton Clothes: Array System . . . 78
4.6.1 Results . . . 79

4.7 Bioimpedance Measurements for Dry and Capacitive Setups 82
4.7.1 Overview 82
4.7.2 Impedance Measurements of Dry Contact Electrode 82
4.7.3 Impedance Measurements of The Dielectric Materials 85
4.8 The Simulation of Dry And Capacitive Models 90
4.8.1 Simulation Results 92
4.9 Conclusion 95

5 Fabric Sensors: Results and Discussion 99
5.1 Overview 99
5.2 Experiment One: Three Fabric Materials Test 102
5.2.1 Experimental Setup 102
5.2.2 Results 104
5.3 Fabric Sensors With GE B450 ECG/PPG Monitor 108
5.4 Experiment Two: GE B450: Sensors' Placement 111
5.4.1 Experimental Setup 111
5.4.2 Results 113
5.4.2.1 DRL Placement Setups 113
5.4.3 PPG Comparison to ECG 116
5.5 Experiment Three : DRL Placement Effect 118
5.5.1 Experimental Setup 118
5.5.2 Results 119
5.6 Experiment Four: Fabric ECG Sensors on Babies 121
5.6.1 Experimental Setup 121
5.6.2 Results 122
5.7 Experiment Five: Bioimpedance measurements on Adults 125
5.8 Fabric Sensors Results Summary and Discussion 127
5.8.1 Overview 127
5.8.2 Results Summary 127

6 Conclusions 131
6.1 Overview 131
6.2 Capacitive Sensors 131
6.3 Fabric Sensors 134
6.3.1 Future Work 135

Bibliography 137

A Materials Datasheets and Certificates **152**

B EPIC Sensors Recordings **162**

C Fabric Sensors Recordings **165**

List of Figures

2.1 Potential Heart rate monitoring methods used on babies immediately after birth. 6
2.2 Resuscitation algorithm for newborns in the delivery room 8
2.3 Infant at 32 weeks gestation in a polyethylene wrap. 9
2.4 Infant wrapped in at towel while performing resuscitation procedure . 9
2.5 The ECG limb leads (right wrist, left wrist, and left leg) 12
2.6 ECG electrodes 16
2.7 The skin–electrode impedance model for the typical Ag/Agcl, dry contact, insulated and capacitive electrodes. 17
2.8 Dry/capacitive electrode topology and schematic circuit 18
2.9 (a) The noise model for the dry/non-contact electrodes. (b) Frequency behaviour of different noise sources. (c) – 19
2.10 The relative power spectrum of noise and motion artefacts in typical ECG signal 21
2.11 ECG recording using non-contact electrode 22
2.12 The wearable garment with fabric sensors on the sleeves for ECG monitoring in the delivery room. 23
2.13 Schematic of the smart-matress (top) and sensor design implementing the EPS sensor (bottom). 24
2.15 Smart Jacket prototype with simple dressing process 25
2.16 Updated Smart Jacket prototype. 25
2.17 The use of conductive foam to close the gap between the ECG sensor and the skin. 26
2.18 Neonatal mattress with integrated capacitive sensors. The mattress is covered with a PU (polyurethane) cover 27
2.19 i-VITAL components and sensors locations. 28
2.20 Simulated and measured cardiac cycles in five head-ECG channels . . 29
2.21 Wearable heart monitor. 29

2.22 DRL circuit for biomedical applications. 31

3.1 Packaging of EPIC PS25101 sensor and its internal design. 33
3.2 The PCB layout of EPIC sensors 34
3.3 The proposed placement of EPIC sensors array inside the resuscitation mattress. 35
3.4 PS2500 ECG recorder box by Plessey connected to EPIC PS25101 sensors 36
3.5 The pilot system which collects one ECG signal using a pair of EPIC sensors. The rectangle in dashed lines represents the internal design of the PS2500 box. 37
3.6 The setup for collecting ECG signal from adult volunteer wrists using PS2500 and two EPIC sensors. 38
3.7 The array system which was designed to couple four ECG signals and process them to choose the best signal for QRS detection. 39
3.8 The wireless system of ECG recorder 42
3.9 The PCB layout of in-house wireless ECG recorde 43
3.10 GE B450 monitor made by GE Health-care 44
3.11 Equivalent circuit alternatives for the electrode/tissue interface 45
3.12 The impedance measurements accuracy graph for 1260 impedance/gain-phase analyser 47
3.13 The impedance measurements accuracy graph for 1260/1294 combined system: the right side is 1294A bioimpedance interface, and the left side is 1294B normal interface 47
3.14 Bioimpedance measurement setup using 1260 impedance analyser and 1294 bioimpedance interface, with a desktop. Smart software provided by Solartron is used with hardware to collect measurements. 48
3.15 The features of ECG signals that are used for heart rate detection . . 49
3.16 The block diagram of the implemented algorithm by Pan and Tompkins. 49

4.1 The setup of dry/capacitive coupling to record ECG signal from adult's wrists and baby's back. 54
4.2 The dielectric material (cotton towel, polyethylene or vinyl) was placed on top of the sensors in the capacitive coupling. 54
4.3 The ECG acquisition system using two EPIC sensors and a DRL (conductive fabric). 55
4.4 Sample of the ECG signal recorded from adult's wrists in dry contact using EPIC PS25101 using the data acquisition system shown in 4.3. 57

4.5 Sample of QRS detection on adult ECG signal collected from wrists in dry contact. It shows the detected QRS on bandpass, moving average raw ECG signals with noise level (Black), signal level (Red) , adaptive threshold (Green) and the QRS detection (Pulse train). 57
4.6 The capacitive ECG signal takes few seconds at the beginning to settle down. 58
4.7 Sample of the introduced motion artefacts, when the volunteers were asked to shake their wrists gently for five seconds. 58
4.8 Sample of ECG signal recorded from eight weeks baby's back in dry contact using EPIC PS25101 and the data acquisition system shown in 4.3. 60
4.9 Sample of QRS detection on baby ECG signal collected in dry contact from the back. It shows the detected QRS on bandpass, moving average raw ECG signals with noise level (Black), signal level (Red) , adaptive threshold (Green) and the QRS detection (Pulse train). 60
4.10 Sample of baby ECG signal distorted by motion artefacts. 61
4.11 Sample of ECG signal recorded from adult's wrists capacitively through the vinyl plastic bag, using EPIC PS25101 and the data acquisition system shown in 4.3. 64
4.12 Sample of QRS detection on adult ECG signal collected from wrists capacitively through the vinyl plastic bag. It shows the detected QRS on bandpass, moving average raw ECG signals with noise level (Black), signal level (Red) , adaptive threshold (Green) and the QRS detection (Pulse train). 64
4.13 Sample of the signal collected from adult's wrists volunteer through polyethylene with no detectable ECG features. 65
4.14 Sample of the signal collected from adult's wrists through cotton towel with no detectable ECG features. 65
4.15 Sample of the signal collected from baby's back through vinyl with no detectable ECG features. 66
4.16 Sample of the signal collected from baby's back through polyethylene with no detectable ECG features. 67
4.17 Sample of the signal collected from baby's back through cotton towels with no detectable ECG features. 67

4.18 Sample of ECG signal recorded from adult's wrists capacitively through 254 μm cotton sheet, using EPIC PS25101 and the data acquisition system shown in 4.3. 71
4.19 Sample of QRS detection on adult ECG signal collected from wrists capacitively through 254 μm cotton sheet. It shows the detected QRS on bandpass, moving average raw ECG signals with noise level (Black), signal level (Red) , adaptive threshold (Green) and the QRS detection (Pulse train). 71
4.20 Sample of ECG signal recorded from adult's wrists capacitively through 355 μm cotton sheet, using EPIC PS25101 and the data acquisition system shown in 4.3. 72
4.21 Sample of QRS detection on adult ECG signal collected from wrists capacitively through 355 μm cotton sheet. It shows the detected QRS on bandpass, moving average raw ECG signals with noise level (Black), signal level (Red) , adaptive threshold (Green) and the QRS detection (Pulse train). 72
4.22 Sample of ECG signal recorded from baby's back capacitively through 254 μm cotton sheet, using EPIC PS25101 and the data acquisition system shown in 4.3. 74
4.23 Sample of QRS detection on baby ECG signal collected from the back capacitively through 254 μm cotton sheet. It shows the detected QRS on bandpass, moving average raw ECG signals with noise level (Black), signal level (Red) , adaptive threshold (Green) and the QRS detection (Pulse train). 74
4.24 The motion artefacts introduced by baby movements and crying. . . . 75
4.25 Sample of the signal collected from baby's back through 355 μm cotton sheet with no detectable ECG features. 75
4.26 Experimental setup for collecting ECG signals from adult back capacitively through cotton clothing using eight EPIC PS25101 sensors. . . 78
4.27 Sample of ECG signal recorded capacitively through single layer of cotton from an adult, using EPIC PS25101 and the setup shown in 4.26. ECGs were collected from shoulders, middle back and waist. A DC offset has been added to these ECG signals in order to show them clearly in the figure. 79

4.28 Sample of ECG signal recorded capacitively through three layers of cotton from adult shoulders, using EPIC PS25101 and the setup shown in 4.26. 80
4.29 The dry contact model of the skin-sensor interface including body layer Stratum corneum, R_i and C_i represent the interface resistor and capacitor while R_b represents the body resistor. The skin interface equivalent model has been used. 83
4.30 The measurement setup of dry sensor - skin interface bioimpedance.Two metal discs were used in contact with adult's wrists. 84
4.31 Impedance measurements of dry contact skin interface before and after skin preparation, using the experimental setup shown in Figures 4.30 and 3.14. 85
4.32 The capacitive contact model of the skin-sensor interface 86
4.33 The capacitance representation of dielectric materials. 87
4.34 The impedance measurements setup of plastic bags, cotton towel and cotton sheets. 88
4.35 Impedance measurements of vinyl bag made of Ethylene vinyl Acetate (EVA) and polyethylene bag made of Low Density polyethylene (LDPE) compared to the calculated capacitance. 89
4.36 Impedance measurements of cotton fabrics are compred to the calculated capacitance. Fabrics' thicknesses are: 2000 μm, 355 μm and 254 μm. The impedance of 2000 μm cotton towels is not shown because it was bigger than the analyser maximum. 90
4.37 Sample of the generated ECG signal that was used as an input for the simulation. 91
4.38 A general representation of the noise and artefacts present in the fetal QRS in the frequency domain 91
4.39 The output ECG of the dry contact model simulation. The impedance measurement at 10 Hz was used with the impedance model shown in Figure 4.29. 92
4.40 The output ECG of the capacitive contact model simulation through $254um$ cotton sheet. The impedance measurement at 10 Hz were used with the impedance model shown in Figure 4.32. 94
4.41 The output ECG of capacitive contact interface simulation through the vinyl plastic bag. The impedance measurement at 10 Hz were used with the impedance model is shown in Figure 4.32. 94

5.1 Proposed fabric placements on newborn babies in the delivery room. The hat is used to hold the forehead sensor, and additional band to hold the forearm sensor and DRL. 101
5.2 Three samples of the conductive fabrics that used in this research. . . 101
5.3 The system used to collect ECG signals over Bluetooth from adult volunteers using fabric sensors in the setups shown in Figure 5.4. . . 103
5.4 Fabric sensors placement arrangements on adult volunteers: (1) Left arm and right arm while the DRL was connected to left leg, and (2) Left forearm and forehead, while the DRL was connected to left wrist. 103
5.5 Sample of QRS detection on adult ECG signals recorded from (LA, RA, LL DRL). It shows the detected QRS on bandpass, moving average raw ECG signals with noise level (Black), signal level (Red) , adaptive threshold (Green) and the QRS detection (Pulse train). 105
5.6 Sample of QRS detection on adult ECG recorded from (Left forearm, Forehead, Wrist DRL). It shows the detected QRS on bandpass, moving average raw ECG signals with noise level (Black), signal level (Red) , adaptive threshold (Green) and the QRS detection (Pulse train). . . 106
5.7 Sample of QRS detection on adult ECG recorded using SP31 fabric. It shows the detected QRS on bandpass, moving average raw ECG signals with noise level (Black), signal level (Red) , adaptive threshold (Green) and the QRS detection (Pulse train).. 107
5.8 The setup of the system that used to record ECG signals from adult and babies volunteers using GE B450 monitor. GE monitor could be powered by either the mains power or Lithium batteries. 109
5.9 The fabric sensors were connected to GE B450 unit using press studs cables while the sensors were attached to stretchy bands. 110
5.10 The GE B450 setup that used to record ECG and PPG signals from adult volunteers using the conductive fabric sensors (silver plated) and the pulse oximeter. 110
5.11 Three different arrangements of the DRL placements on the adult volunteers forearms. The size of each of the senors was 2.5cm×3cm . . . 112
5.12 ECG samples collected from an adult volunteer using three different arrangements of Laird 3080–500 fabric sensors. (a) No DRL, (b) DRL was placed 5cm from forearm sensor, and (c) DRL was placed 1 cm from forearm sensor. 114

5.13 ECG samples collected from an adult volunteer using three different arrangements of Medtex P130 fabric sensors. (a) No DRL, (b) DRL was placed 5 cm from forearm sensor, and (c) DRL was placed 1 cm from forearm sensor. 115
5.14 The PPG signal took time to start at the beginning of recording, while the ECG signal started immediately. 116
5.15 The ECG signal was more robust to mild movements, while the PPG signal was affected. 116
5.16 The PPG signal was completely distorted by motion artefacts, while the ECG signal was still detectable. 117
5.17 Setup of ECG recording with and without DRL. The DRL was placed 1 cm from the forearm sensor. 119
5.18 ECG samples collected from adult volunteer by GE B450 when the monitor was powered by the mains power. 120
5.19 ECG samples collected from adult volunteer by GE B450 when the monitor was powered by Lithium battery. 120
5.20 Proposed fabric placements on newborn babies in the delivery room. The headband used to hold the forehead sensor, while the armband used to hold the arm sensor, and the wrist band was used to hold the DRL. 122
5.21 Samples of ECG recordings from babies using Medtex P130 and Laird 3080–500 fabrics. 123
5.22 Sample of ECG recorded from 65 weeks baby. The signal was heavily affected by the baby's movements. 123
5.23 The fabric sensors with area of 2.5cm*3cm were applied on adult volunteer head and forearm to measure the skin interface bio-impedance. 125
5.24 The Impedance of Laird vs Medtex P130. 126
5.25 Diagram shows the experiments' flow chart; four experiments were conducted on adults (green) and one experiment on babies (orange). . 129

6.1 Newborn's hat designed by SurePulse company for PPG measurements. MedteX P130 fabric ECG sensor was fit into the hat for a clinical setup. 136

Chapter 1

Introduction

1.1 Overview

Approximately 10% of the newborns require intervention to help them begin breathing during their transition from the intrauterine to the extra-uterine environment. The heart and respiration rates are the most vital characteristics that are needed to check the initial status of the newborn and during the resuscitation. The medical guidelines recommend auscultation and palpation methods for heart rate monitoring after birth [1]. The medical staff should pause every 30 seconds during the resuscitation procedure to check the heart rate (HR) and based on the measurement; they should re-evaluate the progress and decide whether to continue or stop [2]. Many studies have suggested that palpation and auscultation may lead to 75% of incorrect interventions after birth and that auscultation can take up to 17 seconds to assess the HR [3, 4]. Despite the inaccuracy and inconsistency of the palpation and auscultation, they are still the most reliable methods by the general medical guidelines for newborns resuscitation.

Many methods have been introduced in the literature for heart rate monitoring immediately after birth. The objective of these studies was to reduce the error rate and time consumed by the manual heart rate monitoring using auscultation and palpation. These methods include pulse oximetry that outputs the HR as well as the oxygen saturation, Doppler ultrasound, forehead reflectance photoplethysmography (PPG) [5–7] and Electrocardiogram (ECG) [4, 6]. Most of the newborn's HR studies concluded that the ECG signal gives the most accurate heart rate measurements and takes less time to be displayed [8, 9]. On the other hand, there are some downsides when the standard ECG wet sensors are used to monitor the newborn's HR, especially the preterms. The wet ECG sensors require skin preparation and adhesive gel application. The skin of the preterms is immature and very fragile and so could be

damaged and scarred by the adhesive in the wet ECG sensors. Also, the time needed for the skin cleaning and careful preparation is relatively long, because the newborns are typically covered by vernix, blood and amniotic fluids [8, 10]. Additionally, the preterm babies need to be wrapped in plastic bags immediately after birth to prevent them from hypothermia and dehydration; these bags must be pulled down to clear the chest for ECG sensors application increasing the probability of hypothermia [8].

Therefore, this research explores different types and technologies of ECG signal sensors that do not require the adhesive gel application or skin preparation.

1.2 Objective

The HR could be extracted via the identification of R peaks [1] of the ECG signals with higher quality compared to other methods. In the most recent medical guidelines, the ECG has been introduced as a potential method for HR assessment in the delivery room, but the appropriate technologies are not available [1]. The research objective is to investigate using capacitive and conductive fabric ECG sensors for newborns HR monitoring in order to bridge this knowledge gap. These types of ECG sensors do not require skin preparation or application of the adhesive gel to the skin. Therefore, they would overcome the limitations of the standard wet ECG sensors.

Fabric and capacitive ECG sensors are widely used in wearable gadgets, sports clothing, car seats and safety measures for adults HR monitoring [11–14]. However, the field is still underexplored for newborn applications, especially for the resuscitation in the delivery room. A limited number of projects had developed wearable chest jackets with fabric sensors for smart newborn monitoring in incubators; for babies in the neonatal intensive care (NICU) [15,16]. Also, some studies have suggested the use of capacitive ECG for babies' heart rate monitoring by placing the sensors between the mattress and bed sheets for the NICU's incubators and home monitoring [17–19].

According to the medical guidelines, the newborn babies should be provided warmth immediately after birth and through the resuscitation procedure [1]. In the delivery room and during the resuscitation, the full term babies are usually cleaned and swaddled in cotton towels, and the preterms are placed in a plastic bag without cleaning [20,21]. In this research, the capacitive sensors were proposed to couple ECG signal from the babies' back through the materials that are used to cover the babies after birth (plastic bags for pre-terms and cotton towels for full-terms). The baby's back was chosen to keep the chest clear and reduce the preparation time since the

[1] R peak is the maximum amplitude of the ECG R wave

sensors would be placed in the resuscitation table in advance. The capacitive ECG sensor that was used in experiments throughout this thesis was the EPIC PS25101 made by Plessey Semiconductors [22,23]. EPIC sensors were tested on adult and baby volunteers in different setups of dry and capacitive contacts. A heart rate extraction algorithm was used to detect the R peaks of the ECG signal and calculate the heart rate. The percentage of accurate R peaks detection was used to quantify the signal quality. After the analysis of the results, it has been concluded that the capacitive sensors are not reliable for the delivery room application, but it might be of interest for the NICU applications.

Therefore, the conductive fabric sensors were proposed to couple the ECG signal in dry contact from the exposed parts of the babies, i.e. head, wrists and forearms. The conductive fabrics are inherently flexible and bendy sensors, and they could be strapped around the forehead and the forearm of the babies. Three conductive fabric materials were initially studied: Medtex P130 by Statex, Laird 3080–500 by Laird Tech and SP31 by Footfalls and Heartbeats. The last fabric (SP31) was later excluded from the study for the poor results. Different placements of fabric sensors were tested on both adult and baby volunteers using a certified medical ECG monitor. The research has assessed the quality of ECG signals based on the signal to noise ratios (SNRs) [in dBs] and the PPG signal collected by the pulse oximeter as a reference signal. The results of this part concluded that the fabric sensors couple high-quality ECG signal and is recommended for the clinical trial.

1.3 Research Impact

According to the newborn resuscitation algorithm in the recent guidelines of 2015 [1], the medical staff needs to reassess the HR every 30 seconds to decide whether to continue or stop. The traditional methods of palpation and auscultation are designed to take six seconds for HR assessment, but usually, it can take about 15–17 seconds, which wastes precious time of the first minutes of the newborn life [8]. The delay during the resuscitation can have a huge impact on the newborns later life, and it may cause severe disability or even death, especially in 1% of the newborns who needs intensive resuscitation [1]. Some studies have reported that the inappropriate or delayed respiratory support during those first minutes may lead to a brain or lung injury [24–26]. Moreover, the palpation and auscultation methods are not accurate and may lead to wrong decisions [3, 4].

Upon a successful solution for this research problem, the ECG signals would be applicable for HR monitoring in the delivery room. The implementation of the ECG would increase the accuracy of the HR assessment, decrease the time needed for HR calculations and provides continuous measurements. The solution could also be extended to HR monitoring in the NICU to minimise the discomfort of adhesive ECG leads.

1.4 Thesis Layout

The thesis consists of six chapters in total: Introduction, Literature Review, Materials and Methods, Capacitive Sensors Results and Discussion, Fabric sensors Results and Discussion, and finally, the Conclusions.

The Literature Review Chapter gives a summary of the related studies. It shows the different methods used for newborns HR monitoring in the delivery room. Then the theoretical background of the ECG signal is explained along with different types of ECG electrodes and their skin interface bioimpedance. After that, the literature of fabric and capacitive electrodes on neonatal applications are reviewed with the different sensor placements that were proposed for this research. Finally, the noise and artefacts that affect the ECG signal are discussed.

In the Material and Methods Chapter, the hardware and software systems that were used during the research experiments are illustrated. The sensors, systems and devices that were used to acquire the ECG signal are listed along with devices used for other measurements. This Chapter also discusses the algorithm used for the heart rate extraction of the ECG signals collected in this research.

Chapter Four summarises all the experiments performed using the capacitive ECG sensors for ECG collection. The ECG was collected from adult and baby volunteers through the cotton towels and plastic bags used in the delivery room. Various setups were used for ECG recording through different cotton sheet thicknesses and different plastic bag materials.

Chapter Five examines the use of conductive fabric sensors for the newborn's HR monitoring in the delivery room. Three types of conductive fabrics for medical applications were tested as potential options for ECG dry coupling. Different setups were tested on adults before deciding the sensors' placements that give a good quality ECG while suiting the newborn's comfort and size at the same time.

Finally, all the results and chapters' conclusions are reviewed in Chapter Six, where all the outcomes are summarised, and a plan for future work is suggested.

Chapter 2

Literature Review

2.1 Overview

The newborn's HR should be assessed immediately after birth in order to evaluate the status of the baby and to determine if there is a need for an intervention. For those babies who are requiring resuscitation or continued respiratory support, a method is needed to monitor the heart rate every 30 seconds during the procedure to indicate whether to continue the procedure or stop [1, 27]. There are two methods for HR assessment that are widely recommended by the international and European guidelines: listening to the apex beat using a stethoscope (auscultation) or by feeling the pulse in the base of the umbilical cord (palpation) [1, 27]. These two methods are considered very cheap, simple and fast ways to calculate the HR in the delivery room. The HR is normally assessed by listening/feeling the cord for six seconds, and then the number of heart beats will be multiplied by ten to give the heart beats by minute [28]. However, practically, both methods give inaccurate estimation and can lead to an incorrect initiation or discontinuity of the resuscitation [29, 30]. Although these methods theoretically assess the HR within six seconds, it can take up to 17 seconds for a HR assessment during the neonatal resuscitation [4]. Generally, the palpation is considered more reliable than the auscultation in the neonatal resuscitation guidelines, especially when the heart rate is healthy (above 100 beats per minute (bpm)) [31]. Chitkara et al. (2013) had claimed in their study that the auscultation had led to incorrect initiation or discontinuity of the resuscitation in 75% of the cases, compared to only 33% when the palpation was used [3].

Over the last three decades, many methods have been studied and reviewed for an immediate heart rate monitoring of newborn babies after birth that gives a more reliable assessment. Among these various methods are pulse oximetry, Doppler ultrasound, forehead reflectance photoplethysmography (PPG) [5–7] and electrocardiog-

raphy [31–33]. Figure 2.1 shows the possible heart rate monitoring methods used on babies in the delivery room and during resuscitation [4].

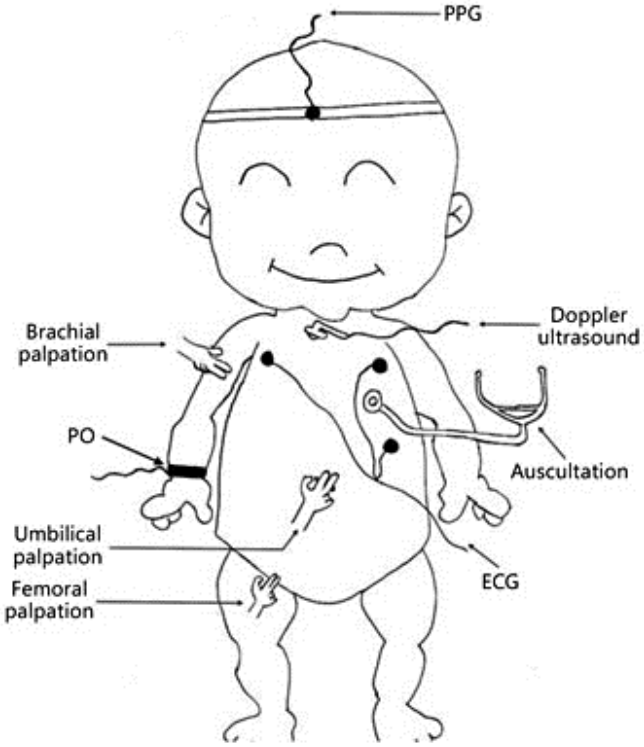


Figure 2.1: Potential heart rate monitoring methods used on babies immediately after birth [4].

Many papers have demonstrated that the ECG signal gives the most accurate heart rate assessment and takes less time to be displayed when compared to heart rate via pulse oximetry [8,9,32–34] or when compared to auscultation [35]. Because of these studies, the ECG was recently introduced as a method for heart rate monitoring in the European guidelines for newborn life support in 2015 [27], as shown in the new life support algorithm in Figure 2.2. These guidelines have pointed out the need for more medical studies in this field and the need for new technologies of ECG sensors to be introduced for this application. The wet ECG sensors have many limitations in the neonatal field because of the adhesive gel use. The application of adhesive gel can damage the fragile babies' skin, especially preterms, and might leave permanent scars, which can disfigure or disable about 10% of the preterms [19]. Also, the standard wet ECG sensors (AG/AgCl), need skin preparation before being applied, and this can take a relatively long time for newborns since they are typically covered by blood, vernix and amniotic fluids. The objective of this research is to bridge the knowledge

gap and investigate different ECG technologies that can be used in the delivery room.

This chapter firstly shows the medical guidelines and the steps taken before starting newborn resuscitation to give an insight into the procedure itself and the situation of the baby when they are resuscitated. Then, it discusses various ways of measuring the HR of the newborn babies in the delivery room in further detail: how they are performed, the measurements' reliability and the methods' limitations. After that, it summarises the theory and applications of the types of the ECG electrodes that do not require skin preparation or adhesive gel application: dry, capacitive, isolated and non-contact electrodes. The advantages,limitations and drawbacks of these electrodes were illustrated along with their skin interface models.

Finally, the chapter reviews the use of different ECG technologies in neonatal care applications, different setups that are used for the ECG acquisition besides the noise and artefacts that generally affect the ECG signal.

2.2 Introduction to Neonatal Resuscitation Guidelines

According to the recent medical guidelines [1], the newborn baby should be kept warm immediately after birth and through the whole resuscitation procedure, as shown in Figure 2.2. The protocol of keeping the baby's body temperature stable depends on the gestation age of the baby, the baby weight and general health. The newborns can generally be classified into two groups, and each group has a different body temperature control mechanism. The first group are the vulnerable babies, those who are born underweight, unhealthy or preterm. This group babies are more prone to hypothermia than infants of a healthy weight or full-term gestational age [20, 21, 36]. The birth is considered premature if the birth takes place at fewer than 32 weeks of gestational age. The second group are the babies who are born after the thirty-second week of gestation age and are not expected to have health complication issues.

A baby from the first group, usually a preterm, should not be cleaned of vernix and amniotic fluids that cover their body. The baby is kept immediately in a plastic bag to keep the body warm, as shown in Figure 2.3 and a hat should be placed to keep the head warm [21, 37]. The plastic bags used to protect the preterm from heat loss are not regulated and are usually supplied by local suppliers. The bags used in hospitals' delivery rooms are made of polyethylene wrap or vinyl plastic [21].

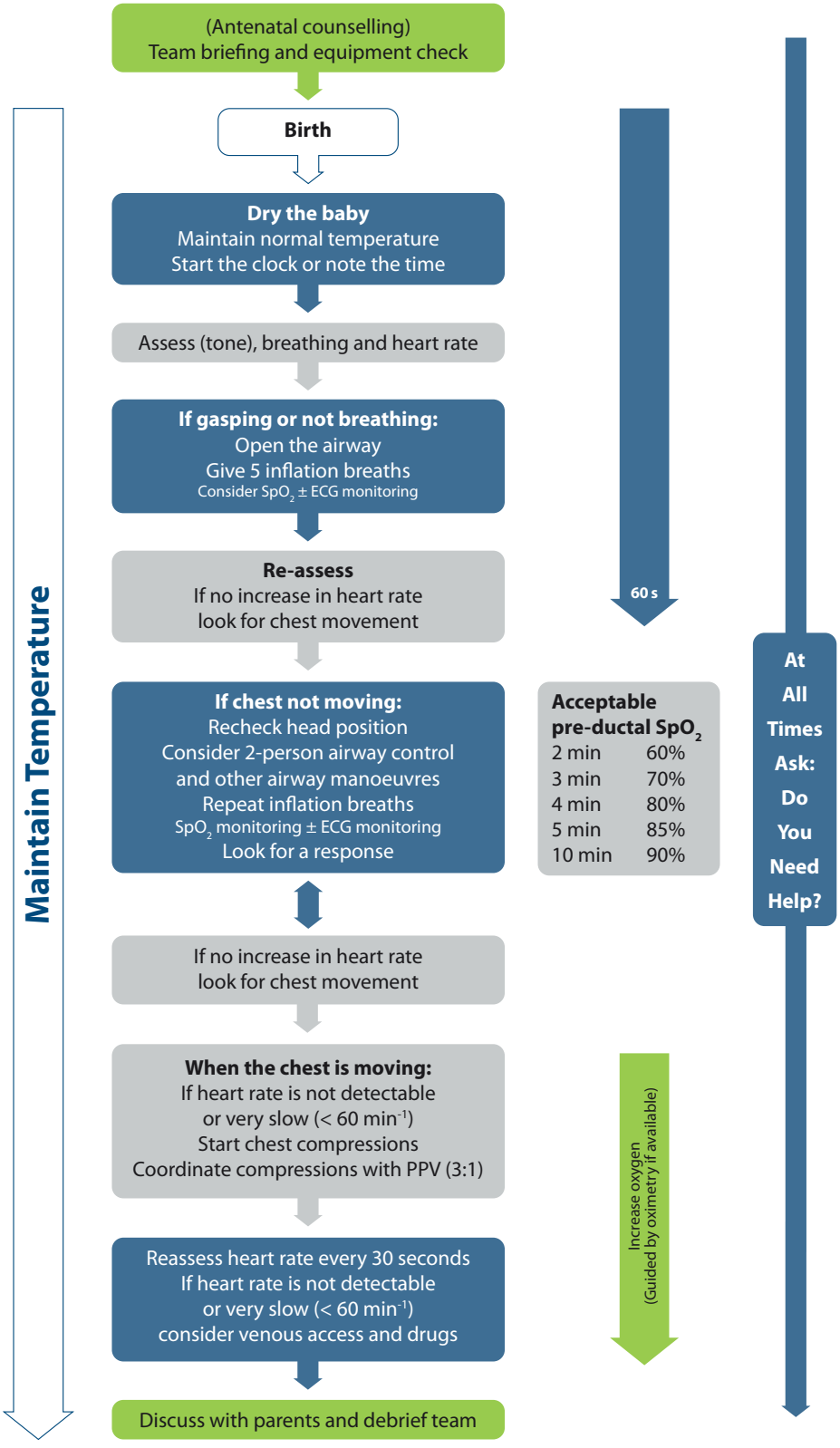


Figure 2.2: Resuscitation algorithm for newborns in the delivery room [1].

Alternatively, a baby from the second group, who are born after 32 weeks gestational age, should be dried and cleaned immediately after birth using warm towels, as shown in Figure 2.4. After cleaning, the baby should be wrapped using clean, dry towels which should not cover the baby's chest or face in order to allow the medical staff to observe the chest movements [27, 37–39].



Figure 2.3: Infant at 32 weeks gestation in a polyethylene wrap [21].

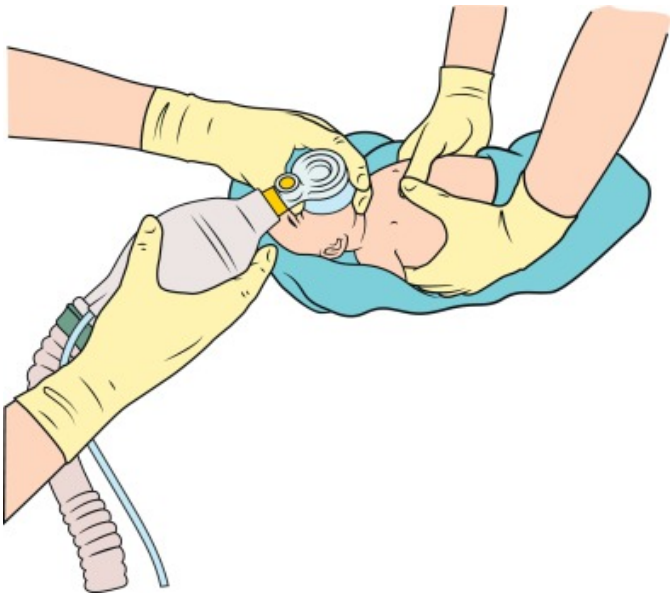


Figure 2.4: Infant wrapped in at towel while performing resuscitation procedure [27].

2.3 Neonatal Heart Rate Detection Methods

As mentioned above, many methods have been studied in the literature to assess the heart rate of newborns in the delivery room. The palpation and auscultation methods were shown as they have been recommended in the international and European guidelines for decades. The ECG has only been introduced in the most recent neonatal resuscitation guidelines of 2015. Although it was pointed out as a potential accurate method for HR assessment, there is still a knowledge gap that needs to be filled before it can be applied. Figure 2.1 summarises the different sensors placements for the potential HR methods that were used in the literature.

2.3.1 PPG and Pulse Oximetry

Photoplethysmography refers to extracting the cardiac-synchronous pulsatile signals, and hence, deriving the heart-rate using changes in the optical characteristics of tissues [4, 40]. Many papers have discussed the use of the PPG signal to detect the heart rate in the delivery room and the neonatal intensive care unit [5–7]. This method could potentially provide a solution for premature babies because of their fragile immature skin. Some studies have suggested the use of a recording camera to detect the PPG signal without physical contact from babies' forehead or cheeks where the signal will be extracted from the recorded video [35]. The problem associated with this method is motion artefacts, which can completely dominate the signal. Many research groups are working on enhancing the PPG signals immunity to motion artefacts [6, 7, 41].

Many papers have studied the pulse oximeter's use for heart rate monitoring in addition to oxygen saturation. In this section, the pulse oximeter is only reviewed for heart rate monitoring application. O'Donnell et al. (2005) found that the fastest way to measure the HR is to place the sensor on the babies wrist or hand before connecting the sensor to the oximeter [42]. Although the pulse oximeter measurements were more accurate than the palpation and auscultation, they were right in only 89% of the cases ($<$100 bpm) because of the poor tissue perfusion [43].

2.3.2 Doppler Ultrasound

Doppler ultrasound is well known for fetal monitoring before birth [44, 45]. Hutchon et al. (2014) have successfully used an ultrasound probe to monitor the heart rate of a baby piglet immediately after birth [46]. Another study has used the Doppler

ultrasound probe on stable neonatal inpatients and used the ECG signal as comparator [47]. The study concluded that HR from the Doppler ultrasound was highly correlated with ECG's HR. In another study, Lemke in (2011) placed a prototype Doppler ultrasound probe clamp on the umbilical cord of 16 babies in the delivery room [48]. The heart rate signals appeared almost immediately after putting the probe, and with relatively low motion artefacts, the signals were also correlated with the palpation signal for at least the first minute. The researchers were also able to get the signal from the preterm babies through a polyethylene bag that was used to keep them warm. Although the mentioned studies above have not explained their methodologies and findings in sufficient detail, the Doppler ultrasound probe might be one of the potential methods in the future for monitoring the heart rate of the newborns in the delivery room. From the limited published studies that covered this method, the estimated HR was more accurate than the palpation and auscultation. The limitations of this method are the delay between the birth and placing the probe (about 90 seconds) for cleaning the cord, as well as its need for an adequate length of the cord (>3 cm).

2.3.3 Electrocardiogram (ECG)

ECG is the recording process of the electrical signal that comes from the heart [49]. The known history of ECG signal started in the year 1786 when Italian physicist Luigi Galvani has noted that an electrical signal could be recorded from the human body muscles [50]. After that, the technologies of the ECG sensors developed rapidly and became one of the most vital signals needed in hospitals and clinics for patient assessment. Normally three ECG sensors are used to collect the signal, as shown in Figure 2.5 [51]. One sensor will be the positive (left upper limb), another one the negative (right upper limb), and the third one is the ground (left leg).

The standard ECG sensors used in hospitals are Ag/AgCl sensors with an adhesive gel used to attach the sensors to the prepared skin [8]. The ECG signal is known to be the most accurate method for clinical heart rate monitoring. Several studies have shown that the ECG is faster and more reliable than the pulse oximeter when measuring the HR of the newborns, especially in the first two minutes. However, the ECG can not replace the pulse oximeter that is recommended to be used in the delivery room for oxygen saturation measurement by the European guidelines. The ECG signal was not introduced in the neonatal resuscitation guidelines until 2015 [1]. One of the reasons is the compromised risks that associated with the Ag/AgCl ECG sensors on the fragile skin of preterms, and there is still a heated debate about

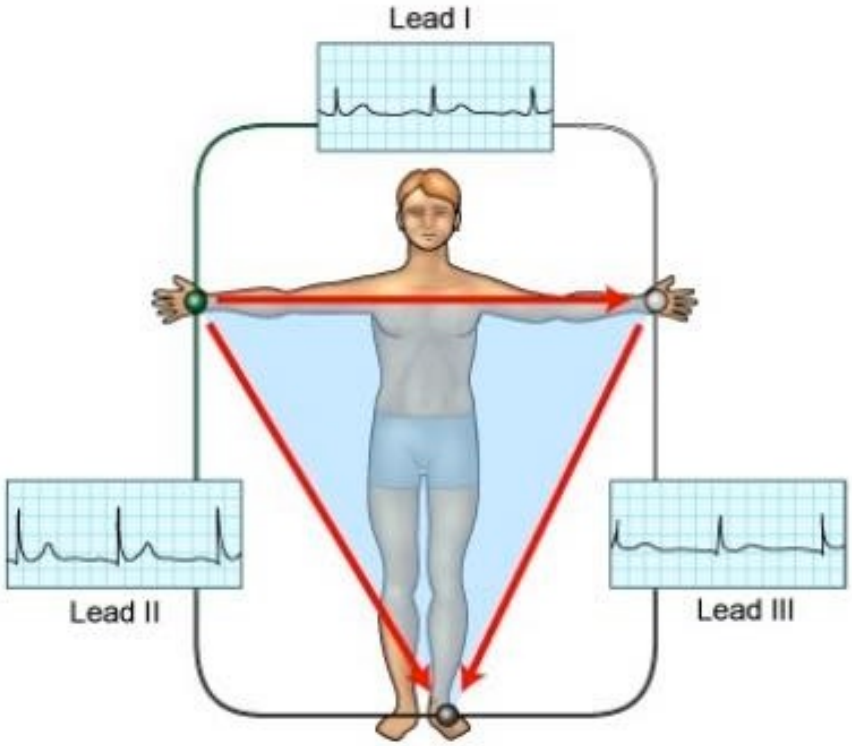


Figure 2.5: The ECG limb leads (RA, LA, and LL) [51].

introducing this signal into neonatal care in the delivery room. Five studies have compared the ECG signal and auscultation during the neonatal resuscitation, and they all found that the ECG signal was more accurate and faster [8,9,32–34]. Another study has also compared between the ECG and pulse oximeter [35] and claimed that the ECG was more accurate than the pulse oximeter and also easier to apply.

However, there are many complications while acquiring the ECG from newborns using the standard wet ECG sensors. Many studies have reported that the adhesive sensors cause epidermal stripping in infants of less than 27 weeks gestational age because the epidermal-dermal junction in these infants is weaker than the bond between the sensor and dermis [52–54]. Moreover, another study indicates that repetitive application and removal of patches can cause significant pain for preterms in particular, and severely affects the infant's development and well-being [15]. This is because the preterms' central nervous system is immature and sensitive to pain and noise. Also, extra time is needed to prepare the skin for the ECG leads because the babies are covered with blood, amniotic fluid and vernix. Moreover, for the preterm babies who are wrapped into plastic bags to prevent heat loss, the bag needs to be pulled down in order for chest sensors placement, which increases the probability of hypothermia [38].

To conclude this section, there is no agreement yet in the literature on which method is the best way to monitor the heart rate of the newborn babies. The ECG and Doppler ultrasound generally give more accurate and reliable heart rate readings than palpation and auscultation [4]. More research is needed to be done on Doppler ultrasound before being introduced clinically. Regarding the ECG, there is still a knowledge gap in ECG technologies and sensors needs to be covered before applying it on babies [1].

2.4 ECG Electrodes

Many studies reviewed in the above section have recommended the ECG as the fastest and most accurate way of assessing the HR of the newborn babies immediately after birth [8, 9, 32, 34, 55]. However, it is not the most used method for estimating the neonatal heart rate because of the inconvenience and discomfort caused by the adhesive and the need for skin preparation before the application [52–54]. The ECG has been recently introduced by the International and European guidelines as an effective method that lacks the technology for being applied in the delivery room [1, 27]. In this section, different types of ECG electrodes are discussed and compared.

2.4.1 Overview

Biopotential recordings are considered vital tools for medical applications to monitor the heart, brain and muscle activities. In order to detect a bio-electric event –in the form of Electrocardiogram (ECG), Electroencephalogram (EEG), Electromyogram (EMG) or Electrooculogram (EOG)–, normally two electrodes at least are needed to perform as a transducer that transfers the event to the input circuit of an amplifier. The amplifier should be designed carefully to match the electrode's characteristics. The essential component of the electrode is the metal-electrolyte interface, where the electrode material represents the metal, and a solution/paste is usually used on the surface as the electrolyte. If the electrodes are designed to be implanted below the skin, then the tissue fluids play the role of the electrolyte. When the metal electrode comes in contact with an electrolyte, the electrode tends to discharge ions into the electrolyte and to combine with the electrolyte's ions. The ions exchanged form two parallel sheets of charges of opposite signs is known as electrical double layer [56].

The standard Ag/AgCl electrodes with a conductive gel have been used over the last decades to record the ECG signals in the hospitals and clinics. The characteristics and proprieties of the Ag/AgCl electrodes, also known as wet electrodes, have been

well studied over the years [57–59]. Despite their high-quality signal, many research groups have been investigating alternative types of electrodes such as dry, insulated and non-contact ECG electrodes [60–62]. In recent years, the demand for dry/non-contact ECG electrodes has increased because of the irritation caused by the standard gel electrodes for long term heart monitoring. However, those types have not yet replaced the Ag/AgCl electrodes in the clinical applications, and they are mainly used for wearable devices, sports and home health care monitoring. [3]. The dry/non-contact electrodes are unlikely to replace the wet electrodes in general, because they need some mechanical solutions to secure the attachment against the skin for patients. However, in some areas where the wet ECG sensors are not applicable or are not considered to be safe, the dry/ non-contact ECG sensors might come into use. These areas are discussed in the next section. These different types of ECG electrodes dry, non-contact electrodes are illustrated in further detail in the next subsections.

2.4.2 Limitations of Wet Electrodes

The dry and capacitive electrodes have been investigated to cover different limitations in the Ag/AgCl electrodes' performance. The biggest limitation of the wet electrodes is the inconvenience of the gel application. One of the common problems is that the quality of the ECG signal is decreased when the gel dehydrates, and in some cases, it is not practical to re-spread the gel [63, 64]. Also, when the electrodes needed to be applied closer to each other, the gel application may cause a short circuit [61]. Moreover, there are some areas where the gel can harm the subject, such as for preterm babies where their skin is very fragile [65] or the patients with burned skin or when the recording is needed from near the eyes [66]. Additionally, some skin treatments may prevent the use of wet electrodes like petroleum ointment [67]. Other worries brought up by dermatologists is that in rare cases the gel used with wet electrodes raises toxicological concerns. So, there is a need for alternative electrodes that are constructed from more acceptable materials [67].

In addition to all the aforementioned limitations caused by the electrolyte, the gel application is also irritating for many patients, especially for long term recording as mentioned earlier [68]. Because of these limitations, the dry and capacitive electrodes which do not require the gel application were studied. Moreover, unlike the wet electrodes, the buffering and amplification can be designed at the dry/capacitive electrode site, improving the performance regarding interference [61, 69].

2.4.3 Dry/Capacitive ECG Electrodes

Generally, the performance and efficiency of the dry, insulated and non-contact electrodes are usually assessed by two aspects. The first aspect is the signal quality, while the second one is the comfort and utility of the device [68]. This section considers those two aspects while addressing the latest developments in the dry and capacitive (non-contact) electrodes.

2.4.3.1 Definitions

The first step towards understanding the difference between various ECG electrodes is to illustrate their skin interface. Some papers classify the insulated sensors as dry contact sensor [68], but generally, they are considered a separate category. The four types of ECG electrodes are shown in Figure 2.6. Wet electrodes need skin preparation before being applied to the skin, while the other three types do not require any kind of skin preparation. Also, the dry and insulated electrodes need to be in direct skin contact in order to couple a signal, while the capacitive electrodes can couple the ECG through dielectric materials such as clothes and hair. The wet electrodes are the conventional Ag/AgCl electrodes that are normally used as disposable ECG sensors in clinical applications. Figure 2.6 (a) shows the layers of the wet sensors, the Ag/AgCl electrode is bathed in the conductive gel (electrolyte) and connected to the amplifier via a snap connector, while the gel is pressed against the skin by adhesive pads.

The capacitive or non-contact electrodes, shown in Figure 2.6 (d), do not require direct contact with the skin and the sensor could be separated from the skin with cotton layer, air or hair [62]. The capacitive sensors are usually designed as active sensors in order to minimise the interference and the effect of motion artefacts.

2.4.3.2 The Electrical Model of Skin Interface

As mentioned above, the most important component of the electrodes is the skin interface. In this section, the electrical model of skin interface is presented for the different types of ECG electrodes. The interface is characterised by the conductance and the capacitance of each contact layer between the electrodes and the skin. As shown in Figure 2.7, different structures of RC parallel circuits is used to model the electrodes' skin interfaces. Some of these interfaces are dominated by the conductance and others are dominated by the capacitance. In the case of Ag/AgCl, the electrode is modelled as half cell potential and a double layer of capacitors in parallel with

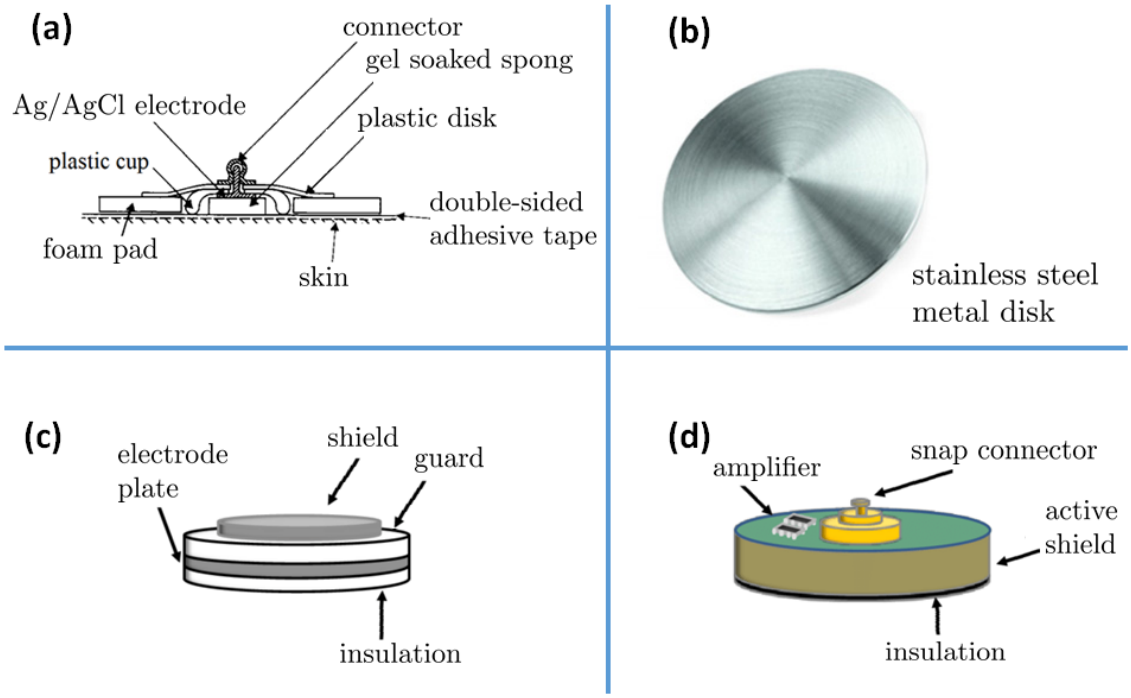


Figure 2.6: ECG electrodes: (a) Wet electrodes needs an adhesive gel to be applied between the skin and electrode surface [70]. (b) Simple passive dry contact electrode of stainless steel metal disc [71]. (c) Insulated electrode which was made of a conductive layer and insulation layer (usually thin film). These electrodes need direct skin contact [72]. (d) Active capacitive electrode (non-contact) which can couple ECG signal through clothes [68, 72].

the resistor. The dry electrodes are modelled with only one RC layer, where the interface resistance is about ten times higher than the wet electrodes' [68]. The high impedance of the dry electrode interface could be reduced by abrading or hydrating the skin, and many studies have suggested using micro-fabricated needles to penetrate $10 - 40$ μm which will give results as good as Ag/AgCl electrodes without the need to skin preparation or using gel [73, 74].

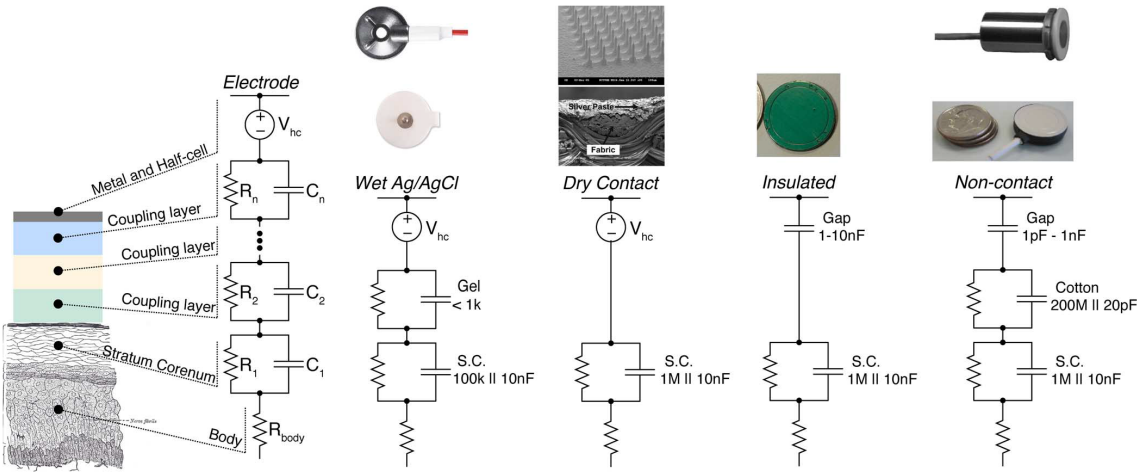


Figure 2.7: Skin–electrode impedance models for the typical Ag/Agcl, dry contact, insulated and capacitive electrodes [68].

The wet, dry and insulated electrodes need direct physical contact with the skin to operate, but the non-contact electrodes (also known as capacitive electrodes) can couple the signal through clothes or air without skin contact. Interestingly, the capacitive electrodes are usually dominated by the resistive component of the dielectric RC layer, because of the poor conductivity of the clothes and air [75]. On the other hand, the dry electrodes are more dominated by the capacitive component of the skin interface layer [62, 76].

One of the interesting points regarding the skin interface impedance is that the high resistance of the interface can be beneficial to the ECG coupling [68]. This was proved by Chi et al. (2010) [68] using the dry/capacitive electrode model, shown in Figure 2.8 and 2.9, to define the electrical signals and parameters of the mathematical equations.

Figure 2.9 (a) shows the circuit noise model of dry / capacitive electrode. Figure 2.9 (b) shows the relevant frequency behaviour of different sources of noise: amplifier thermal noise, interface thermal noise and the interface excess noise. Figure 2.9 (c)

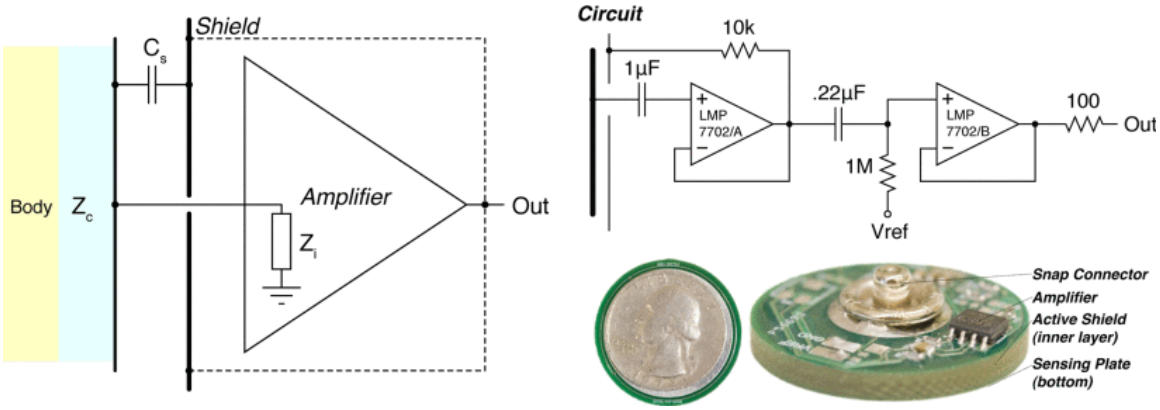


Figure 2.8: Dry/capacitive electrode topology and schematic circuit [68].

shows the effect of increasing and decreasing the resistance of the RC layer on the noise contribution.

The model of the dry contact shown in Figures 2.8 and 2.9 is considered in order to mathematically describe the input referred noise, and to find the conditions that achieve the minimum noise. The parameters need to be defined from the mentioned model are:

$v_s(j\omega)$	signal source on skin surface;
$v_o(j\omega)$	signal recorded at amplifier output;
$v_{i,n}(j\omega)$	input referred amplifier voltage noise;
$i_{i,n}(j\omega)$	net current noise at amplifier input;
$Y_c(j\omega)$	$g_c + j\omega C_c$, skin-electrode coupling admittance;
$Y_i(j\omega)$	$g_i + j\omega C_i$, amplifier input admittance;
C_s	active shield to electrode capacitance;
A_v	amplifier voltage gain.

With source to output gain:

$$v_o = G(j\omega)\left(v_s + v_{s,n}\right) , \tag{2.1}$$

and source input referred noise:

$$\begin{aligned} G(j\omega) &= A_v \frac{Y_c(j\omega)}{Y_c(j\omega) + Y_i(j\omega) + j\omega\left(1 - A_v\right) C_s} \\ &= A_v \frac{g_c + j\omega C_c}{g_c + g_i + j\omega\left(C_c + C_i + \left(1 - A_v\right) C_s\right)} \end{aligned} \tag{2.2}$$

$$\begin{aligned} v_{s,n} &= \frac{Y_c(j\omega) + Y_i(j\omega) + j\omega C_s}{Y_c(j\omega)} v_{i,n} + \frac{i_{i,n}}{Y_c(j\omega)} \\ &= \frac{g_c + g_i + j\omega\left(C_c + C_i + C_s\right)}{g_c + j\omega C_c} v_{i,n} + \frac{i_{i,n}}{g_c + j\omega C_c} \end{aligned} \tag{2.3}$$

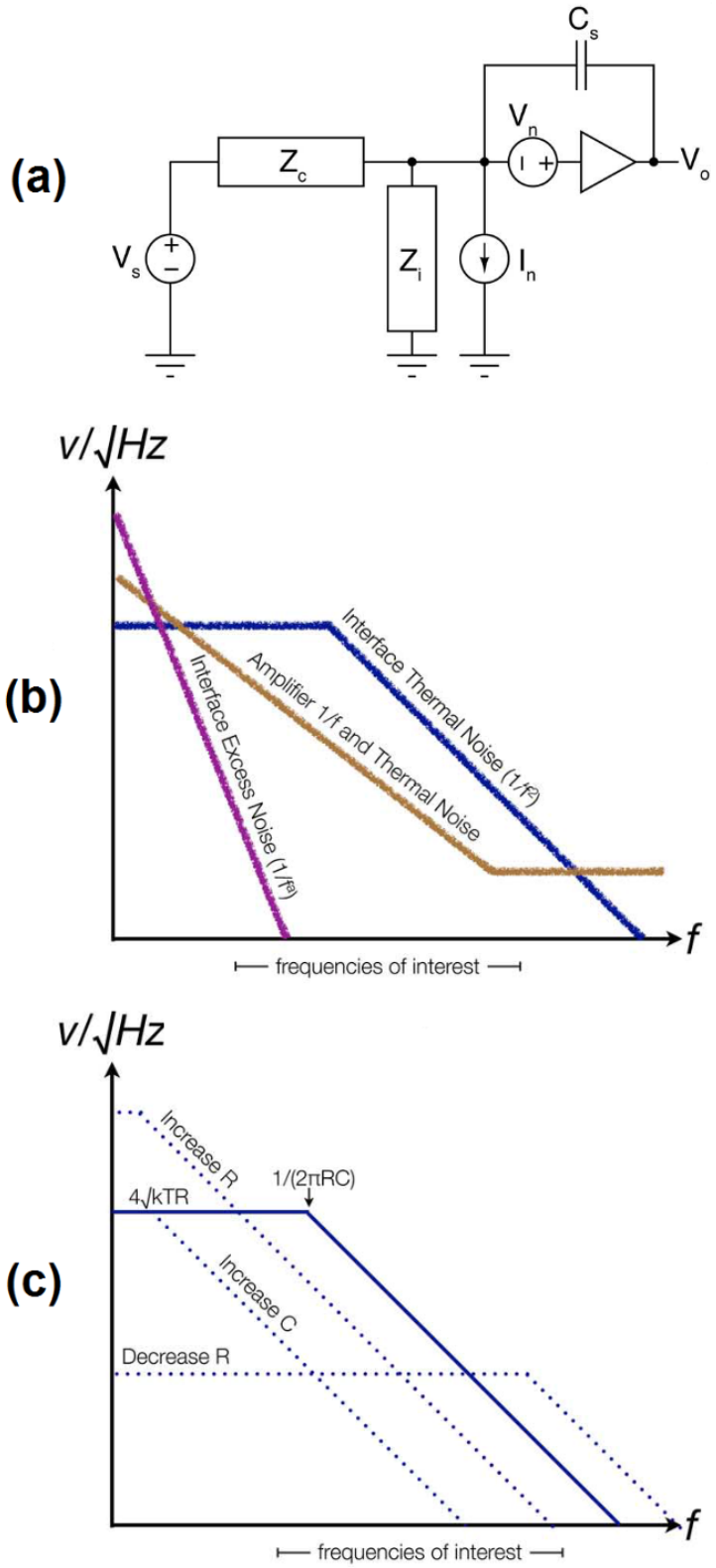


Figure 2.9: (a) The noise model for the dry/non-contact electrodes shown in Figure 2.8. (b) Frequency behaviour of different noise sources. (c) The effect on the noise contributions when the changing the R and C values[68].

The source input-referred noise power density follows directly from Equation 2.3 where $v_{i,rms}^2$ and $i_{i,rms}^2$ represent the power (RMS squared) of the two input noise generators, $v_{i,n}$ and $i_{i,n}$:

$$v_{s,rms}^2 = \frac{|Y_c(j\omega) + Y_i(j\omega) + Y_s(j\omega)|^2}{|Y_c(j\omega)|^2} v_{i,rms}^2 + \frac{i_{i,rms}^2}{|Y_c(j\omega)|^2} \tag{2.4}$$

$$= \frac{(g_c + g_i)^2 + \omega^2 (C_c + C_i + C_s)^2}{g_c^2 + \omega^2 C_c^2} v_{i,rms}^2 + \frac{i_{i,rms}^2}{g_c^2 + \omega^2 C_c^2} \tag{2.5}$$

The first component of Equation 2.5 ($v_{i,rms}^2$) does not dominate the ECG bandwidth unless the dry/capacitive electrode were poorly coupled to the skin. The second component of the noise ($i_{i,rms}^2$) is more likely to dominate the noise contribution. This noise current includes the conductance of both interface coupling and amplifier input, as well as the thermal noise. Therefore, the noise contribution to the signal can be reduced to:

$$v_{s,rms}^2 \approx \frac{4kTg_c}{|Y_c(j\omega)|^2} = \frac{4kT}{g_c + \frac{\omega^2 C_c^2}{g_c}} \tag{2.6}$$

Equation 2.6 shows that the minimum input referred noise will be achieved when the coupling impedance equals zero or infinity. The two extreme cases achieve the optimum solution for the minimum noise when the interface impedance is reduced to be zero, or when the interface impedance is infinite, i.e. capacitive sensors.

2.4.4 Limitations of Dry/Capacitive Electrodes

Decreasing the effect of artefacts is one of the most challenging aspects of designing dry/capacitive electrodes. The dry/capacitive electrodes are more prone to the relative electrode motion because of the lack of gel layer. The skin interface's impedance changes suddenly according to the distance change, which produces instant spikes in the ECG signal [77, 78]. The motion artefacts share the same spectrum domain as the ECG signal, as shown in Figure 2.10.

The dry/capacitive electrodes should be designed to minimise the effect of motion artefacts by implementing a high input impedance amplifier. Also, many designs have adopted using unity gain active shielding along with decreasing the input capacitance of the amplifier [68]. Some models have been proposed to suppress the displacement artefacts of the capacitive electrodes [77, 78]. However, they demand knowledge of the coupling capacitance and still need to be tested on real ECG recording.

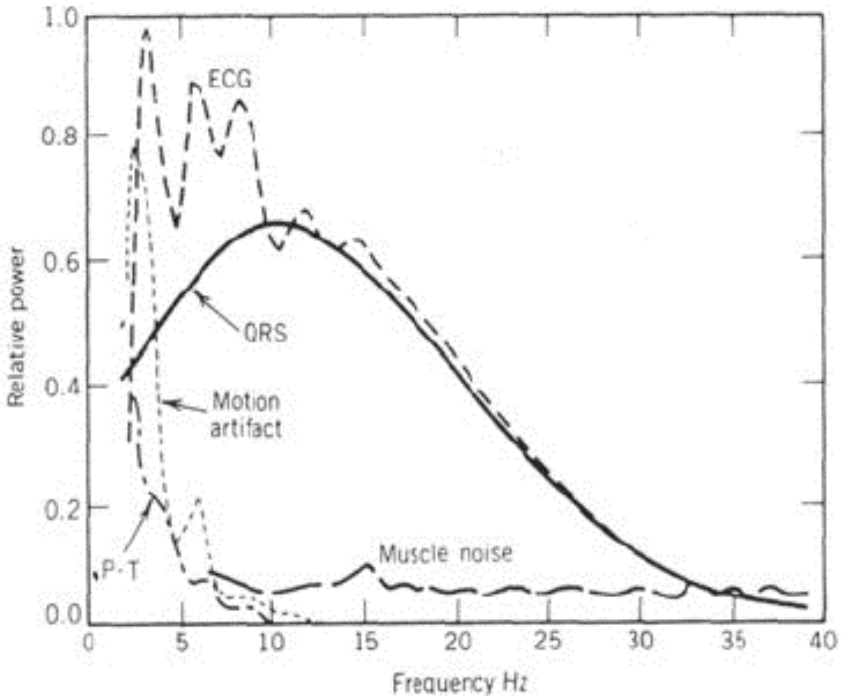


Figure 2.10: The relative power spectrum of noise and motion artefacts in a typical ECG signal [79].

Another source of artefacts is the friction between the electrodes and the skin in case of dry contact, or the electrodes and dielectric material in case of capacitive electrodes. An additional problem of the capacitive electrodes is the time needed for the signal to settle down. As shown in Figure 2.11, after a recording disruption, the signal took about 15 seconds to settle down. This behaviour is caused by the high pass filter characteristics of the capacitive electrode frequency response. The lower frequency in the frequency response should be 0.05 Hz maximum in order to reserve the ECG signal morphology. However, some sensors are designed with a high lower frequency of $0.5 - 1$ Hz [68]. This approach can distort the ECG signal and might not be acceptable for some diagnosis of medical applications [80].

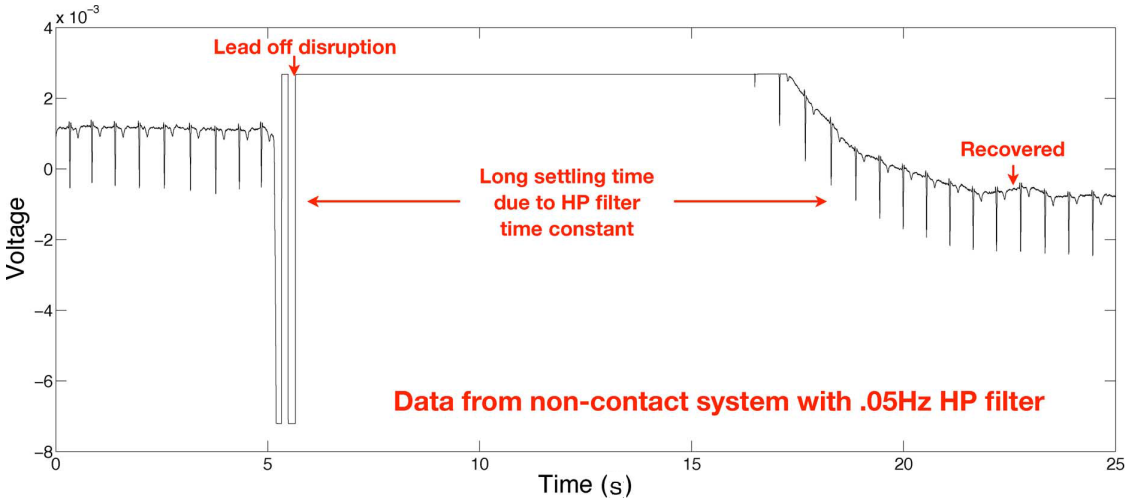


Figure 2.11: ECG recording using non-contact electrode. The signal takes approximately 15 seconds to settle down [68].

2.5 The Applications of Dry/Capacitive ECG in Neonatal Care

2.5.1 Delivery Room Monitoring

There is limited research discussing dry/capacitive ECG applications in the field of newborn heart rate in the delivery room.

One clinical trial was performed on newborns in the delivery room using ECG fabric sensors in dry contact [81]. A hypoallergenic garment was used to cover the top of the babies, as shown in Figure 2.12, where the conductive fabric sensors were attached to the sleeves, recording the ECG signal from lead I. The data were sent wirelessly over Bluetooth to a computer for storage and further processing. The recordings were performed during the first hours of the newborns' life and performed on 29 babies.

The average percentage of good quality ECG recordings in this study was 75.8% ± 18.9 SD. The quality was lowered by the introduced motion artefacts, and the signal was also absent for several intervals due to software bugs in the communication system.

An additional, recent study which was published in March 2019 by the University of Sussex, has introduced the use of active dry electrodes as a potential method of recording ECG signal in the delivery room [82]. The sensing plate was printed on a mattress cotton cover using silver ink and then connected to the analogue circuit of the processing unit. The study has successfully collected ECG signal from the back of

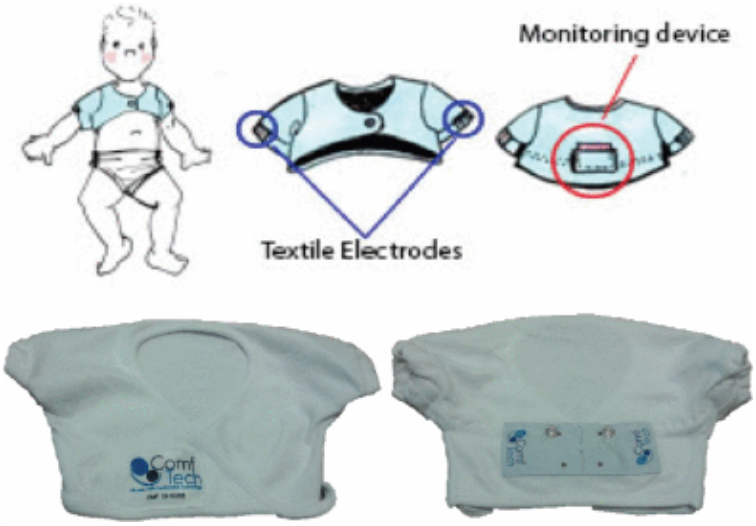


Figure 2.12: The wearable garment with fabric sensors on the sleeves for ECG monitoring in the delivery room. The transmitter base unit is placed at the back [81].

one baby aged 18 months, using the sensors printed on the mattress cover, as shown in Figure 2.13. The study is waiting for approval in order to extend to a clinical trial. Those two studies were the only available studies in the literature regarding dry or capacitive electrodes applications in heart rate monitoring in the delivery room.

On the other hand, few studies have tested the dry/capacitive ECG for neonatal intensive care unit (NICU) when the babies are placed in their incubators. These studies will be discussed in the next section. The babies in the NICU are mostly placed naked in the incubator apart from their nappies, in order to control the heat [83]. However, in some cases, they might be snuggled in cotton sheets [19]. There are also different positions for the babies in the NICU; the babies are placed on their back, chest, right side and left side [19].

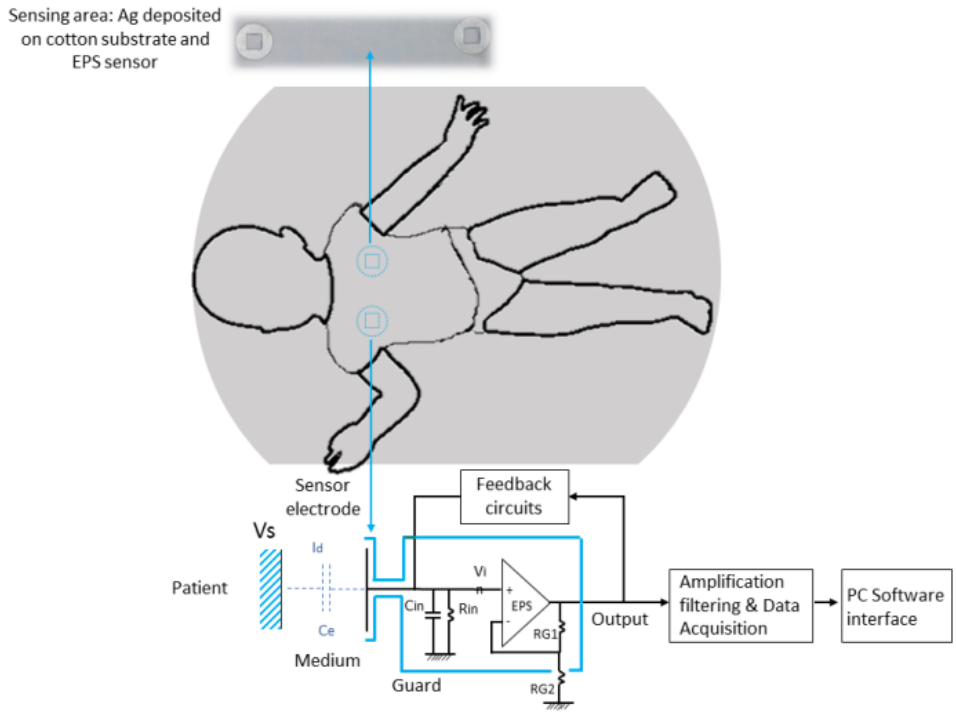


Figure 2.13: Schematic of the smart-matress (top) and sensor design implementing the EPS sensor (bottom) [82].



Figure 2.14: Naked newborn in the NICU incubator [16].

2.5.2 NICU Monitoring

Many papers have suggested the use of fabric sensors in the NICU for long term ECG monitoring. The fabrics are comfortable and could be sewn to the bedding or babies clothes.

One of these proposals is a project called Smart Jacket, where patches of silver plated and gold plated sensors were sewn into a wearable jacket for babies in the incubators. The initial design of the jacket is shown in Figure 2.15 and the updated version with bigger sensors' area is shown in Figure 2.16 [16, 84]. The textile used in this project was the same textile provided by Statex company for silver plated fabrics.



Figure 2.15: Smart Jacket prototype with simple dressing process [16].



Figure 2.16: Updated smart Jacket prototype [16].

The recorded ECG from the preterm volunteer using the design in Figure 2.15 was of good quality. The smooth skin of the preterms resulted in better sensor contact, primarily because of the continuous pressure when the babies are lying down or when being held. Also, the motion artefacts were relatively little because of the limited movements of the newborns. Another study has suggested the use of conductive foam with flexible dry electrodes on preterm babies. This arrangement can reduce the high impedance due to the air gap, as shown in Figure 2.17.

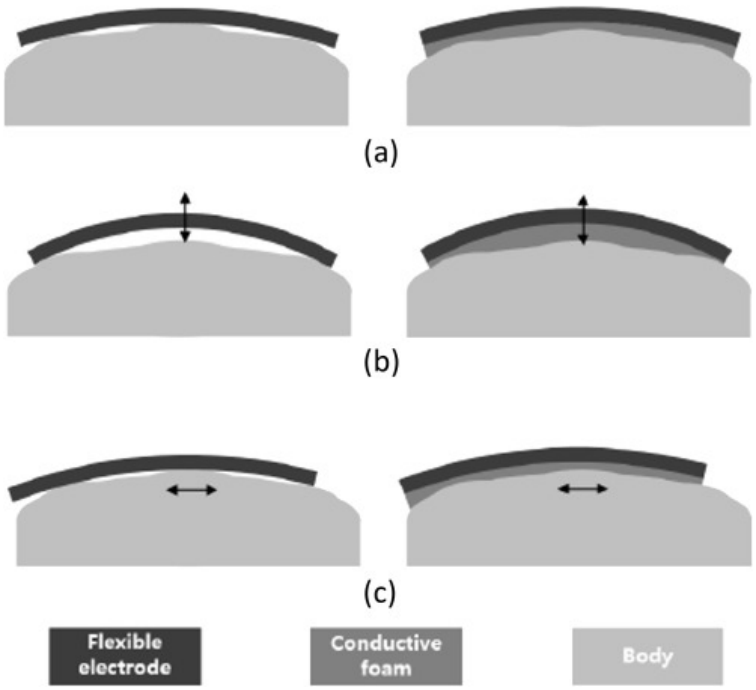


Figure 2.17: The conductive foam is used to close the gap between the ECG sensor and the skin [85].

Atallah et al. (2014) [19] has proposed using an array of capacitive sensors embedded in a mattress to record the ECG capacitively through the cotton sheet in the NICU [19]. The system in Figure 2.18, was used to collect ECG signals capacitively through layers of bedding and clothing of 15 babies in the NICU and neonatal medium care unit (NMCU). The babies were snuggled in a different number of cotton layers (up to four layers), a mattress cover (polyurethane) was used in all the recordings. The babies were put in different positions throughout the recording on their chest, right side, left side and back. When the collected capacitive ECG was compared to reference ECG for heart rate detection, the accuracy of R peak detection varied significantly from only 7% for one baby to 86% for another baby. The reason for that was the different positions of the babies, the different clothing layers and the introduced motion artefacts by every baby movements. The best results were collected from the babies placed on their chests and from the naked babies.

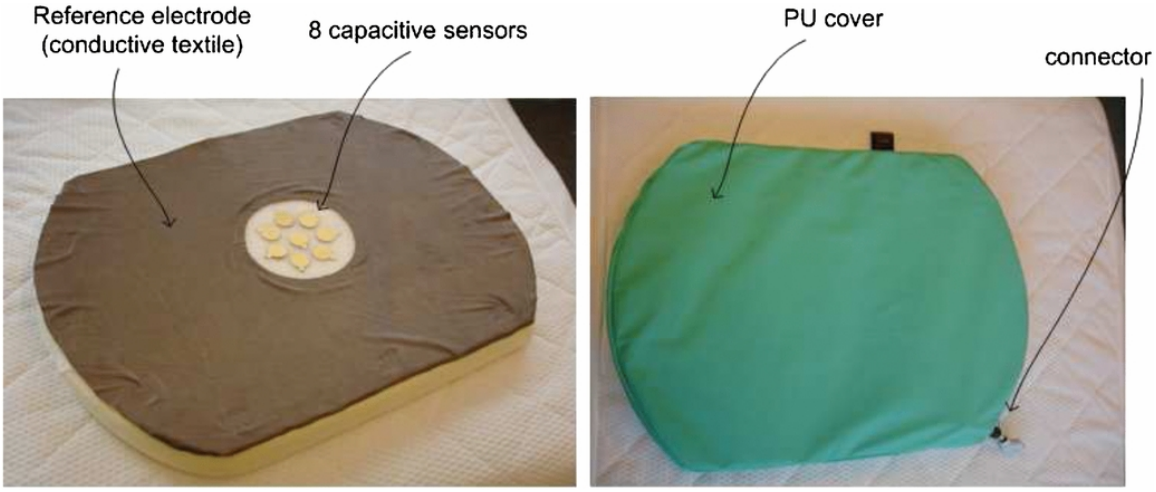


Figure 2.18: Neonatal mattress with integrated capacitive sensors. The mattress is covered with a polyurethane (PU) cover [19].

2.6 ECG from Head

One of the proposed ECG sensors placement in this research is the forehead. Therefore, this section is devoted to discussing such a placement. Some papers in the literature have discussed the possibility of recording ECG signal from the head, but the field is still underexplored, and most of the available research treats the ECG signals from the head areas as artefacts or interference on EEG, EOG and EMG signals [86], [87], [88]. The papers which are concerned with recording the ECG signal from head and neck are mostly associated with motorcycles' safety and investigating the ability to develop ECG embedded in helmets or in the area of hearing aids and earplugs.

Various types of ECG sensors were used in helmet applications: Ag/AgCl [89], dry sensors [90, 91] and fabric sensors [92]. The EU-funded i-VITAL project [90] has developed an ECG monitoring system integrated with helmets. The objective of the product is to monitor vital signs in real-time and send them to emergency teams in motorcycles accidents. The system has used EPIC sensors PS25101 in dry contact with face and neck to capture an ECG-like signal, as shown in Figure 2.19. The research has successfully recorded ECG-like signals, which could be used mainly to calculate HR.

Other research has simulated the biophysics of ECG signals from head [93]. Five channels were studied, where the sensors were placed symmetrically from the neck, jaw centre, jaw joint, cheek and forehead. The ground was placed in the forehead centre, and the results of both measured and simulated ECGs are shown in Figure

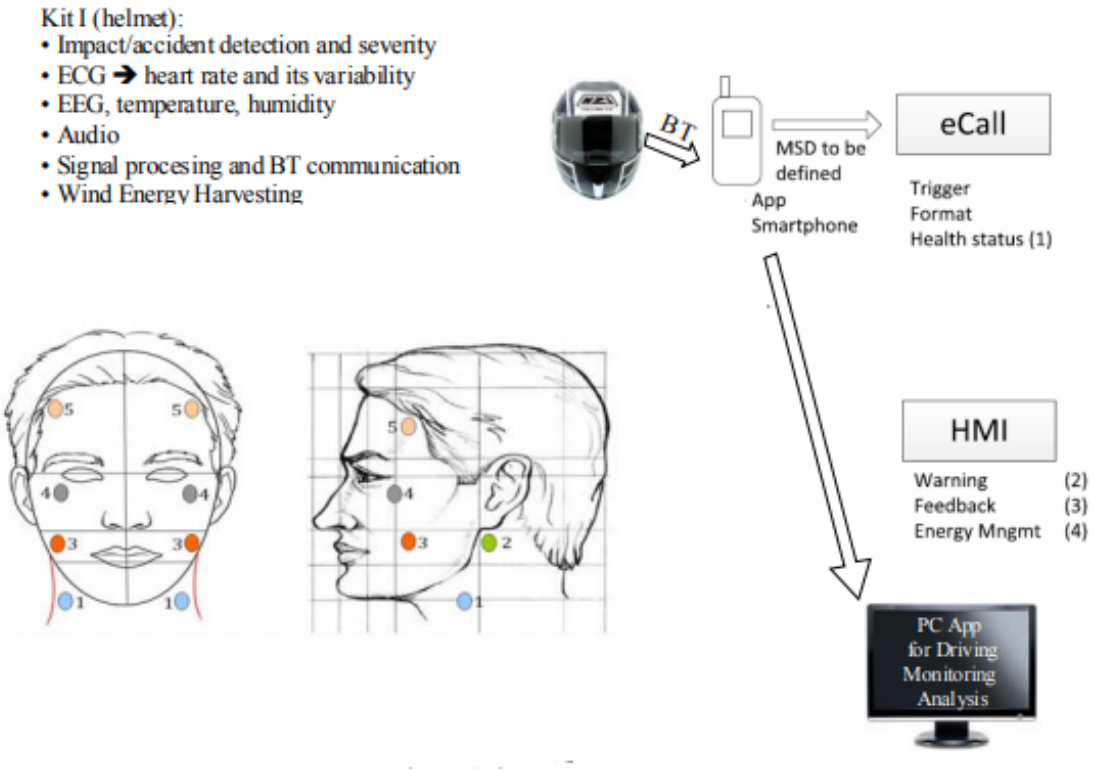


Figure 2.19: i-VITAL components and sensors locations [90].

2.20. The head ECG signal was also considered in eye wears' designs, where the frame bridge was used to record ECG from the forehead, and the glasses temples were used to record PPG signal from the earlobe [94].

Moreover, other papers have explored collecting ECG signal from the area around the ear by attaching the sensors to hearing aids or earplugs [95–97]. As shown in Figure 2.21, such a wearable device was used to collect ECG signal from the mastoid area. Because of its flat surface, it minimises the motion artefacts and produces a stable signal.

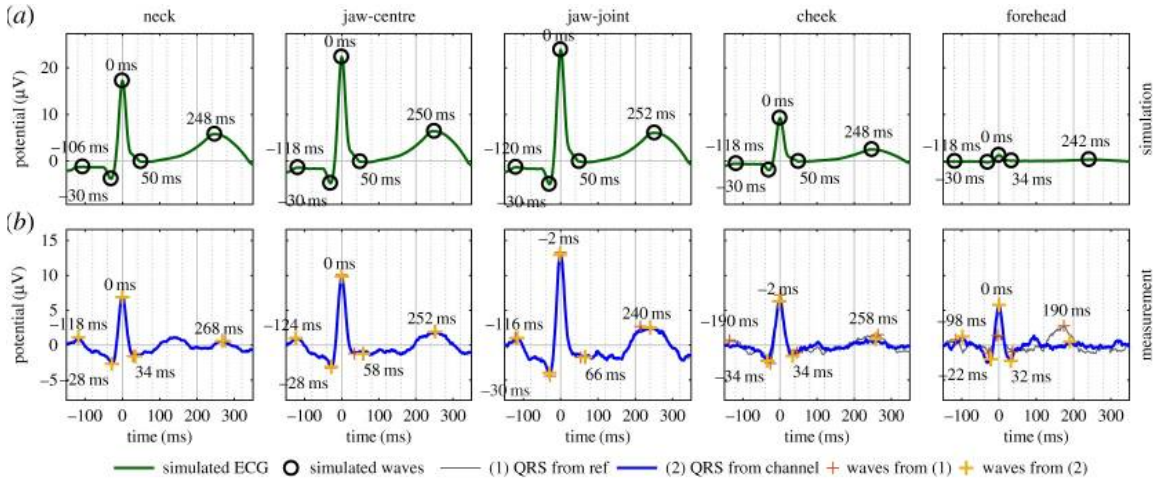


Figure 2.20: Simulated and measured cardiac cycles in five head-ECG channels [93].

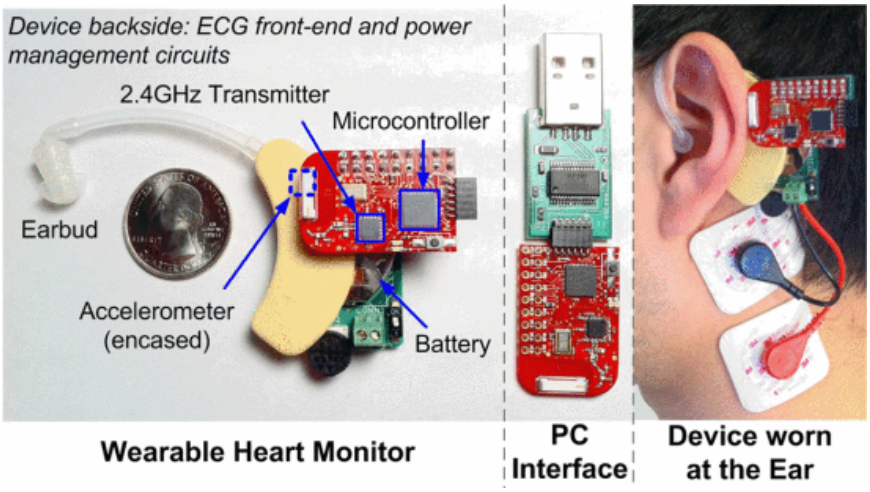


Figure 2.21: Wearable heart monitor [97].

2.7 ECG Noise and Interference

The are many types of noise that affect the bioelectrical signals recording, with most of it being introduced by the electrodes. Most of the noise generation mechanisms are not fully understood, yet some papers have suggested some of the elements that contribute to the biomedical signals [58,98,99]. In order to model the expected noise in the signal, Gondranet al. (1995) found that the noise introduced to biomedical signals decreases at higher frequencies [66,98,99], and noted that the metal-electrolyte interface could introduce significant voltage fluctuations. However, the noise amount mainly depends on the subject test, electrode area and skin preparation.

Power line interference in biomedical signals (at 50 Hz or 60 Hz), can happen due to capacitive coupling when there is impedance mismatch of the electrodes, and hence, a differential voltage at the amplifier input (simple Ohm's law). The power line noise can also be introduced when the body common mode signal is converted to differential voltage [57]. The 50 Hz noise can be decreased by minimising the electrode impedance because this will automatically minimise the impedance mismatch. From what was mentioned above, the coupled noise could be reduced by reducing the noise differential voltage at the amplifier input, and the minimum noise could be coupled if the resistance of the electrode equals zero or infinity as proved earlier.

One of the most popular approaches to minimise the common mode noise is to design an active ground known as Driven Right Leg (DRL). The DRL circuit is designed by feeding back the anti-phase of the ECG electrodes' mean. However, some papers have pointed out that the DRL can introduce interference to the differential mode of the isolated amplifier, and so they discourage the use of DRL when the system is isolated from the powerlines according to the safety guidelines. They claimed that the interference is unpredictable and need more investigation and research [100] & and [101].

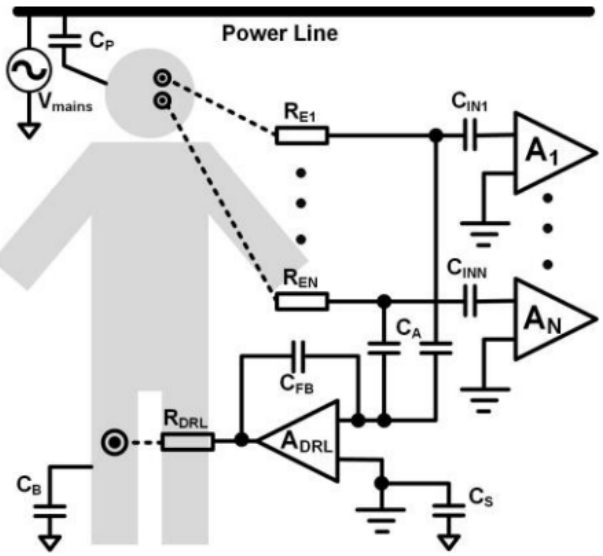


Figure 2.22: DRL circuit for biomedical applications [101].

2.8 Conclusions

This research investigates potential methods for heart rate monitoring in the delivery room. The first section of the literature review has listed the different HR monitoring methods that are used immediately after birth. The ECG signal was recommended by many research papers as the most accurate method for HR assessment. The ECG has been introduced in the recent European guidelines for newborns' resuscitation as a potential method that lacks the appropriate technology.

After that, the medical guidelines for the newborns were reviewed for a better understanding of the delivery room environment and how the babies are wrapped into cotton towels or plastic bags to control their body heat. Then the dry/capacitive ECG electrodes were compared against Ag/AgCl electrodes, which have many limitations in the neonatal applications. The electrical model of the skin impedance interface for the dry/capacitive electrodes was illustrated, and then the design, which can suppress most of the noise power was discussed. The limitation of the dry/capacitive electrodes was listed, including the artefacts and friction. Moreover, the different applications of these electrodes in neonatal care were studied.

Finally, the noise contributions were summarised with one of the 50 Hz noise solutions, the driven right leg. In the next chapter, the materials and methods used in this research are illustrated along with the ECG acquisition systems.

Chapter 3

Materials and Methods

3.1 Overview

This chapter describes the different materials that were used in the experimental setups in this research. Ethics approval was sought and obtained from the Faculty of Engineering for the experiments presented in this thesis. A sample of ethics application information sheet and a participant consent form are shown in appendix A. The second section discusses the materials and systems that were used for the capacitive sensors experiments. The third section illustrates the different material and systems that were used for the fabric sensors experiment. The fourth and fifth sections discuss the methods of skin impedance measurements and heart rate detection. These two methods were used for capacitive and fabric sensors experiments.

3.2 Capacitive Sensors Materials and Systems

3.2.1 EPIC Sensor Overview

Plessey Semiconductors Ltd. has produced an electric potential integrated circuit (EPIC) sensor in collaboration with Sussex University, UK. Some papers have discussed that the EPIC sensor offers an outstanding ability to detect very low electric fields, with or without physical contact [102].

The sensor works as a very sensitive non-contact voltmeter which has a lower corner frequency of 0.2 Hz and an upper corner frequency of 10 kHz [22, 23]. The frequency of the lower corner is relatively high, compared to the standard 0.05 Hz prescribed for the ECG signal [68]. Prance et al. (2008) have tested the EPIC sensors developed by Plessey in 2008 and claimed that the sensors could detect the heart rate capacitively through fabrics and dielectric materials and the signals could be detected

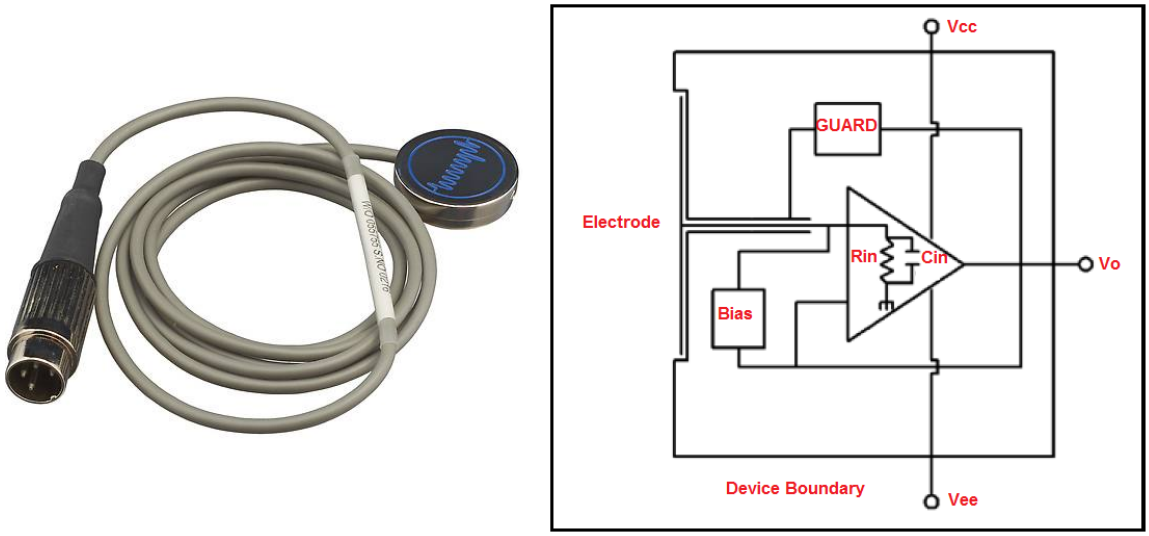


Figure 3.1: Packaging of EPIC PS25101 sensor and its internal design.

through the air up to 40 cm of air distance between the sensor and the adult human [103].

EPIC sensors have been produced in many versions. In this research, EPIC PS25101 sensors have been used because they are biocompatible according to ISO 10993. The sensor is an ultra-high impedance device, made of titanium electrode and protected by a capping layer of dielectric material in order to isolate the titanium electrode from the body being measured. As shown in Figure 3.1, the EPIC PS25101 sensor is designed in a metal disc-style package with a diameter of 1.4 cm, equipped with a connecting lead and mini-DIN plug termination.

The internal PCB layout of the sensor is shown in Figure 3.2, where two pins are used to power the sensor, and one pin is the output signal. The product is classified as a IIa certified medical product, and the electrodes follow the ISO 10933 compatibility regulations and the IEC 60601 safety regulations.

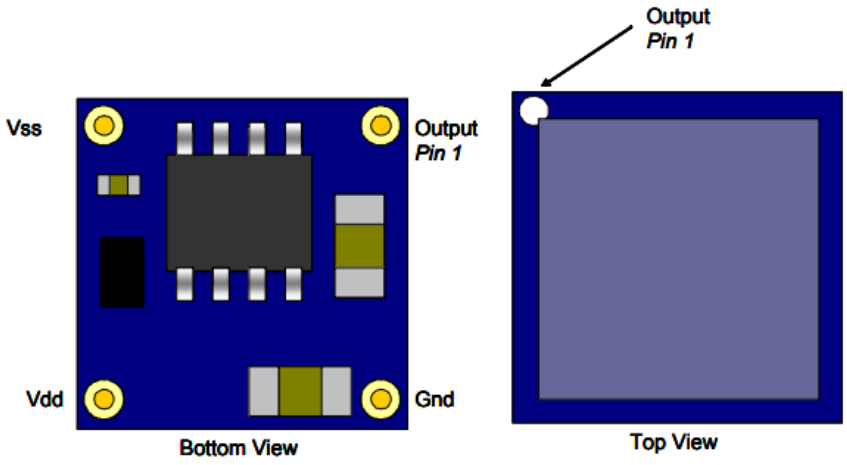


Figure 3.2: The PCB layout of EPIC sensors [104].

3.2.2 EPIC Sensors Placement

As illustrated in the Literature Review Chapter, newborn babies in the delivery room are wrapped into cotton towels or plastic bags to prevent heat loss and protect them from hypothermia. EPIC PS25101 sensors were used in this research to couple the ECG signal capacitively through these materials. The active capacitive sensors are relatively bulky compared to the standard wet ECG sensors, which makes them difficult for limb attachment. The most practical placement for EPIC sensors for the newborns is under the babies back. There are many advantages of collecting ECG signal from the back of the baby as listed below:

(1) The back is the closest part to the heart after the chest, and the chest cannot be used to strap relatively bulky sensors during the resuscitation. Because the medical guidelines advise the medical staff to observe the chest while resuscitating [1].

(2) The contact area from the back is bigger than the hands and legs which enhance the signal to noise ratio.

(3) The babies are placed in the supine position during the resuscitation, and pressure from the baby's body weight would be useful to hold the sensor contact.

(4) Unlike the limbs, the muscles of the back are not fully matured in the newborn babies, and hence the movement of the baby back is limited compared to the hands and legs, which decreases the introduced motion artefacts.

(5) The possibility of arranging an array with more than one channel to record simultaneous ECG signals which would increase the efficiency of the system and may reduce the effect of motion artefacts at the same time.

Therefore, the proposed placement for the sensors was to be embedded in the mattress of the resuscitation table, where the baby would be placed during the resuscitation. In the first stage, a pair of sensors was tested to record the ECG signal from babies backs through the cotton towels and plastic bags that are used to wrap the newborns in the delivery room. Upon the success of these experiments, the second stage is designed to use four pairs of EPIC sensors to be embedded in the mattress in order to couple four ECG signals. Then, the best signal will be chosen for HR detection. During movements, motion artefacts are created by the sudden change in coupling capacitance. With four ECG signals, the effect of motion artefacts will hopefully be significantly reduced. Figure 3.3 shows the top and side views of the proposed placement of EPIC sensors.

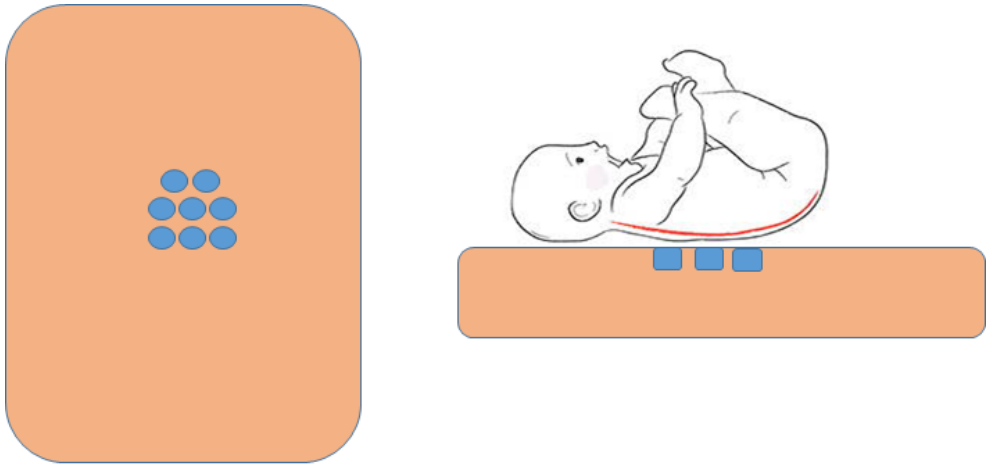


Figure 3.3: The proposed placement of EPIC sensors array inside the resuscitation mattress.

Before testing the array placement, a pilot system with two sensors was used to test if EPIC sensors can couple the ECG through the delivery room materials. This system was used to record ECG signals from babies' backs in dry contact and through the dielectric materials. The array systems with eight EPIC sensors was designed but was only used to acquire ECG from adult volunteers. These systems and their sensors placement are discussed in the next section.

3.2.3 ECG Acquisition Systems

As mentioned above, two systems were used to collect ECG signals using EPIC sensors. The first system was a pilot system to acquire one ECG signal at a time in order to assess the ability of the sensors to record ECG signals capacitively through cotton towels and plastic bags. This system was used on both adult and baby volunteers. The second system was designed to collect four ECG signals but was only used on adult volunteers. Both systems have used EPIC PS25101 sensors and the DRL as advised by the sensors' manufacturer (Plessey semiconductor).



Figure 3.4: PS2500 ECG recorder box by Plessey connected to EPIC PS25101 sensors [22].

3.2.3.1 Pilot System

The pilot system was an ECG recorder provided by Plessey Company known as the PS2500 box and is compatible with EPIC PS25101 sensors. The PS2500 box acquires two analogue inputs from two EPIC sensors and generates a DRL. Figure 3.4 shows the PS2500 box, and its internal design is shown in Figure 3.5, where two inputs are coupled from EPIC sensors leads. The signals are amplified, filtered with a low pass filter of 35 Hz and then with a 50 Hz notch filter before being digitised. A DAQ 6008 is used to convert the analogue ECG signal into a digital one with a sampling frequency of 1k sample/second. The bandwidth of the EPIC sensor is 0.2–10k Hz (as mentioned earlier), which means that the collected ECG signal bandwidth is 0.2–35 Hz. PS25100 made by Plessey is classified as a class IIa medical device with BS EN 60601 certification.

The digital ECG signal is then sent to the computer for further processing and heart rate detection. This pilot system was used in this research to test the ability of EPIC sensors to collect the ECG capacitively through the materials used to warms

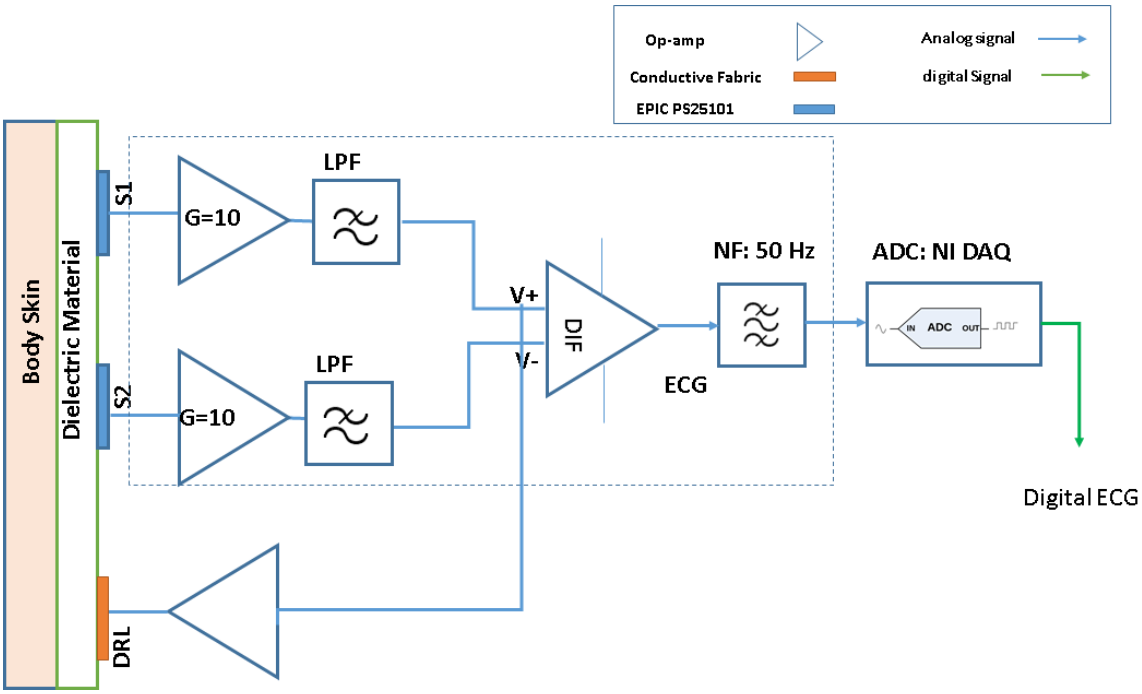


Figure 3.5: The pilot system which collects one ECG signal using a pair of EPIC sensors. The rectangle in dashed lines represents the internal design of the PS2500 box.

the newborns. The sensors were initially tested on adults wrists. The adults' wrists were chosen for the test because:

(1) Their weight pressure on the sensors is similar to the newborn's body.

(2) The potential ECG components at the wrists have smaller amplitude compared to upper parts of the body, and the expected newborns ECG is expected to have small R amplitude [105].

(3) They are accessible for dry ECG contact. The hands were ruled out because their skin is naturally developed to be harder than the rest of the body.

Figure 3.6 shows the complete setup of ECG recording from adult volunteer wrists. The digital ECG signals were collected and stored using LabVIEW software and further processed using Matlab. The laptop was disconnected from the mains power during all the ECG recordings to minimise the interference.

3.2.3.2 Array System

The array system was designed for this research to collect four ECG signals from volunteers using eight EPIC sensors. The system was built using four differential

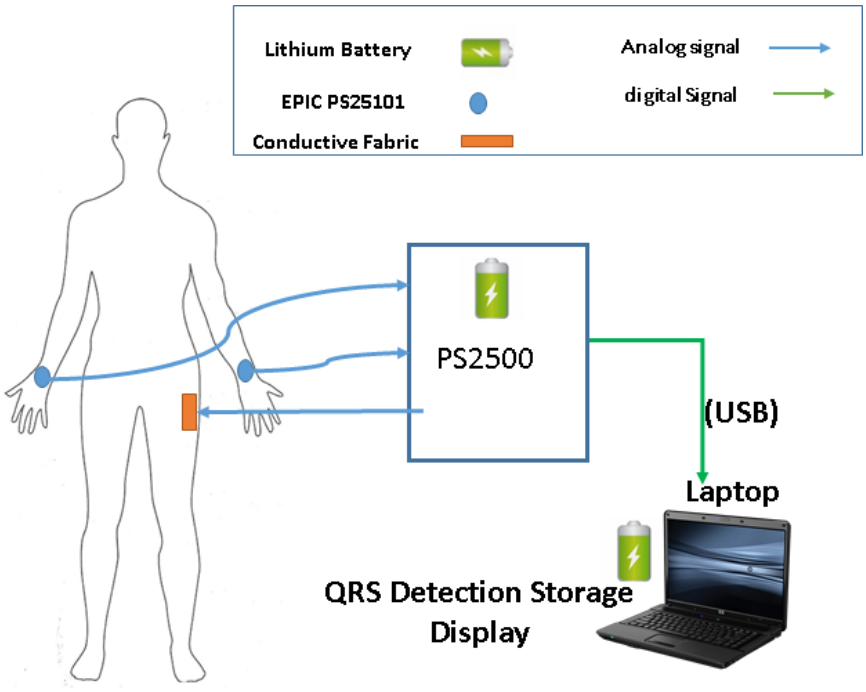


Figure 3.6: The setup for collecting ECG signal from adult volunteer wrists using PS2500 and two EPIC sensors.

circuits using the same design that was used to build Plessey PS2500. The eight sensors were attached to different points to create an array that produces four ECG signals. The signals were then processed with Matlab to choose the ECG signal with the best quality for the QRS[1] detection. This setup should increase the accuracy of the acquisition system and also increase its robustness against the motion artefacts. This because some of the sensors are not in contact with the volunteer due to movement, another pairs of sensors could be able to pick up the signal and hence the probability of the ECG acquisition increases by increasing the sensors. The proposed system is shown in Figure 3.7.

[1]QRS complex is the combination of three of the graphical deflections on the ECG signal.

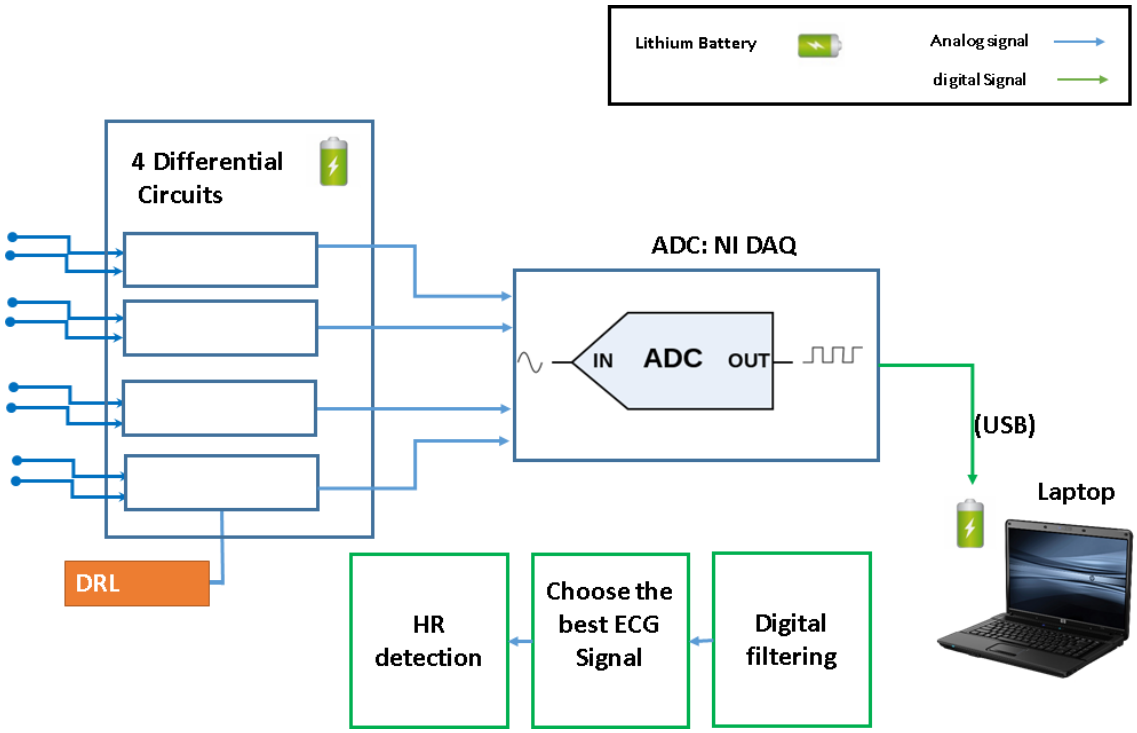


Figure 3.7: The array system which was designed to couple four ECG signals and process them to choose the best signal for QRS detection.

3.3 Fabric Sensors Materials and Systems

3.3.1 Overview

As mentioned earlier, most of the newborn body is expected to be covered, but the forehead and the forearms of the babies are usually exposed. However, it is not practical to attach a bulky active dry sensor on the head of the newborns. Therefore, the conductive fabric was proposed as a potential method to record the ECG signal from the head and arm of the newborn.

It has been illustrated in the literature review that the ECG signal is recorded from the head using fabric sensors in some applications, but there were no available data about this method for newborn babies applications.

In Chapter Five, the conductive fabric sensors were tested for the application of a newborn's heart rate monitoring in the delivery room. The sensors were proposed to be placed on the forehead and left forearm of the newborn babies in dry skin contact. This section discusses the materials and systems used for fabric sensors experiments in Chapter Five.

3.3.2 Fabric Sensors Placement

As mentioned above, the fabric sensors are introduced in this research as a potential method of coupling dry ECG signal from newborns during resuscitation. The initial proposal was to record the ECG from the forehead and forearm. The forehead sensor would be sewn into the babies hat, while the forearm sensor and the driven right leg would be attached to the babies forearm using a stretchable cotton armband. The experiments in Chapter Five were designed to test if the conductive fabric can collect ECG signals from babies using this setup.

The size of the fabric sensors was restricted by the average size of newborns. The average length of the forearm for a newborn baby is 60.2 mm [106]. In order to use one armband to hold the forearm sensor and the driven right leg, the distance between these two fabrics will be restricted by the forearm length. Also, the width of the sensors is limited by the wrist circumferences, which is 62 mm on average and can be as low as 50 cm for newborns [106].

3.3.3 Fabric Sensors Materials

Three fabric materials were tested as passive dry contact sensors on adult and baby volunteers.

1) Medtex P130 Fabric:

This product is made by Statex for medical applications as a base material for many fungicidal products, mattress/pillow covers for allergen protection, medical clothes, compression wrap, and wound dressing. The substrate of the fabric is made of 78% nylon and 22% elastomer and is plated by pure silver [107]. The thickness of the fabric is 0.55 mm ±10%. The fabric is biocompatible according to the ISO 10993 and is also classified as class I by Oeko-Tex Standard 100. The data sheet, biocompatibility certificate and Oeko-Tex certificate are all attached in Appendix A. Medtex P130 fabric was used as an ECG sensor for military applications [92].

2) Laird 3080–500 Fabric:

The product is made by Laird Tech [108] as antibacterial fabric for medical and military applications. The substrate of the fabric is made of 78% nylon and 22% spandex and plated with pure silver. The fabric is flexible, lightweight and very thin (0.45 mm thickness). The fabric is biocompatible according to the ISO 10993 tests, the biocompatibility certification and tests are all enclosed in Appendix A,

along with the product data sheet. It was introduced in the applications of wound dressings, compression wraps and antimicrobial garments.

3) SP31 Fabric:

This product is made by Footfalls and Heartbeats [109] for medical applications. The fabric is made of 20% stainless steel and 80% polyester fibres. Isaia et al. (2016) have investigated the electrical and mechanical proprieties of this fabric [110].

These three fabric materials were used to couple ECG signal from adult and baby volunteers, using two systems. The first system used a wireless ECG recorder 102 developed by Butler in 2018 [111] at the University of Nottingham, and the second system used the clinical ECG monitor, GE B450.

3.3.4 Wireless ECG Recorder

This in-house wireless ECG recorder, shown in Figure 3.8, is designed to collect ECG signals using passive dry contact sensors. It is a portable recorder that works on a battery and has a low power Bluetooth transmission base. The recorder was developed by Butler (2018) [111] at The University of Nottingham with an isolated amplifier. The ECG signal is acquired using an ADS1298 and converted to a digital signal with a sampling frequency of 400 sample/second. The sampling rate was restricted because of the use of the low energy Bluetooth which allows a maximum sampling rate of 400 sample/second in order to maintain the battery life. Despite the relatively low sampling rate compared to the typical of 1K sample/second, the detected ECG signal quality was good. Generally, decreasing the sampling rate decreases the quality of the signal, therefore the ECG recorder was initially tested using simulated ECG in order to compare the quality of the received and the original ECG signals. Figure 3.9 shows the PCB layout of the in-house wireless ECG 102 recorder.



Figure 3.8: The wireless system of ECG recorder .

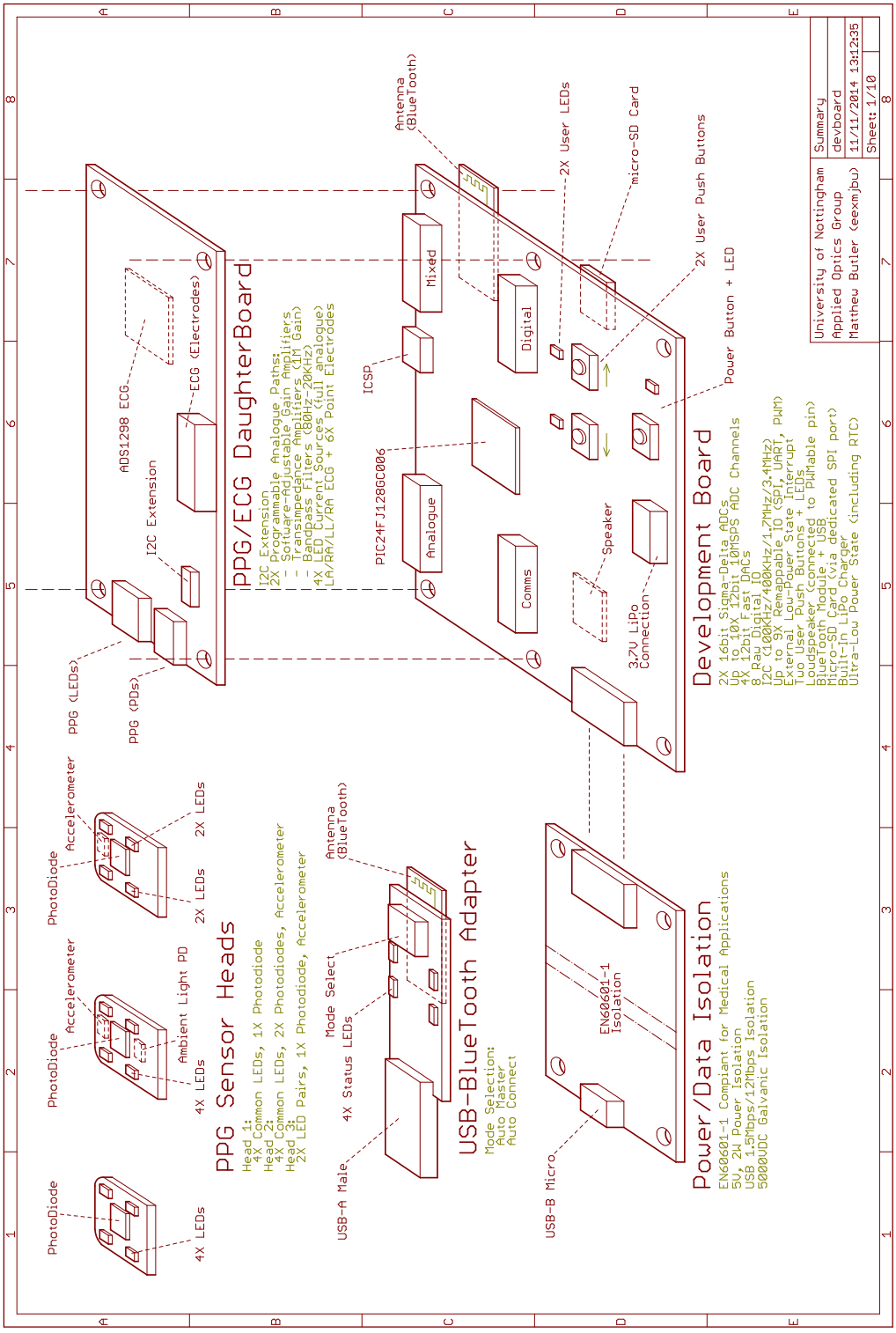


Figure 3.9: The PCB layout of in-house wireless ECG recorder [111].

3.3.5 GE B450 Monitor

The clinical monitor GE B450 was used in Chapter Five to record ECG signals using the passive fabric sensors instead of standard wet ECG sensors. The monitor shown in Figure 3.10 is typically connected to the person using three ECG leads (LA, RA, and LL) and a pulse oximeter (R index finger) [112]. The monitor shows the ECG signal, Oxygen saturation, Heart rate and PPG signal. This monitor was connected to adult volunteers to collect the ECG signal and compare it with the PPG from the pulse oximeter.



Figure 3.10: GE B450 monitor made by GE Health-care [112].

3.4 Skin Interface Impedance Measurement

The skin/electrode interface impedance is an aspect that should be considered in order to model the coupling efficiency of the biomedical system. The interface impedance of dry and capacitive coupling was measured in Chapter Four and Five. This section illustrates the tools used to measure bioimpedance accurately.

3.4.1 Electrode Impedance

Each electrode has an impedance that is dependent on the nature of the electrical double layer between the metal and the gel. This impedance is usually referred to as the polarisation impedance [56]. The polarisation impedance is normally neglected because the electrical layer impedance is small compared to the input impedance, which makes the voltage drop due to the electrode impedance negligible. The term electrode impedance refers to the interface impedance between the electrode and the

biological material. However, it is important to note that, sometimes the electrode impedance is used to describe the total impedance between the two electrodes, including the impedance of the biological material between the two electrodes. Figure 3.11 illustrates two popular approaches in the literature to explain the electrodes/tissue impedance, which is represented by a capacitor shunted by resistance in series with the half cell Voltage E [56]. The unusual part is that both the resistance and capacitance values are frequency dependent, and the magnitude of the impedance decreases with higher frequencies. Geddes proved in 1972 and 1975 that for the wet electrodes, the skin resistance is almost equal to the capacitance at any frequency with the ECG bandwidth [56, 66]. The input impedance of the recorder should be very high compared to the electrode polarization impedance.

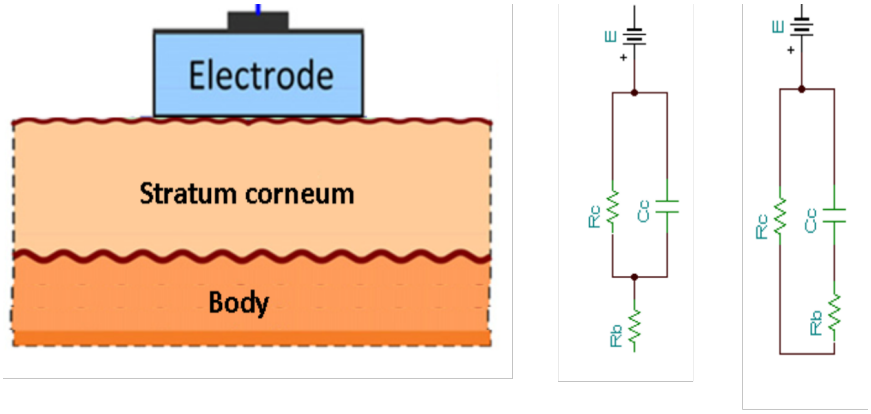


Figure 3.11: Equivalent circuit alternatives for the electrode/tissue interface. Where: R_b is the body resistor,R_c and C_c are skin resistor and capacitor respectively [56].

In order to measure the interface bioimpedance for the sensors used in this research, two devices were used: 1260 Impedance/gain-phase analyser and 1294 Bioimpedance interface. Both of the devices are manufactured by Solartron.

3.4.2 Impedance Measurements Setups

The 1260 impedance analyser was used to measure the electrode-skin impedance in a wide frequency range from 1 Hz to 1 MHz. However, the accuracy of the device is limited when the impedance is higher than 1 Mohm, as shown in Figure 3.12. Also, the 1260 analyser is not biocompatible to direct human applications. Therefore, the 1294 Bioimpedance interface was used, which acts as a buffer and increases the measurement accuracy for higher impedances while providing a human interface. In

addition to accuracy increase, the 1294 interface could be directly connected to a human through a biocompatible and safe interface.

The 1294 has two types of interfaces: (1) 1294A bio-impedance interface with IEC 601 connections which is used to measure the skin impedance layer, and (2) 1294B normal interface which is used to measure the impedance of dielectric materials. As suggested by the name, the bioimpedance interface protect the live subject from any excess current according to the IEC 602 standard. The IEC connections allow a maximum of ± 10 μA of a DC current and 10 mA (RMS) of an AC current. The graph of the measurement accuracy when using the 1294 bioimpedance interface is shown in Figure 3.13.

All the setups of the impedance measurements in this research were conducted using two terminal setup connections. For the skin/electrode impedance measurements, 1294A bio-impedance interface was used. For the dielectric materials impedance measurements, 1294B normal interface was used.

The setup of the measurements is shown in Figure 3.14, where the subjects were connected to 1294 interface via IEC 602 triaxial cables. Then 1294 interface was connected to the impedance amplifier via BNC cables. The 1260 Impedance analyser was connected to a computer via Keithly to USB (KUSB) cable and parallel port. The measurements results were displayed and imported using SMART software made by Solartron. This method was used to measure the skin impedance interface for the dry contact, and the impedance of the cotton towels, polyethelene and vinyl plastic bags which are used to wrap the newborns.

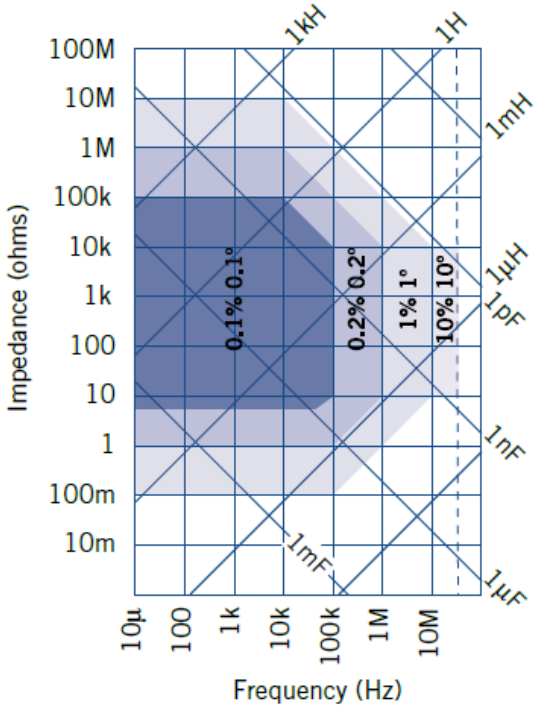


Figure 3.12: The impedance measurements accuracy graph for 1260 impedance/gain-phase analyser [113].

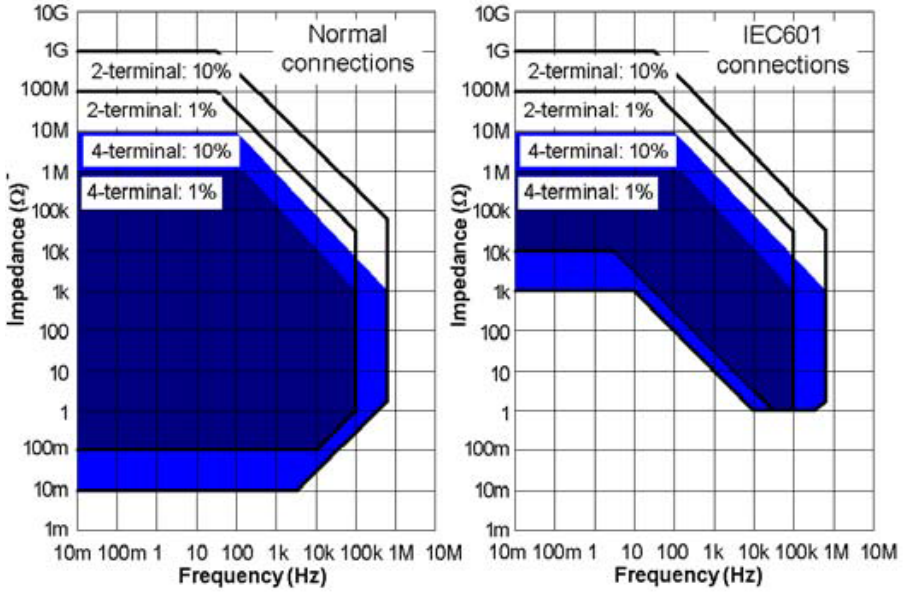


Figure 3.13: The impedance measurements accuracy graph for 1260/1294 combined system: the right side is 1294A bioimpedance interface, and the left side is 1294B normal interface [114].

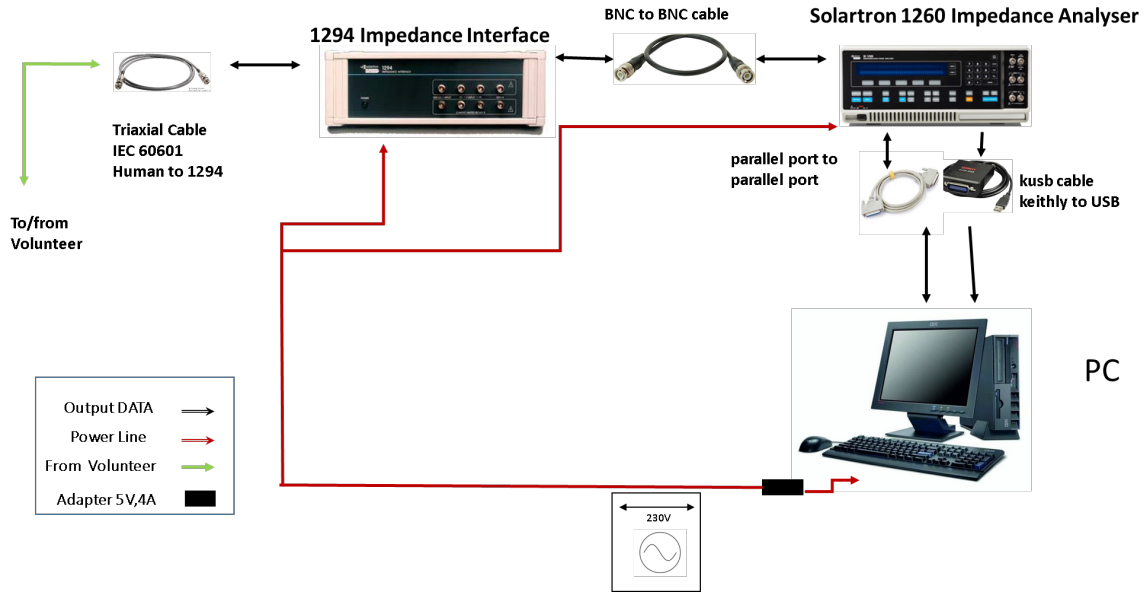


Figure 3.14: Bioimpedance measurement setup using 1260 impedance analyser and 1294 bioimpedance interface, with a desktop. Smart software provided by Solartron is used with hardware to collect measurements.

3.5 Heart Rate Detection Algorithm

Many techniques have been investigated in the literature to detect the heart rate from ECG signals. The features of the ECG are shown in Figure 3.15. Most of the available HR detection techniques are associated with QRS complex detection because the P and T detection is more difficult due to their relatively lower amplitude and their possible overlapping [115]. However, there are still no universal solutions for the QRS detection because of the wide range of QRS waveforms, ECG artefacts and the different medical abnormalities [116].

In this research, the QRS complex detection was used as the main feature for heart rate detection. The algorithm developed by Pan and Tompkins in 1985 for real-time QRS detection was used [117], where the heart rate is calculated from R-R intervals. Pan and Tompkins's algorithm was implemented using Matlab code. The block diagram of the implementation is shown in Figure 3.16.

The implemented algorithm was designed to calculate and update the heart rate every five seconds and was applied to sixty adult ECG recordings which were collected using the clinically approved monitor GE B450 in Section 3.3.5. The output of the heart rate detection algorithm was compared to the HR readings using GE B450 monitor. The deviation range between the HR calculated using the implemented algorithm (i.e. Pan and Tompkins algorithm) and GE B450 HR was $\pm 4\%$ when

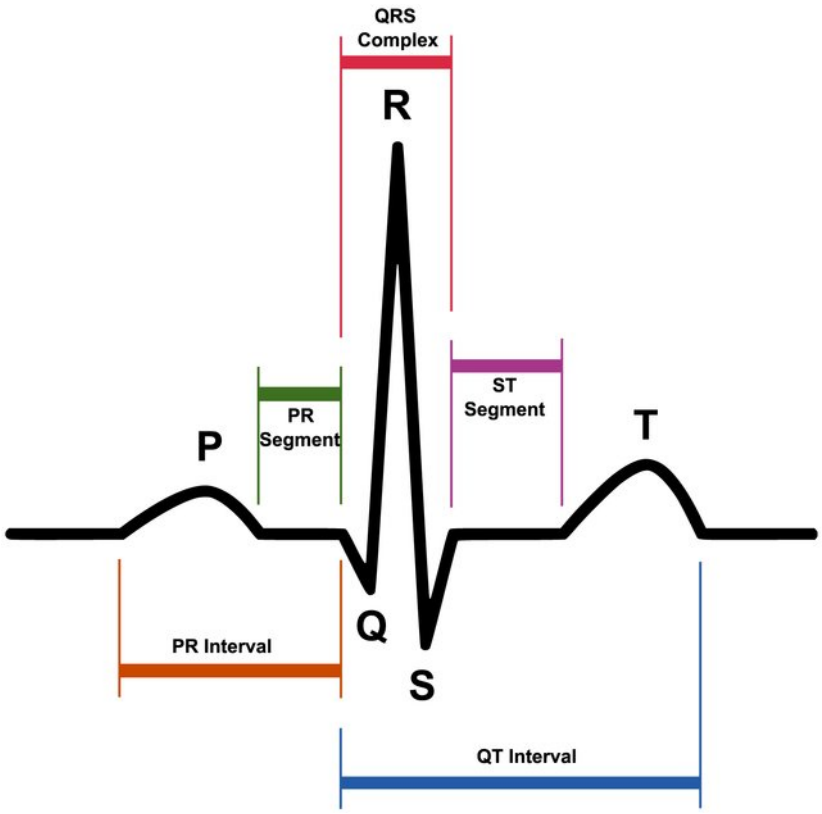


Figure 3.15: The features of ECG signals that are used for heart rate detection[115].

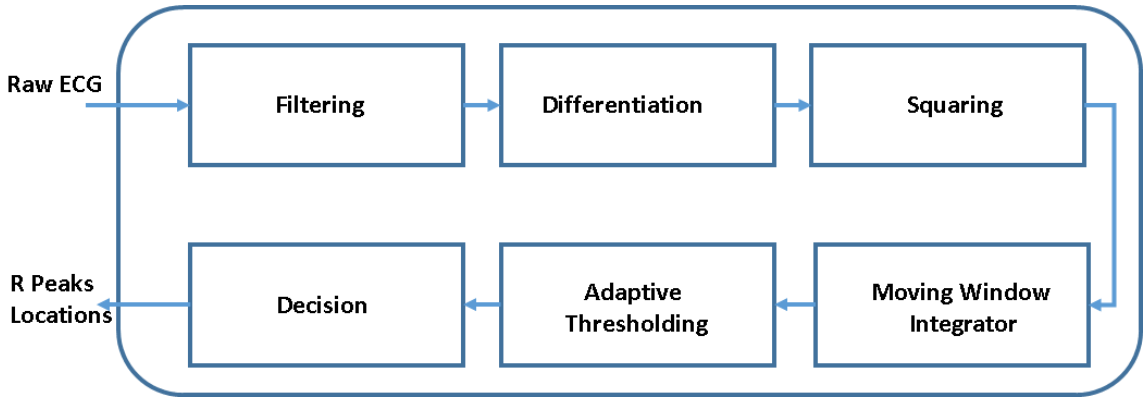


Figure 3.16: The block diagram of the implemented algorithm by Pan and Tompkins.

the ECG was stable. However, when there are motion artefacts, the algorithm HR calculations were more accurate than GE B450 monitor when compared to the visual calculations.

Chapter 4

Capacitive Sensors: Results and Discussion

4.1 Introduction

The conclusion from the literature review in Chapter Two suggested that the use of the ECG signal is the most accurate approach to estimate the heart rate of newborn babies. Moreover, it is often considered as a reference signal to evaluate other methods' reliability [8, 9, 32, 34, 55, 118]. However, the standard Ag/AgCl ECG sensors are not the ideal sensors to be applied to newborn babies in the delivery room because of the discomfort, delay for skin preparation and the scarring caused by applying the adhesive gel to newborns. These disadvantages have discouraged the use of the wet ECG sensors during resuscitation.

On the other hand, the dry and capacitive ECG sensors do not require gel application or skin preparation, as discussed in Chapter Two, which makes them a potential choice for the newborns' applications. The main challenge when applying dry/capacitive electrodes is to reduce the artefacts caused by the relative electrode motion or friction. Two types of ECG sensors were studied in this research to replace the Ag/AgCl sensors for the application of newborns' heart rate monitoring during resuscitation, capacitive ECG sensors and conductive fabric sensors. This chapter discusses the application of capacitive sensors (EPIC capacitive sensors made by Plessey), and the next chapter discusses the conductive fabric sensors. EPIC PS25101 sensors had been used in previous studies of wearable ECG monitoring devices [119], car seat HR monitoring [13] and even a helmet-based ECG recorder for motorcyclists [93]. Many papers have used EPIC sensors in capacitive setup and concluded that the sensors were able to couple capacitive ECG signals with good quality through cotton clothing with thickness up to 2.37 mm [93, 120]. They have also claimed that the

sensor could detect an ECG signal through 40 cm of air gap [120]. In this research, the EPIC sensors were introduced to couple the ECG signals through the dielectric materials that are used for swaddling the newborns in the delivery room.

The initially proposed placement for these capacitive sensors was to place an array of eight sensors in the mattress of the resuscitation table to collect four ECG signals simultaneously from the baby's back as discussed in Chapter Three, Section 3.2.2. The use of four ECG signals from different points of the body would reduce the effect of the motion artefacts and enhance the signal quality. However, before implementing this array setup, a pilot system was used to test the performance of the EPIC sensor when applied capacitively to adult and baby volunteers. As mentioned in the literature review in Chapter Two, the full-term babies are immediately cleaned after birth and swaddled in cotton towels. The preterm babies are wrapped into polyethylene or vinyl plastic bags without cleaning in order to protect them from heat loss and possible hypothermia [21,36,38]. Samples of the delivery room materials were brought from the Queens Medical Centre Hospital in Nottingham city, UK, in order to use them as a capacitive medium in the experiments tests. The thickness of the cotton towel sample was 2000 μm $\pm$10%, and the thickness of plastic bags was 10 μm $\pm$10% each.

Five experiments were conducted throughout this Chapter. The first experiment was designed to evaluate the performance of EPIC PS25201 when coupling the ECG signals in dry contact setup without skin preparation or applying a conductive gel. The second experiment was designed to test the ability of EPIC ECG sensors to couple the ECG capacitively through the cotton towels and plastic bags that are typically used in the delivery room. The outcomes of this experiment were negative. Therefore, the third experiment was designed to couple the ECG signals capacitively through thinner cotton sheets with different thicknesses of 254μm and 355 μm. This experiment aimed to investigate the application of the capacitive sensors in the neonatal intensive care unit, where the newborn babies are usually kept without clothing and in supine or prone positions [19]. The pilot system used for the setups mentioned above used two EPIC sensors to generate a single ECG signal during the recordings.

However, in the fourth experiment, eight EPIC sensors were used to collect four capacitive ECG signals simultaneously through the clothing. The array system used in this experiment was further discussed in Chapter Three, section 3.2.3. Finally, the fifth experiment was designed to measure the electrode's impedance for the dry and capacitive contact setups in order to model the skin interface and simulate the output ECG signal.

All the ECG recording experiments in this chapter were conducted firstly on seven adult volunteers and then on three baby volunteers of age: 8, 15 and 42 weeks. The heart rate was extracted from the ECG signals using the QRS detection algorithm that was based on Pan and Tompkins method [117], which was further discussed in Chapter Three, Section 3.5. The quality of the recorded ECG signals was quantified by the QRS accuracy detection. The accuracy was calculated visually from the missed R peaks and the duration of the motion artefacts if the QRS was not visible. The ECG recorded from the same volunteer in different setups were compared in terms of signal to noise ratio and the robustness against motion artefacts. The different setups of the adults and babies experiments are described in the next sections and compared to simulated models' outputs.

4.2 The Experimental Setup of Dry/Capacitive Contact

It has been shown earlier that the newborn babies in the delivery room are swaddled in either plastic bags or cotton towels in order to control their bodies' temperature. According to the medical guidelines, the newborn must be kept warm immediately after birth and throughout the resuscitation procedure, leaving only the face and forearms skin area accessible for direct skin contact. Therefore, the EPIC capacitive sensors were proposed to couple the ECG signal through the cotton towels and plastic bags.

Two sensors were used to collect ECG signals from adults wrists and babies' backs in both dry and capacitive contact. For the baby volunteers, the EPIC sensors were placed on a mattress to collect the ECG signal, as shown in Figure 4.1. The babies' backs were chosen for the sensors' placement because the active capacitive sensors are bulkier than the standard wet sensors, and it would be difficult to attach them to hands or legs with straps or stretchy bands. Additionally, when the sensors are placed under the back, the baby weight pressure would hold the sensor contact and reduce the artefacts.

For adult volunteers, the EPIC sensors were placed on a wooden desk and under the volunteer's wrists, as shown in Figure 4.1. The volunteers were asked to relax and not press down onto the sensors. The wrists were chosen to record the ECG signals from adult volunteers because their weight pressure on the sensors is closer to the pressure caused by newborns back. The wrists are also accessible for dry/capacitive ECG recordings; the hands were ruled out because their skin is naturally developed

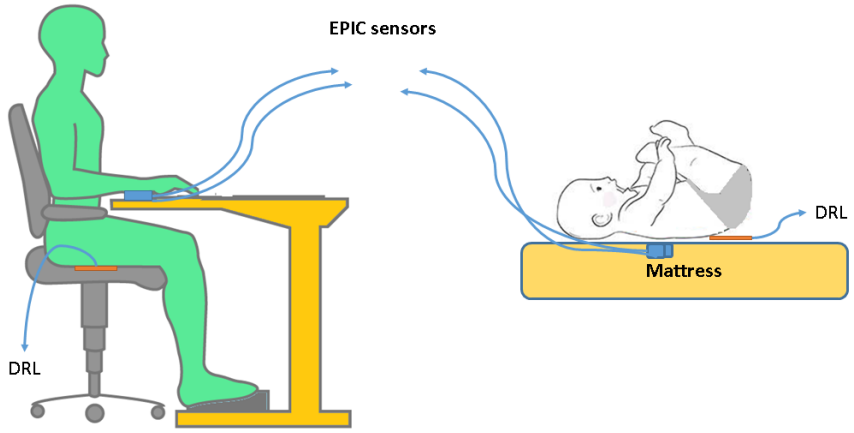


Figure 4.1: The setup of dry/capacitive coupling to record ECG signal from adult's wrists and baby's back.

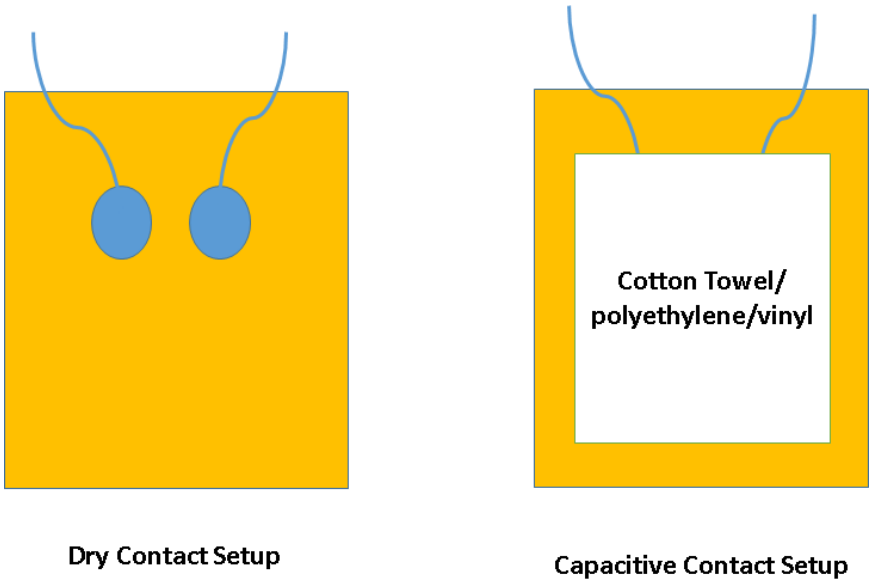


Figure 4.2: The dielectric material (cotton towel, polyethylene or vinyl) was placed on top of the sensors in the capacitive coupling.

to be harder than the rest of the body. The sensors' placement for babies and adults are further discussed in Chapter Three, Section 3.2.2.

The driven right leg (DRL) used with the ECG recording system was made of conductive fabric and was placed under the bottoms of babies and adults in order to reduce the mains power interference. Figure 4.2 shows the placement of the dielectric material on top of the EPIC sensors for capacitive ECG coupling. The dielectric materials used for the delivery room capacitive setup were: cotton towels with 2000 μm of thickness, polyethylene and vinyl plastic bags with 10 μm of thickness each. Additionally, two cotton sheets were used with a thickness of 254 μm and 355 μm.

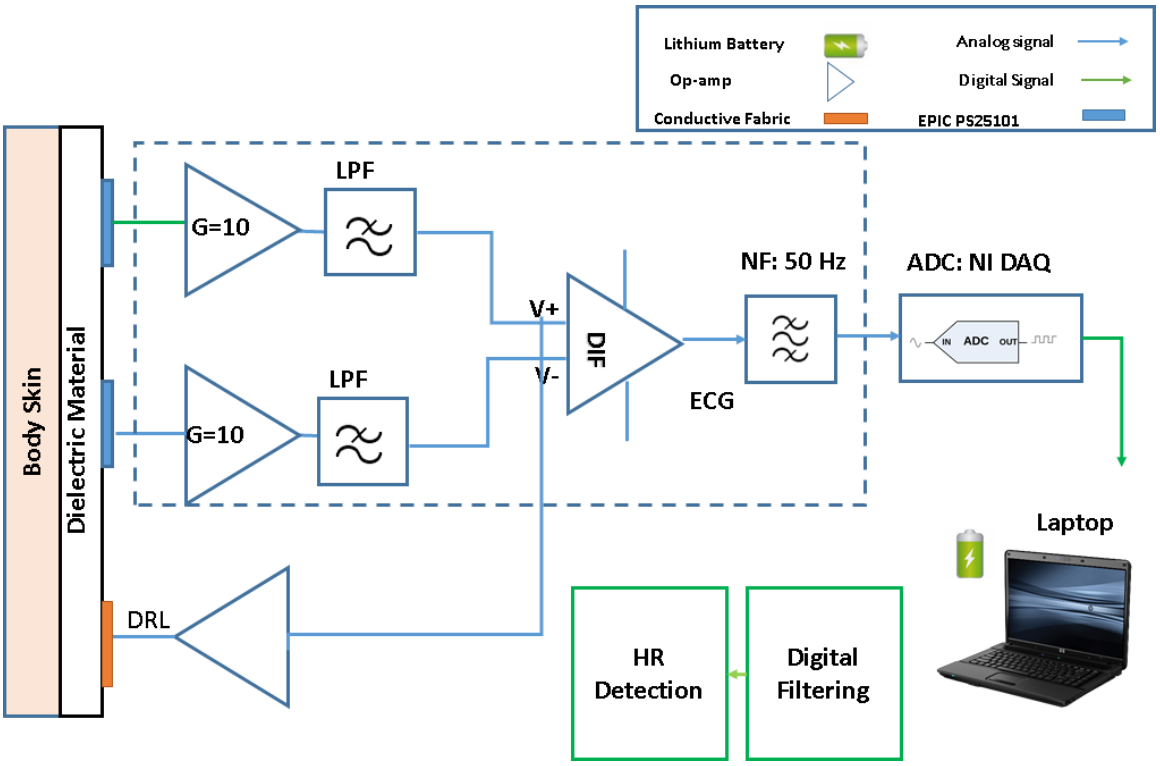


Figure 4.3: The ECG acquisition system using two EPIC sensors and a DRL (conductive fabric).

The system used for ECG acquisition is shown in Figure 4.3, where two EPIC sensors were used to collect the ECG signals in either dry or capacitive contact. The analogue ECG signal was amplified and filtered by anti-aliasing and low pass filtering of 35 Hz and digitised using a 6008 DAQ (National Instruments). The signal was digitised at 16-bits per sample and a $1k$ sample per second rate and sent to a laptop over a USB for storage and further digital processing by Labview and Matlab. The laptop was disconnected from the mains during the recording in order to decrease the

power line interface. The ECG circuit schematic of the ECG acquisition system is further discussed in Section 3.2.3.1.

The digital ECG signal was collected by Labview and further processed by Matlab using a bandpass filter with cut-off frequencies of 0.5 Hz and 35 Hz. After that, the signal was filtered by a derivative filter and squared to calculate the adaptive thresholds of the signal and noise to detect the QRS complex, the most dominant feature of the ECG signal. These steps were adapted from Pan and Tompkins algorithm [117] and modified to accommodate the dry and capacitive ECG signals with expected high motion artefacts, the algorithm was further discussed in Chapter Three, Section 3.5.

4.3 The Dry Contact Coupling

In the dry contact experiment, the EPIC sensors were applied directly to the volunteers' skin without applying a conductive gel on the skin. The dry experimental setup was designed to evaluate the quality of the ECG signals collected by EPIC sensors without skin preparations. For the adult volunteers, two sensors were placed on a wooden desk, and the adult volunteers were asked to place their wrists on top of the sensors. For the baby volunteers, two EPIC sensors were used to record the ECG signals from three babies' backs in dry contact with skin, as shown in Figure 4.1. The parents of the baby volunteers were asked to bring their baby's mattress for the experiment. The sensors were firstly placed on the mattress, and then the babies were placed on top of the sensors.

4.3.1 Adult Volunteers Results

The ECG signal was recorded from wrists of seven adult volunteers for five minutes each, using EPIC sensors in dry contact. The adult volunteers were asked to gently shake their wrists and fingers once every minute during the recording without moving their wrists completely from the sensors in order to test the performance of the system when handling motion artefacts.

Figure 4.4 shows a representative sample of the collected data from one adult volunteer. The figure shows the ECG signal after the digital filtering, where the motion noise and the DC baseline of the raw signal were filtered out by a digital bandpass filter 0.5 Hz-35 Hz. In the beginning of the ECG recording, the signal took about five seconds to settle down, as shown in Figure 4.6. On average, the ECG signals collected from the adults took between five and ten seconds before settling down. The adults' ECG signals were generally robust against the motion artefacts

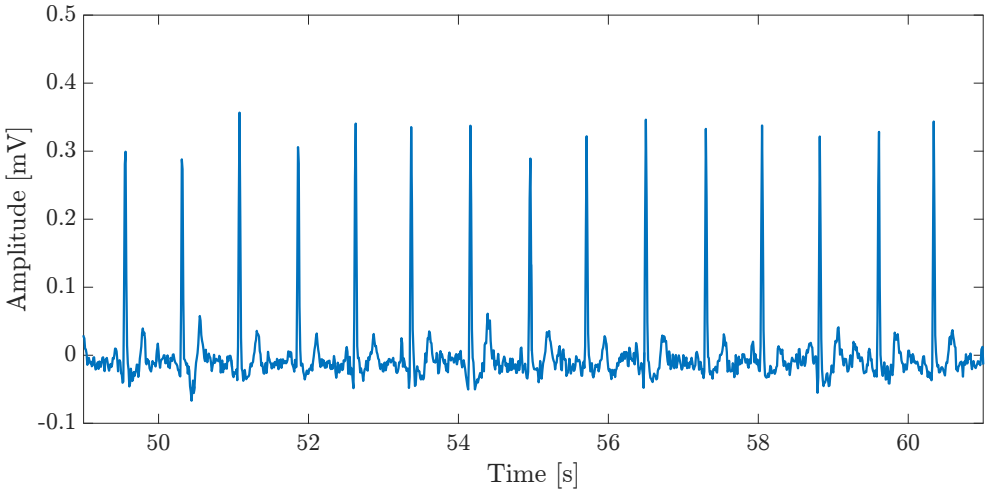


Figure 4.4: Sample of the ECG signal recorded from adult's wrists in dry contact using EPIC PS25101 using the data acquisition system shown in 4.3.

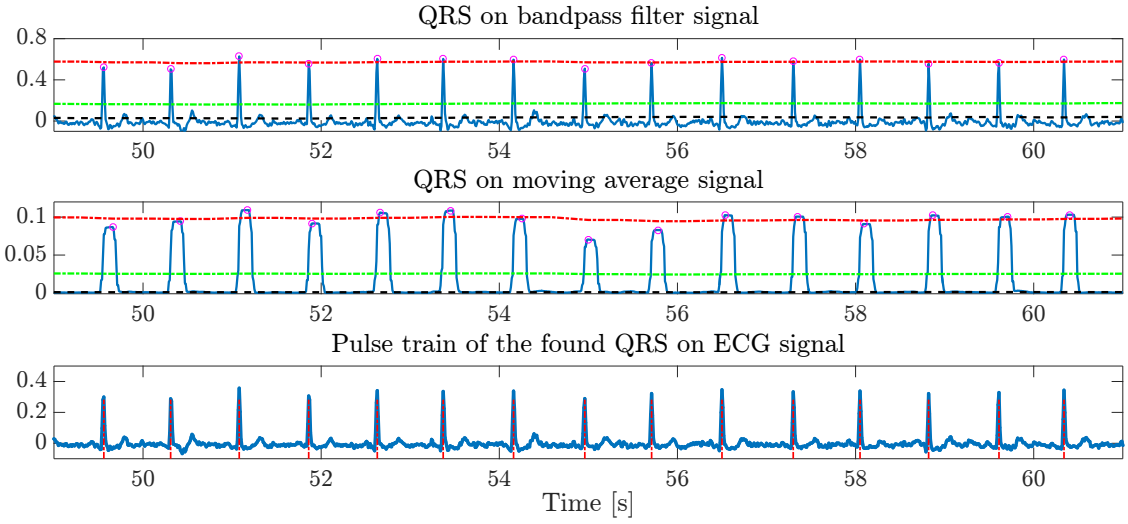


Figure 4.5: Sample of QRS detection on adult ECG signal collected from wrists in dry contact. It shows the detected QRS on bandpass, moving average raw ECG signals with noise level (Black), signal level (Red) , adaptive threshold (Green) and the QRS detection (Pulse train).

created intentionally by the volunteers during the recording as shown in Figure 4.7. This volunteer was asked to gently shake her wrists for five seconds (295−300 seconds).

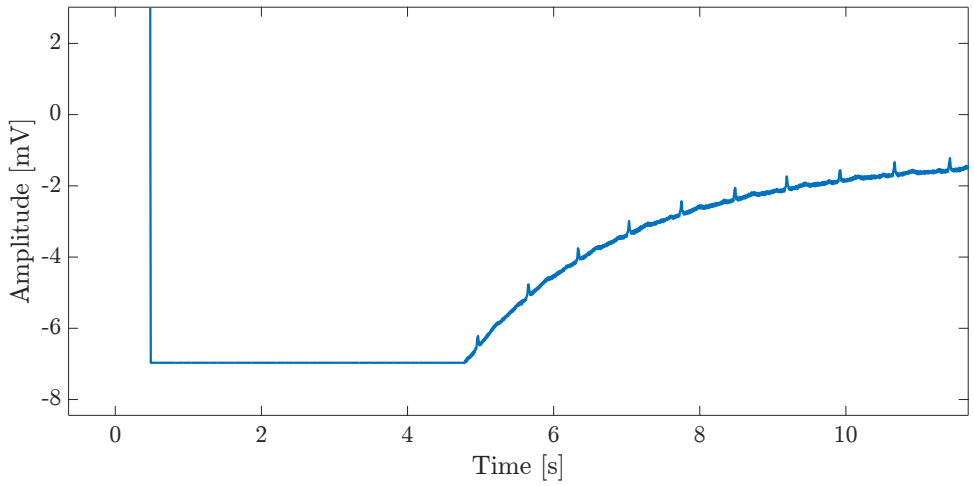


Figure 4.6: The capacitive ECG signal takes few seconds at the beginning to settle down.

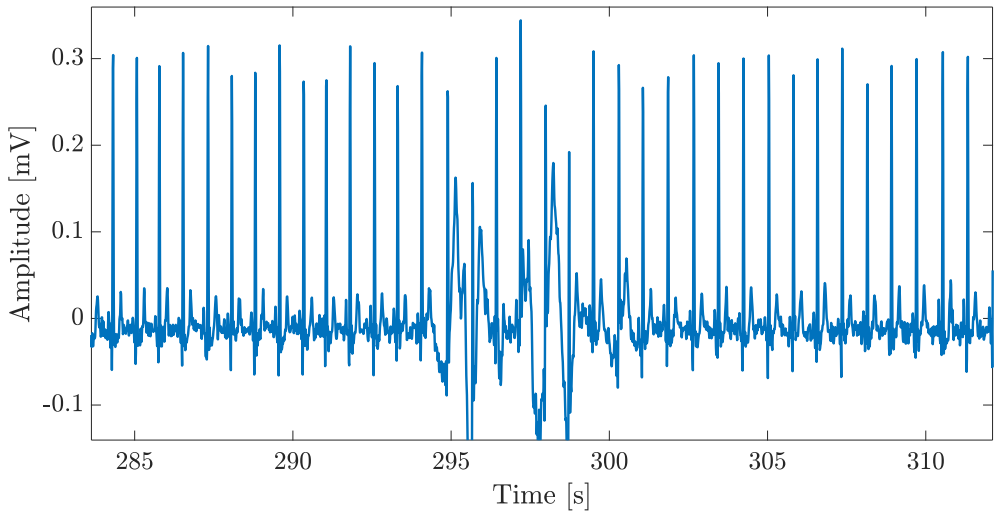


Figure 4.7: Sample of the introduced motion artefacts, when the volunteers were asked to shake their wrists gently for five seconds.

The QRS peaks were the dominant feature of the ECG and were easily recognised in both raw and filtered signal. The ECG signal was then processed by the QRS algorithm detection to extract the heart rate of the volunteer. Figure 4.5 shows a sample of the QRS algorithm outputs and the adaptive thresholds of signal and noise. The peaks above the green line were detected as R peaks, 100% of the QRS peaks

in this volunteers data were detectable, and no QRS was missed. One minute of this volunteer data is shown in Appendix B. The percentages of the detectable QRS of the ECG signals collected from adult volunteers signals are shown in Table 4.1 at the end of this section. On overage, 99.84% of adults' dry contact ECG was successfully detectable.

4.3.2 Baby Volunteers Results

Two EPIC sensors recorded five minutes of ECG data from the baby volunteers backs; the sensors were placed just under the shoulders to secure better contact. The collected ECG data was then filtered, digitised and processed by the QRS detection Matlab code. As mentioned earlier, the ages of the babies were 8, 15 and 42 weeks. The ECG signal recorded from the eight weeks baby had the least motion artefacts interference compared to the other two babies because the baby movement was limited. A representative sample from the eight weeks baby's ECG is shown in Figure 4.8.

As shown in the figure, the baby's heart rate was very high compared to an adult's. This was expected since the typical heart rate of the babies under 78 weeks is between $80 - 130$ bpm [105]. Parts of the signal were noise and affected by the motion artefacts, as shown in Figure 4.10. The three ECG signals collected from the babies were processed using the QRS detection algorithm. A representative sample of the eight weeks baby processed ECG signal after the QRS detection is shown in Figure 4.9. For this baby volunteer, 93% of the ECG signal was detectable. The undetectable 7% of the data was mainly dominated by the motion artefacts. On average, 89% of the babies signals were detectable. For the older babies, the ECG signal was more affected by the motion artefacts, because their muscles were stronger and they were able to move their backs.

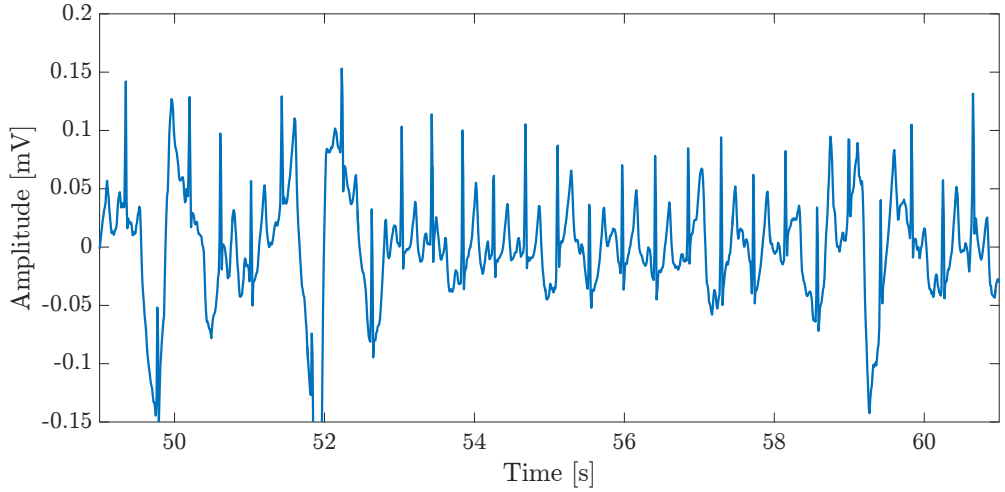


Figure 4.8: Sample of ECG signal recorded from eight weeks baby's back in dry contact using EPIC PS25101 and the data acquisition system shown in 4.3.

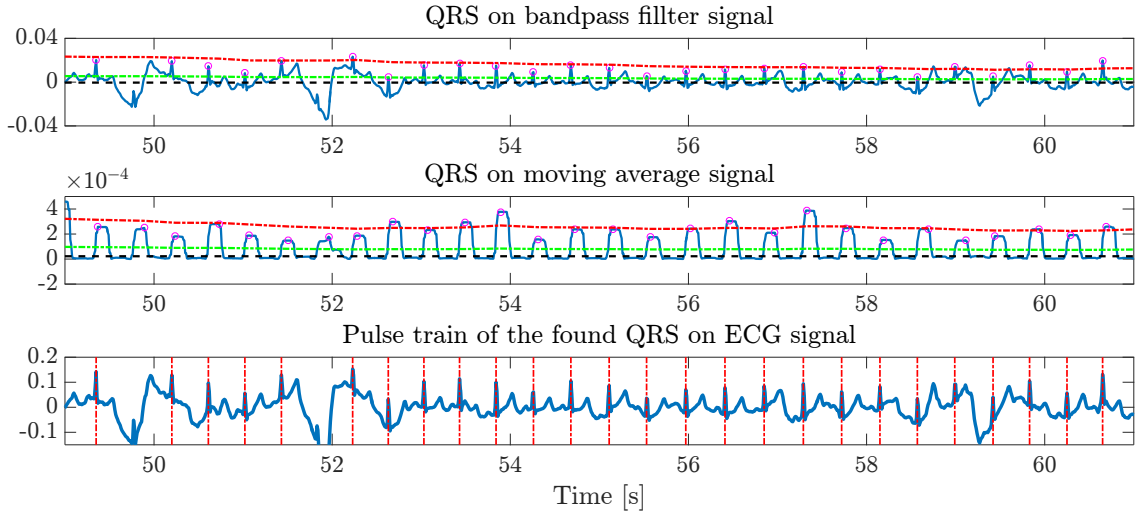


Figure 4.9: Sample of QRS detection on baby ECG signal collected in dry contact from the back. It shows the detected QRS on bandpass, moving average raw ECG signals with noise level (Black), signal level (Red) , adaptive threshold (Green) and the QRS detection (Pulse train).

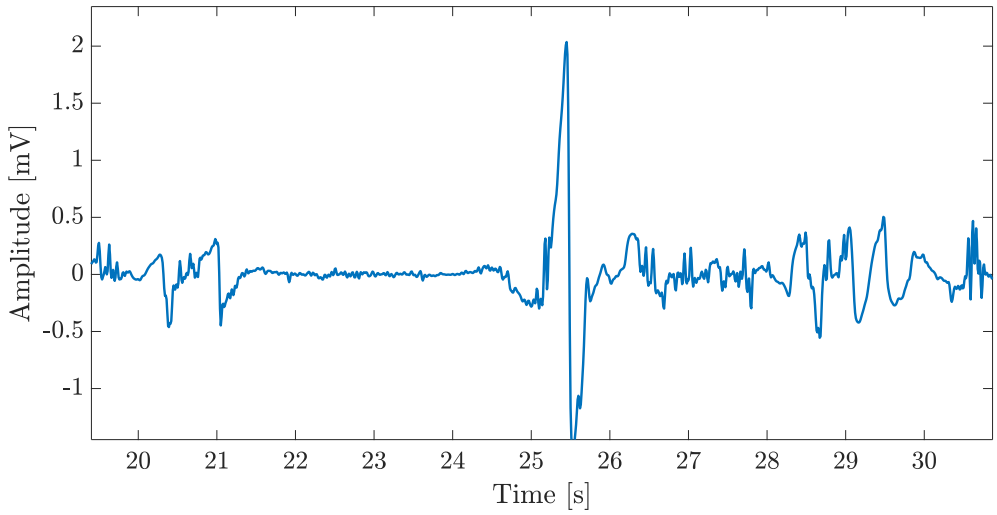


Figure 4.10: Sample of baby ECG signal distorted by motion artefacts.

4.3.3 Summary

The accuracy of the QRS detection on the adult and baby volunteers are shown in Table 4.1. The average accuracy for adults' ECG was 99.87%, and the minimum one was 99.3%. All of the babies were crying during the recording and moving their limbs, so their ECGs were heavily affected by the motion artefacts introduced by their mobility, crying and respiration rate. However, the average QRS detection accuracy of babies' ECG was still acceptable of about 89.33%. The deviation of the ECG quality was very high, because of the age difference, which has huge impacts on babies mobility. As the age of the baby increased, the baby's ability to move increased, and as a result, the detection accuracy decreased. The accuracy for the eight weeks baby was 93%, and the accuracy for newborns is expected to be more since they would not be able to move. The samples of the data shown in this section were part of the ECGs highlighted in yellow colour in table 4.1. One minute of the eight weeks ECG data is in Appendix B.

It was shown earlier, that the dry ECG signal collected using EPIC sensors took a few seconds, in the beginning, to settle down. This transient effect happened every time after the sensors were separated from the volunteers' skin. The reason for that is EPIC bandwidth of 0.2 Hz - $10k$ Hz; which makes the sensor act as a high pass filter. However, the settling time of EPIC sensors was relatively small compared to the average delay in capacitive sensors of 15 seconds [68]. The reason for this relatively faster response is EPIC sensor design. The lower cut off frequency of the sensor was designed to be 0.2 Hz instead of the recommended 0.05Hz. This design would distort

Volunteers gender/age	Sensors position	QRS detection percentage
Female 25Y	wrists	100%
Male 29Y	wrists	99.6%
Male 28Y	wrists	100%
Male 33Y	wrists	100%
Male 24Y	wrists	100%
Female 29Y	wrists	100%
Male 30Y	wrists	99.3%
Female 8W	back	93%
Male 4M	back	91%
Female 11M	back	84%

Table 4.1: QRS detection accuracy of ECG signals collected in dry contact from adults' wrists and babies' backs using PS25101 sensors. Samples of the yellow colour rows data were shown in this chapter and Appendix B.

the ECG signal for the diagnosis applications, but since the ECG signal is only used for the HR detection in this application, the minor distortion would not impact the results.

4.4 The Capacitive Coupling Through The Delivery Room Materials

As explained earlier, the newborns are wrapped immediately after birth with cotton towels or plastic bags, in order to prevent them from becoming hypothermic. There are no rules in the medical guidelines to specify the type of plastic bag used in the

delivery rooms to keep the babies warm, but many papers refer to using two types of plastic bags: vinyl and polyethylene [21, 37].

This experiment was designed to test the possibility of collecting ECG signals from babies through the cotton towels and plastic bags used in the delivery rooms. The cotton towels are made of 100% cotton, and their thickness was 2000 μm.The polyethylene plastic bag used in this experiment was made of Low-Density polyethylene (LDPE) while the vinyl plastic bag was made of Ethylene-vinyl Acetate (EVA). They would be identified in this chapter as polyethylene and vinyl plastic bags. The thickness of both plastic bags was 10 μm.

The experimental setup shown previously in Figures 4.1 and 4.2 was used for this experiment as well. For adults, the sensors were placed on top of a desk and were covered by a towel or plastic bag, and the volunteers were asked to put their wrists comfortably on top of the covered sensors. The ECG signal was recorded from seven adult volunteers capacitively through the cotton towel and the two plastic bags.

For babies, the sensors were placed on the baby's mattress and covered by the cotton towel or plastic bag, then the baby's bare back was placed on top of the covered sensors. The ECG signal was recorded from each of the three baby volunteers for five minutes. The age of the babies at the time of the experiment was: 8 weeks, 15 and 42 weeks.

4.4.1 Adult Volunteers Results

The materials were used separately with each volunteer as a dielectric medium between the sensors and the volunteer's wrists. The capacitively coupled signals were very noisy and vulnerable to motion artefacts from respiration. After further processing by Matlab, the R peaks were not identified in any of the volunteers' signals, collected through the cotton towel or the polyethylene plastic bag as shown in Figures 4.14 and 4.13. However, the R peaks were identified among five of ECG signals that were coupled through the vinyl bag. A sample of the ECG signal recorded from adult wrists through the vinyl plastic bag is shown in 4.11. As shown in the figure, the QRS peaks of the volunteer ECG signal could be seen, but the noise was very high compared to the dry contact ECG signal. The adults ECG through the vinyl plastic bag was processed by Matlab in order to extract the heart rate. The QRS detection accuracy of these signals was very low compared to the signals collected in the dry contact setup. A sample of the output of the Pan and Tompkins algorithm is shown in Figure 4.12. As it can be shown in the figure, some of the artefacts were mistakenly

identified as R peaks by the QRS detection algorithm. One minute recording of this ECG data is shown in Appendix B.

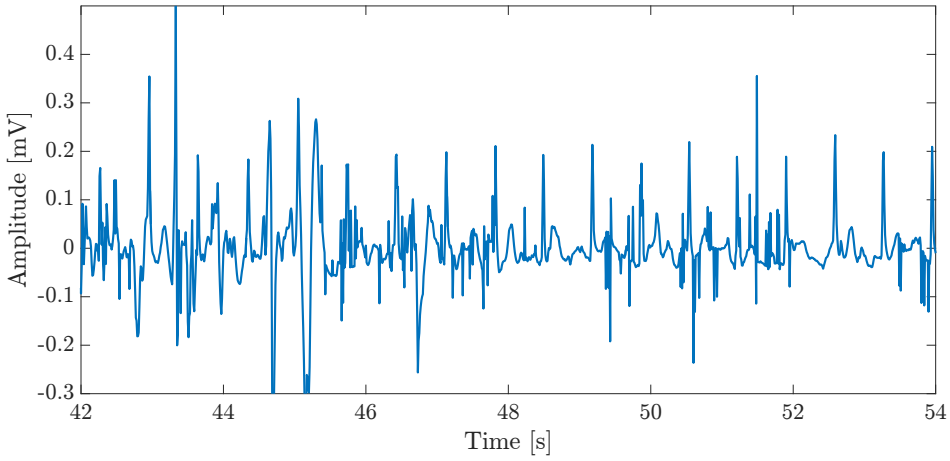


Figure 4.11: Sample of ECG signal recorded from adult's wrists capacitively through the vinyl plastic bag, using EPIC PS25101 and the data acquisition system shown in 4.3.

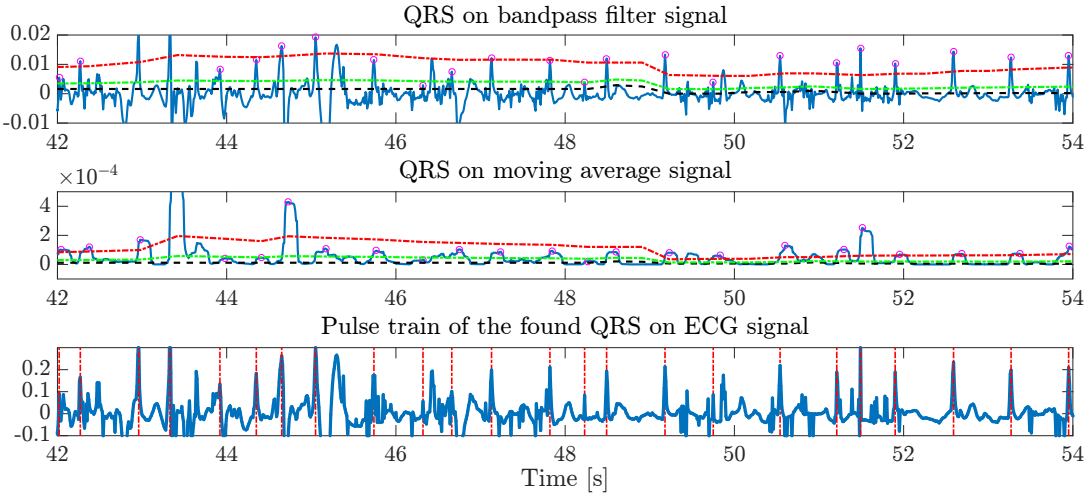


Figure 4.12: Sample of QRS detection on adult ECG signal collected from wrists capacitively through the vinyl plastic bag. It shows the detected QRS on bandpass, moving average raw ECG signals with noise level (Black), signal level (Red) , adaptive threshold (Green) and the QRS detection (Pulse train).

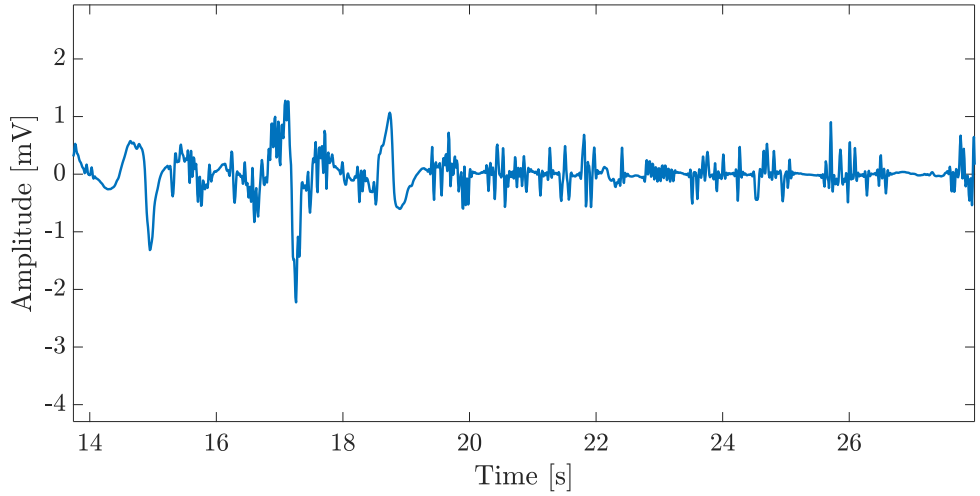


Figure 4.13: Sample of the signal collected from adult's wrists volunteer through polyethylene with no detectable ECG features.

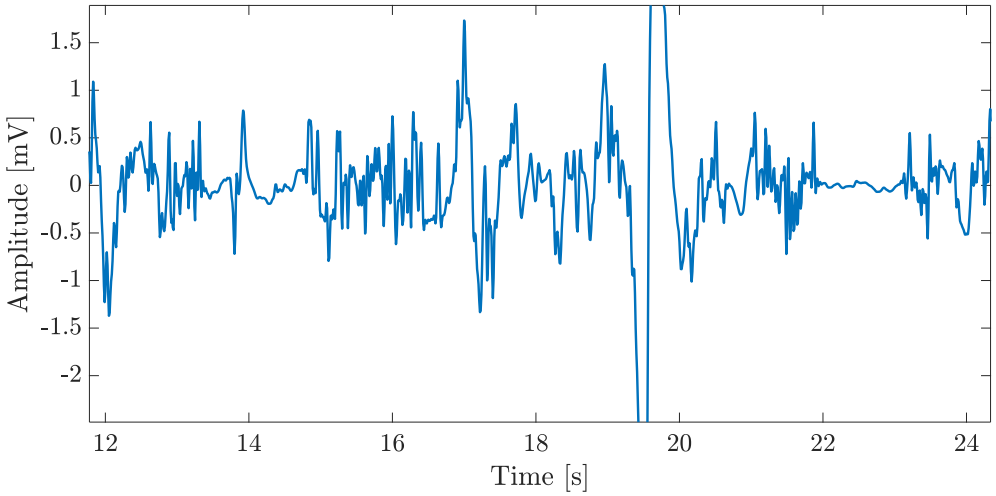


Figure 4.14: Sample of the signal collected from adult's wrists through cotton towel with no detectable ECG features.

4.4.2 Baby Volunteers Results

In this experiment, a pair of EPIC sensors were placed on the baby volunteer's mattress. The sensors were covered with a plastic bag or cotton towel, and the baby volunteer was placed on top of the covered sensors with his/her bare back, as illustrated previously in Figure 4.1. The plastic bags used for baby volunteers were the same type of bags used for adults: polyethylene and vinyl plastic.

The signals were collected from three different babies of ages: 8, 14 and 42 weeks. No ECG signals could be identified from any of the babies. The nine signals were processed by the QRS detection algorithm, and the algorithm only detected meaningless artefacts peaks. Samples of the recorded signals are shown in Figures 4.15, 4.16 and 4.17.

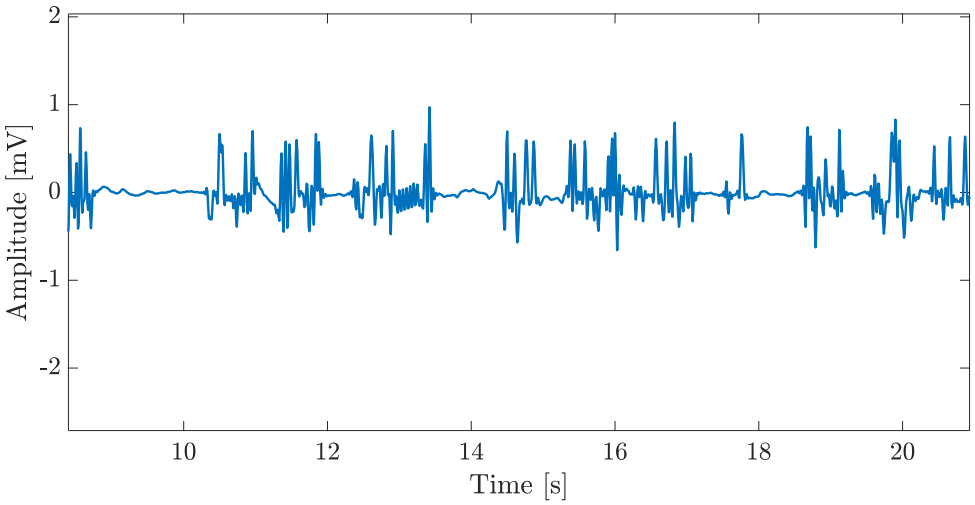


Figure 4.15: Sample of the signal collected from baby's back through vinyl with no detectable ECG features.

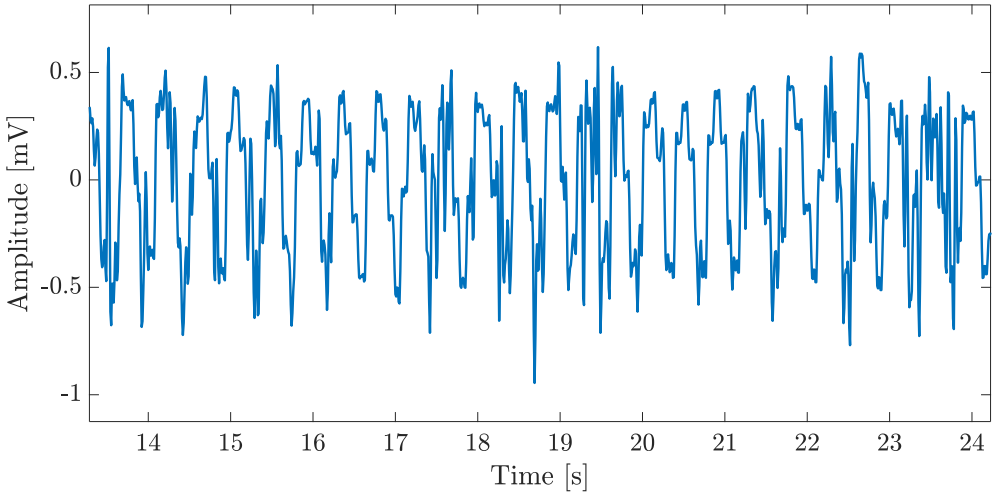


Figure 4.16: Sample of the signal collected from baby's back through polyethylene with no detectable ECG features.

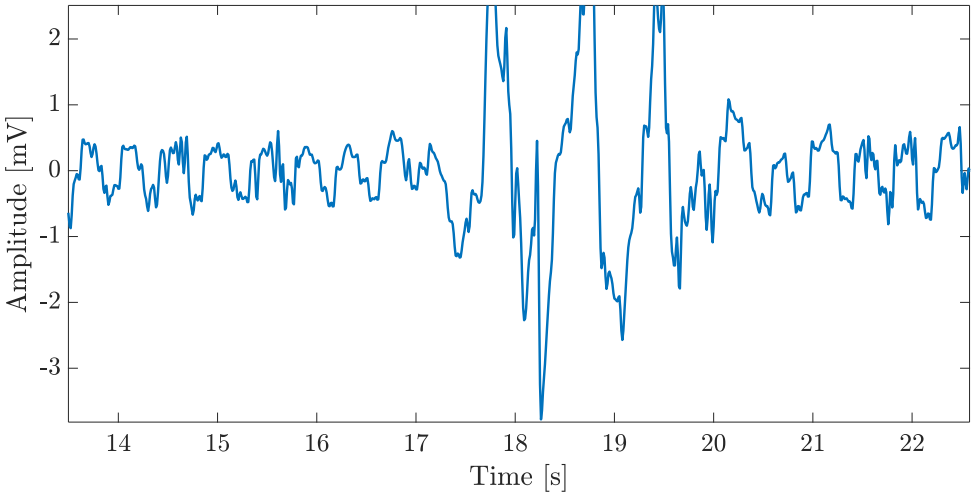


Figure 4.17: Sample of the signal collected from baby's back through cotton towels with no detectable ECG features.

4.4.3 Summary

The capacitive sensing of ECG signals was performed using a cotton towel, vinyl and polyethylene plastic bags which were provided by the Queens Medical centre in the city of Nottingham. The experiment was performed on seven adults and three babies. Five of the adult signals were coupled through vinyl plastic and recognised as ECG signals. The QRS peaks were detected among those five signals, although many R peaks were not detected due to low signal to noise ratio. On the other hand, all the signals coupled through polyethylene bags or cotton towel were not recognised as ECG.

The capacitively coupled signals collected from the babies were not identified as ECG signal. The QRS were not visible within the nine collected signals. Table 4.2 summarises the results of the capacitive ECG coupling through the cotton towel and plastic bags. Based on these findings, the capacitive coupling ECG in the delivery room using EPIC sensors is not likely applicable. However, more experiments were conducted in order to evaluate the sensor performance through thinner sheets. This setup might be of interest for the HR monitoring in the neonatal intensive care, where the newborns are kept with minimal clothing inside the incubators.

Volunteers gender/age	Sensors position	Vinyl QRS detection	Polyethylene QRS detection	Cotton towel QRS detection
Female 25Y	wrists	69.2%	–	–
Male 29Y	wrists	72.1%	–	–
Male 28Y	wrists	–	–	–
Male 33Y	wrists	61.0%	–	–
Male 24Y	wrists	–	–	–
Female 29Y	wrists	58.4%	–	–
Male 30Y	wrists	70.6%	–	–
Female 8W	back	–	–	–
Male 4M	back	–	–	–
Female 11M	back	–	–	–

Table 4.2: QRS detection accuracy in ECG signals collected capacitively though vinyl, polyethylene and cotton towels; from adult and baby volunteers using PS25101 sensors. Samples of the yellow colour row data was shown in this chapter and Appendix B.

4.5 Capacitive Coupling Through Cotton Sheets

As shown in the previous section, EPIC sensors were not able to couple ECG signals through cotton towels or polyethylene plastic bags. Some of the signals were coupled through the vinyl bags and recognised as ECG signal, but with a low detection accuracy, compared to the dry contact ECG.

The experiments in this section were designed to test the possibility of coupling ECG signal through thinner cotton sheets using EPIC sensors. EPIC sensors have been used in the literature to couple ECG signals through sweaters and cotton shirts [121]. The EPIC sensors were used in this experiment to couple ECG through two different cotton sheets of a thickness of 254 μm and 355 μm$\pm$10%.

The capacitive setup was similar to the dry contact setup in the previous section and was also performed on seven adults and three babies of 8, 15 and 42 weeks. The experimental setup was the same as the previous experiments, where the ECG signal was collected from the adults' writs and babies' backs, as shown in Figures 4.1 and 4.2. For adult volunteers, the sensors were placed on a desk and then covered by a cotton sheet before asking the volunteers to place their wrists on the covered sensors. For baby volunteers, the sensors were placed on the baby's mattress and then covered by a cotton sheet before placing the baby's bare back above the covered sensors. After collecting the ECG for five minutes, the 254 μm cotton sheet was replaced by 355 μm cotton sheet.

4.5.1 Adult Volunteers Results

In this experiment, two cotton sheets with thicknesses of 254 μm and 355 μm were used to cover the capacitive sensor. The ECG signal was collected capacitively through these cotton sheets from seven adult volunteers for five minutes each and was then processed offline using the QRS detection algorithm in Matlab.

Recognisable ECG signals were coupled through both of the cotton sheets; representative samples of these ECGs are shown in Figures 4.18 and 4.20. The ECG QRS peaks were visible in both cases, but the signal coupled through the thicker fabric was more distorted by noise and motion artefacts.

The QRS detection accuracy of the thin cotton sheet was higher than the thick cotton sheet as expected. Representative samples of the detected QRS peaks through 254 μm and 355 μm are shown in Figure 4.19 and Figure 4.21 respectively. One minute recording of these samples' signals are shown in Appendix B. The calculated

accuracy of QRS detection of ECG signals collected from adult volunteers through cotton sheets are summarised in Table 4.3 at the end of this section.

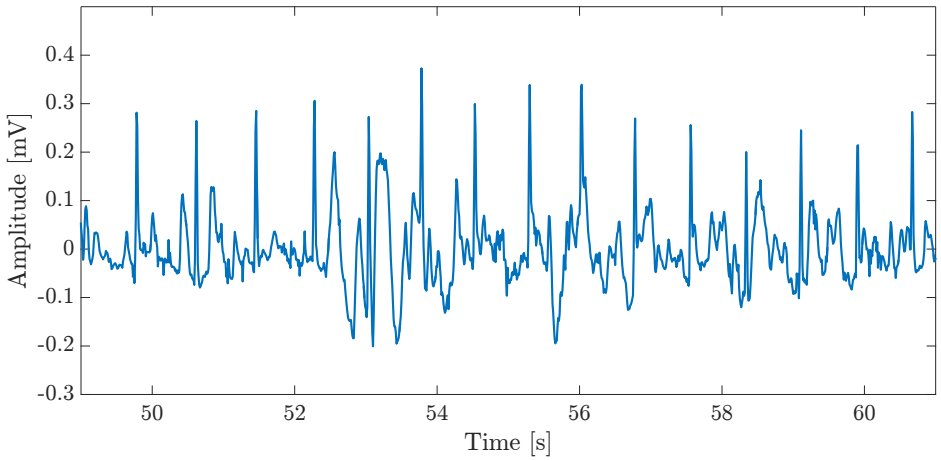


Figure 4.18: Sample of ECG signal recorded from adult's wrists capacitively through 254 μm cotton sheet, using EPIC PS25101 and the data acquisition system shown in 4.3.

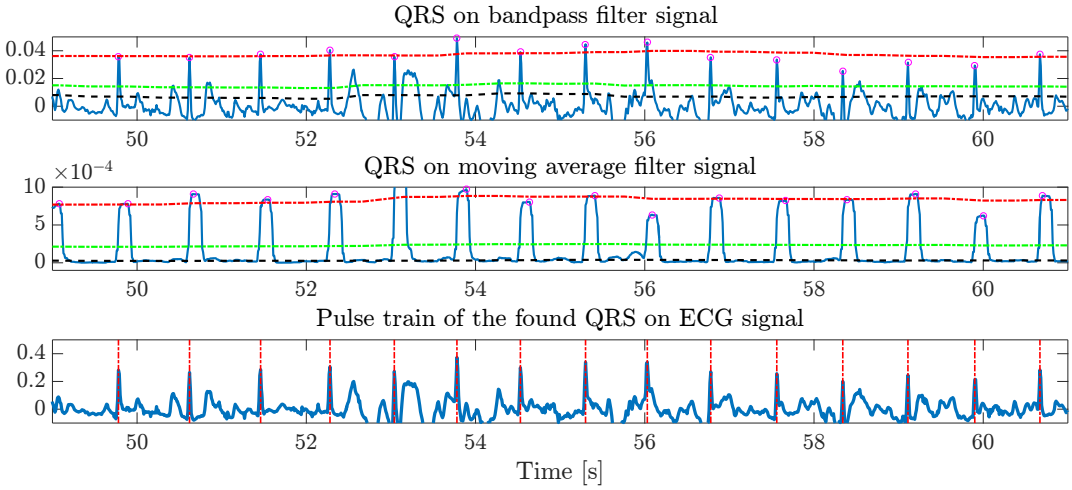


Figure 4.19: Sample of QRS detection on adult ECG signal collected from wrists capacitively through 254 μm cotton sheet. It shows the detected QRS on bandpass, moving average raw ECG signals with noise level (Black), signal level (Red) , adaptive threshold (Green) and the QRS detection (Pulse train).

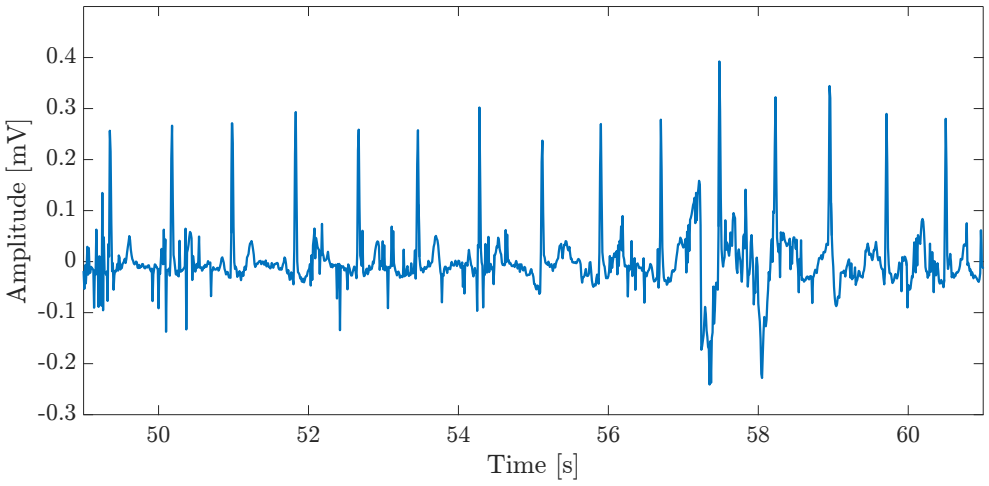


Figure 4.20: Sample of ECG signal recorded from adult's wrists capacitively through 355 μm cotton sheet, using EPIC PS25101 and the data acquisition system shown in 4.3.

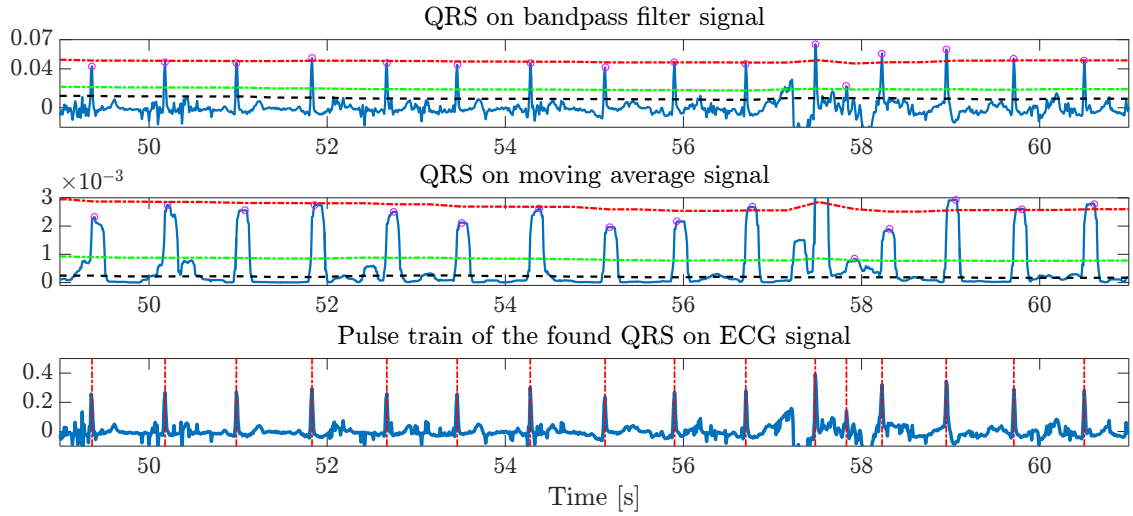


Figure 4.21: Sample of QRS detection on adult ECG signal collected from wrists capacitively through 355 μm cotton sheet. It shows the detected QRS on bandpass, moving average raw ECG signals with noise level (Black), signal level (Red) , adaptive threshold (Green) and the QRS detection (Pulse train).

4.5.2 Baby Volunteers Results

In this experiment setup, two Plessey sensors were placed on the babies' mattresses, which were brought by the parents and covered by cotton fabric. Then the babies were put on top of the cotton fabric without wearing any clothes apart from their nappies. The sensors collected the signals from babies' bare backs capacitively through the cotton sheets with a thickness of 254 μm and 355 μm. Five minutes of ECG recordings were collected from each baby.

The ECG morphology was recognised within the signals that were coupled capacitively through 254 μm sheet. They were affected by the noise and motion artefacts more than the dry contact ECG signal, but the R peaks were still recognised by the naked eye among most of the signal. A sample of ECG signal collected capacitively through 254 μm cotton sheet, from an eight weeks baby volunteer, is shown in Figure 4.22. The babies were not comfortable and cried through the experiments. The quality of ECG signal recorded from the youngest baby of eight weeks was the best because the older babies had more muscles and hence introduced more motion artefacts. The QRS peaks have been detected in the collected ECG signals using the QRS detection algorithm. A sample of detected QRS is shown in Figure 4.23. Some parts of the ECG were entirely taken by motion artefacts due to baby's movements or crying, as shown in Figure 4.24. The QRS detection accuracy through 254 μm cotton sheet for the three babies are shown in Table 4.3 at the end of this section. On the other hand, no ECG signals were detected through the cotton sheets with 355 μm of thickness; a sample of the collected signal is shown in Figure 4.25.

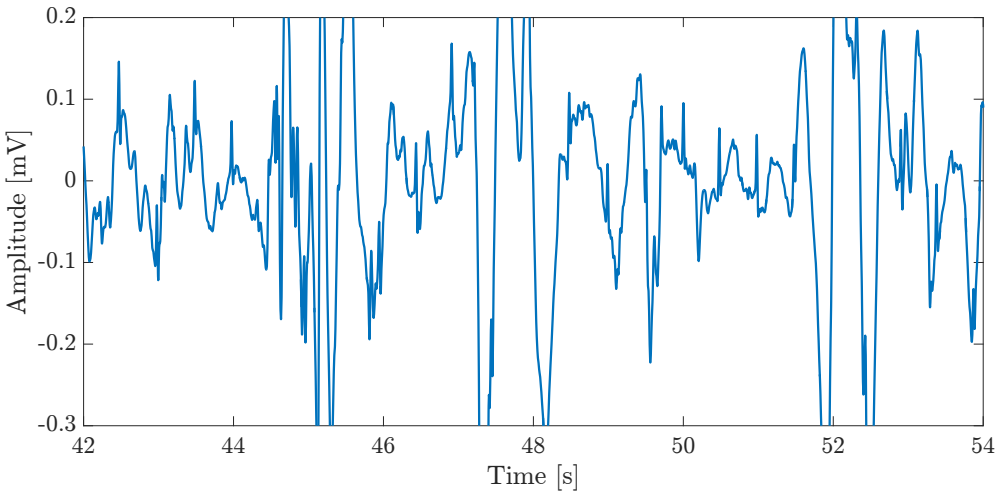


Figure 4.22: Sample of ECG signal recorded from baby's back capacitively through 254 μm cotton sheet, using EPIC PS25101 and the data acquisition system shown in 4.3.

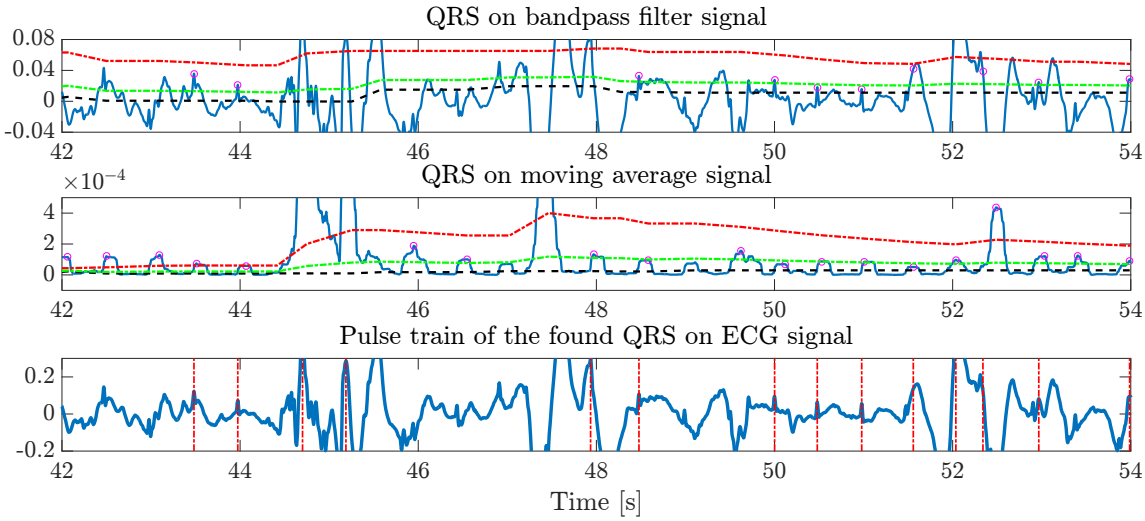


Figure 4.23: Sample of QRS detection on baby ECG signal collected from the back capacitively through 254 μm cotton sheet. It shows the detected QRS on bandpass, moving average raw ECG signals with noise level (Black), signal level (Red) , adaptive threshold (Green) and the QRS detection (Pulse train).

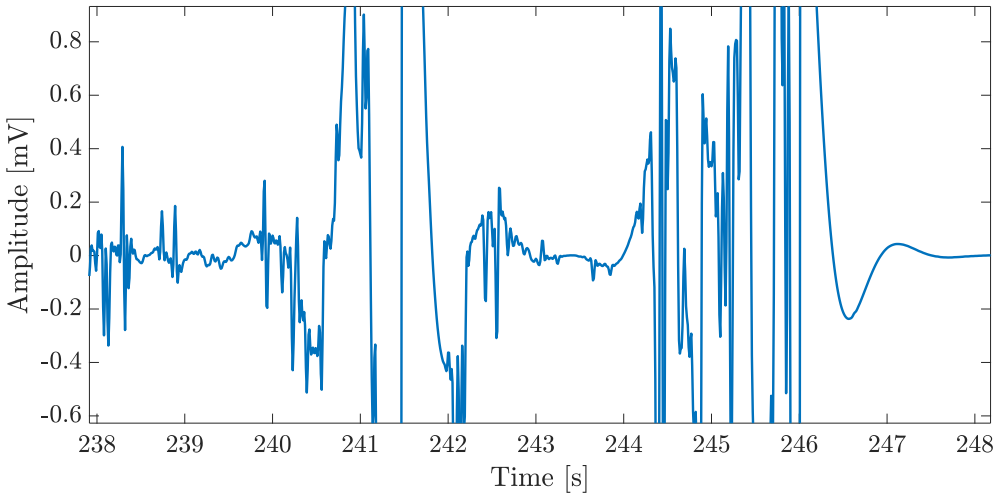


Figure 4.24: The motion artefacts introduced by baby movements and crying.

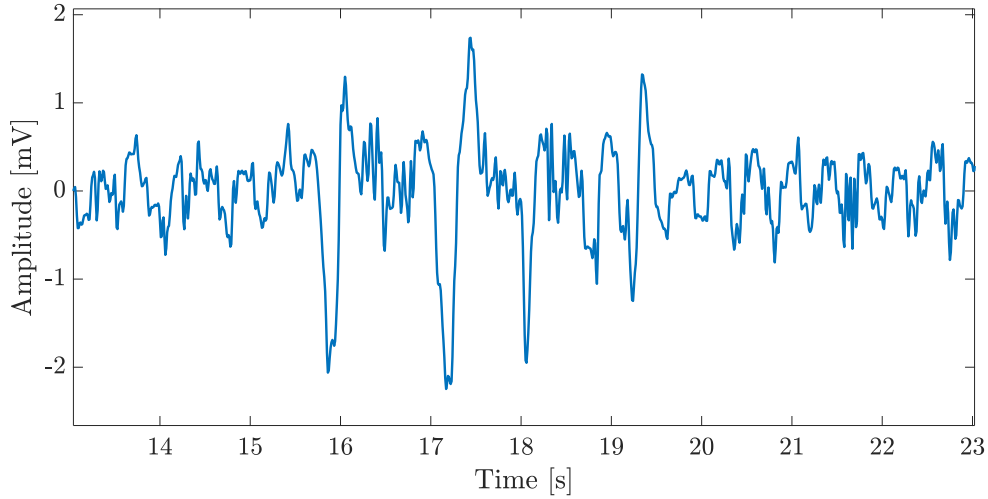


Figure 4.25: Sample of the signal collected from baby's back through 355 μm cotton sheet with no detectable ECG features.

4.5.3 Summary

The accuracy of the QRS peaks detection from adult and baby volunteers are summarised in Table 4.3. The QRS peaks could be visually identified in the capacitive ECG signals collected from adults and babies through the 254 μm cotton sheet. The accuracy of QRS detection was generally higher among the adults' ECG signals than babies'. For the 355 μm cotton sheet, the QRS peaks could only be detected from adult ECG signals and were not identified from the babies' neither visually nor using the detection algorithm. Based on this data, the capacitive coupling might be of interest for the NICU applications. EPIC sensors could couple an ECG signal in dry contact without applying the conductive gel with relatively good quality. The sensor was also able to couple the ECG signal through the cotton sheet of 254 μm despite the motion artefacts introduced by the baby active movements during the recording.

Volunteers gender/age	**Sensors position**	254 μ**m QRS detection**	355 μ**m QRS detection**
Female 25Y	wrists	99%	94.6%
Male 29Y	wrists	100%	94.3%
Male 28Y	wrists	99.5%	94.0%
Male 33Y	wrists	99.2%	95.5%
Male 24Y	wrists	99.5%	85.6%
Female 29Y	wrists	100%	93.4%
Male 30Y	wrists	100%	95.7%
Female 8W	back	71.3%	–
Male 4M	back	75.6	–
Female 11M	back	67.4	–

Table 4.3: QRS detection accuracy in ECG signals collected capacitively though cotton sheets from adult and baby volunteers using PS25101 sensors. Samples of the yellow colour rows data were shown in this chapter and in Appendix B.

4.6 Capacitive Coupling Through Cotton Clothes: Array System

In the previous section, the ECG signals were successfully collected from the adult volunteers capacitively through cotton sheets. In this section, a non-controlled experiment was performed on adult volunteers in order to find out if the EPIC sensors can detect ECG through cotton clothes with different layers. Eight sensors were used to record four ECG signals simultaneously in the form of an array. The setup of this experiment is shown in Figure 4.26, where the sensors were placed under the shoulders, middle back, waist and lower back. In this experiment, the adult volunteers were asked to lie down on a yoga mat fully clothed, wearing 100% pure cotton shirts and trousers of their choices. Several holes were made on the yoga mat to accommodate the eight EPIC sensors for an unobtrusive system. All the volunteers wore at least one layer of cotton material on their upper part, and two layers on their lower part. This system was initially fabricated in order to increase the accuracy of ECG acquisition from babies through the delivery room materials. However after the initial analysis, the system was only tested on adults.

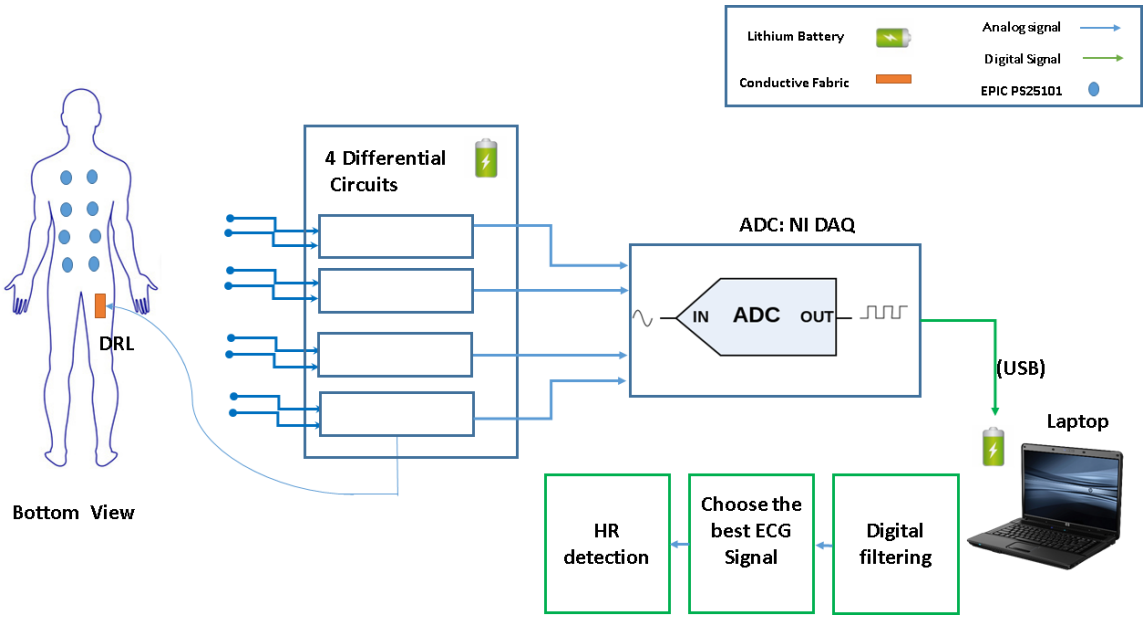


Figure 4.26: Experimental setup for collecting ECG signals from adult back capacitively through cotton clothing using eight EPIC PS25101 sensors.

4.6.1 Results

In this experiment, four ECG signals were collected simultaneously from each adult volunteers back through his/her cotton clothes with different thicknesses and layers. The ECG signals were collected successfully from the bodies' upper parts, i.e. shoulders, middle back and waist; but no ECG signal was collected from the lower back sensors because of the thick multi-layers of clothing. The experiment was performed on seven adult volunteers to collect five minutes of recording. Samples of one adult volunteer ECG signals recorded capacitively from shoulders, middle back and waist are shown in Figure 4.27. This sample was taken of a volunteer who was wearing a single cotton layer. However, the morphology of capacitive ECG signals through the multi-layers was distorted. Figure 4.28 shows the ECG signal that was coupled through three layers of clothes after filtering.

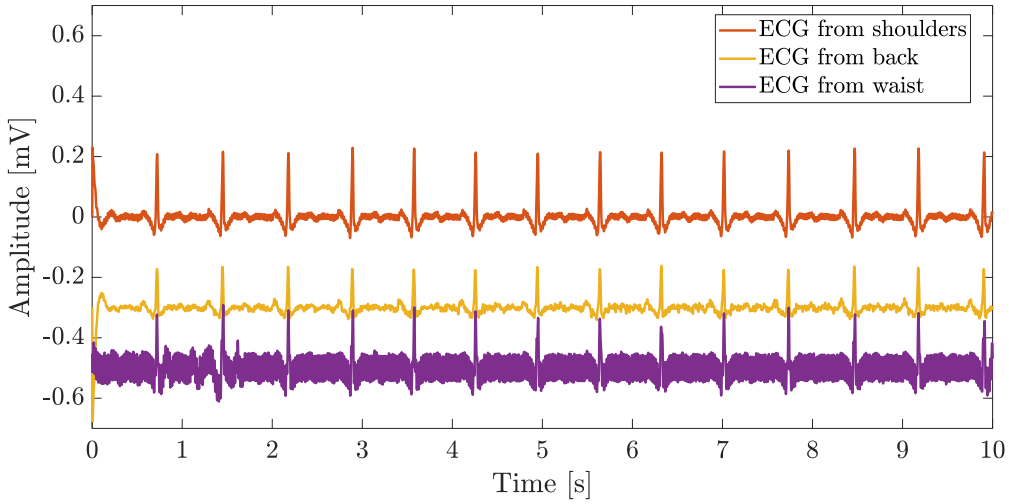


Figure 4.27: Sample of ECG signal recorded capacitively through single layer of cotton from an adult, using EPIC PS25101 and the setup shown in 4.26. ECGs were collected from shoulders, middle back and waist. A DC offset has been added to these ECG signals in order to show them clearly in the figure.

The shoulders' ECG had a higher amplitude than the other capacitive ECGs because of the better contact and reduced the air gap at the shoulders when the volunteer was lying on the back, besides they were the closest to the heart among the eight contact points. The features of typical ECG signals were visible in the capacitive ECG signals of all volunteers. The QRS complex was not visible from the lower back ECG signals, as mentioned above. An algorithm was used to choose the signal with the highest SNR at the time, and calculate the HR based on that signal, the ECG

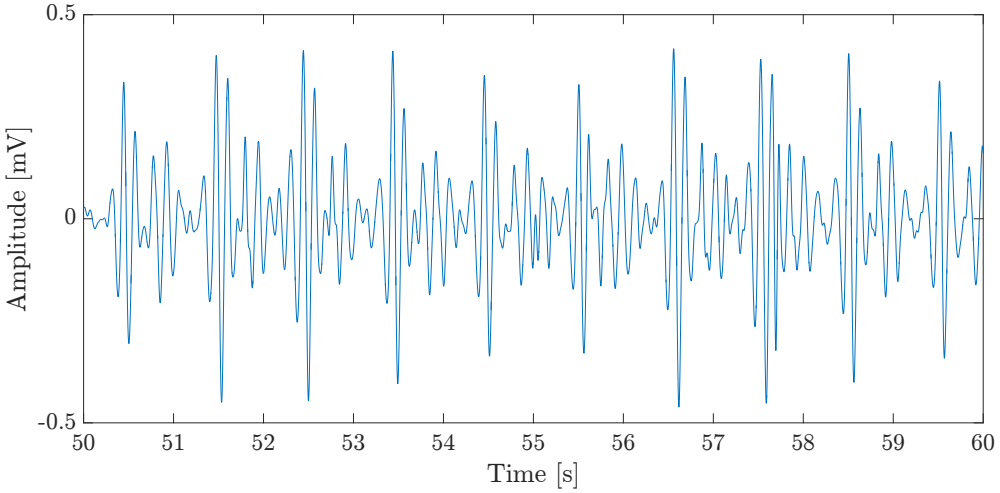


Figure 4.28: Sample of ECG signal recorded capacitively through three layers of cotton from adult shoulders, using EPIC PS25101 and the setup shown in 4.26.

from the lower back was always ruled out of the HR calculations due to low SNR. The percentages of the detectable ECG signals from adult and baby volunteers are shown in Table 4.4. The detectable part of the ECG signal is inversely proportional to the number of clothing layers. The best signal, in terms of QRS detection accuracy (96.3%), was collected through one layer of clothing, and the worst signal of 78.8% was collected through three layers of clothing.

Volunteers gender/age	**Sensors position**	**# Cotton layers in upper parts**	**QRS detection**
Male 29Y	back	1	96.3% 359/473
Female 25Y	back	2	91.6 % 306/334
Male 28Y	back	2	92.4% 316/342
Male 33Y	back	2	91.8% 324/353
Male 24Y	back	1	94.8 295/311 %
Female 29Y	back	3	78.6% 245/311
Male 30Y	back	2	92.4% 304/329

Table 4.4: QRS detection accuracy in ECG signals collected capacitively though cotton clothes from adult volunteers. Samples of the yellow colour row data was shown in this chapter.

4.7 Bioimpedance Measurements for Dry and Capacitive Setups

4.7.1 Overview

The ECG signal is generated by the excitable cells of the heart muscles. The ion currents carried by $Cl-$, $Na+$ are converted to electrical current by the ECG electrodes which work as a transducer. The outer skin layer -the stratum corneum- impedes the transfer of the ions in the tissue to electrons in the electrode leads. Many studies in the literature review have discussed that the skin-electrode interface can be described as a series of parallel R and C circuits, where each circuit represents one of the contact layers [56,68,99]. The interface impedance between the skin and the typical standard wet ECG sensors are modelled using the Warburg model and its modifications. In the Warburg model, the resistive component of the skin is frequency dependent, and the magnitude changes significantly within the bandwidth of the ECG signal. The model suggests that when using the wet ECG sensors the resistance of the skin is almost equal to the skin capacitance $Rsc(f) \approx Xsc(f)$ at every frequency within the ECG bandwidth [56]. Some papers have suggested that the resistive component of the skin interface could increase up to a few ohms, as shown in chapter two, Figure 2.7 [122].

Different interface impedance models representing wet, dry and capacitive electrodes were shown in chapter two, Figure 2.7 and explained in Section 2.4.3. In the case of dry contact, there are only two layers of impedance: stratum corneum and the ECG electrode. While in capacitive contact, the layers are stratum corneum layer, cotton or plastic layer and then the ECG electrode. The skin impedance was measured using the combination of the 1260 Solartron impedance analyser and 1294 bioimpedance interface which can measure up to 100MΩ ±1% or up to 1 GΩ ±10%.

In order to model the dry contact skin interface, an experiment was carried out using a Solartron impedance analyser 1260 and the bioimpedance interface 1294. The bioimpedance measurements system was further discussed in Chapter Three, Section 3.4, and was shown in Figure 3.14. The system was used to measure the dry skin interface impedance and the cotton and plastic materials' impedance.

4.7.2 Impedance Measurements of Dry Contact Electrode

Typically, the impedance of the dry contact interface is represented by Figure 4.29. In order to measure the skin interface impedance when the sensors are applied in dry

contact setup, two metal discs were used for the measurement. The discs were cut of the same shape and area of EPIC sensors. The previous experiments in this chapter were conducted without skin preparation. However, the skin interface impedance was measured from the adult volunteer before and after skin preparation in order to compare.

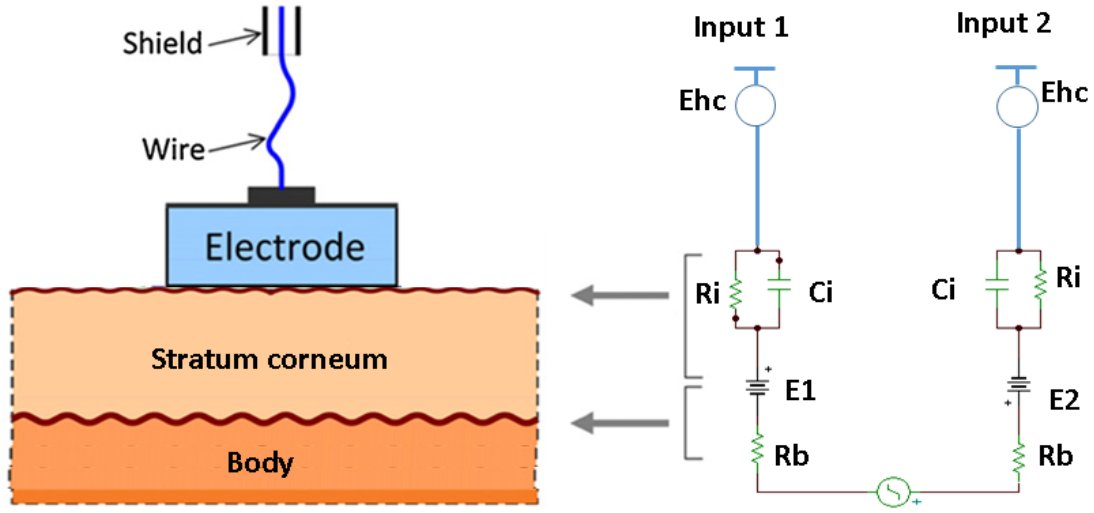


Figure 4.29: The dry contact model of the skin-sensor interface including body layer Stratum corneum, R_i and C_i represent the interface resistor and capacitor while R_b represents the body resistor. The skin interface equivalent model has been used [56].

Figure 4.29 shows the impedance model of recording the ECG signal capacitively. The Rb resistor was used to represent the body resistivity. The R_i and C_i components represented the impedance of the Stratum corneum contact layer.

Figure 4.30 illustrates how the metal plates were applied to the adult volunteers' wrists to measure the dry contact interface between the plates and the volunteers' skin. The copper plates were placed on top of the wooden desk, and the volunteers were asked to place their wrists just over the plates (the same setup of ECG signal recording). However, in this setup, the metal discs were strapped and secured using wrist bands to maintain accurate readings. The bioimpedance interface 1294, which was designed for the human interface, was connected to the metal discs by IEC 60601 certified triaxial cables. The IEC60601 connections allow a maximum of ± 10 μA of a DC and 10 mA (RMS) of an AC. The measurements were taken twice on the volunteer: first without skin preparation, and then after the skin preparation (includes shaving the hair of the selected area, abrasion and proper cleansing using ECG prep pad).

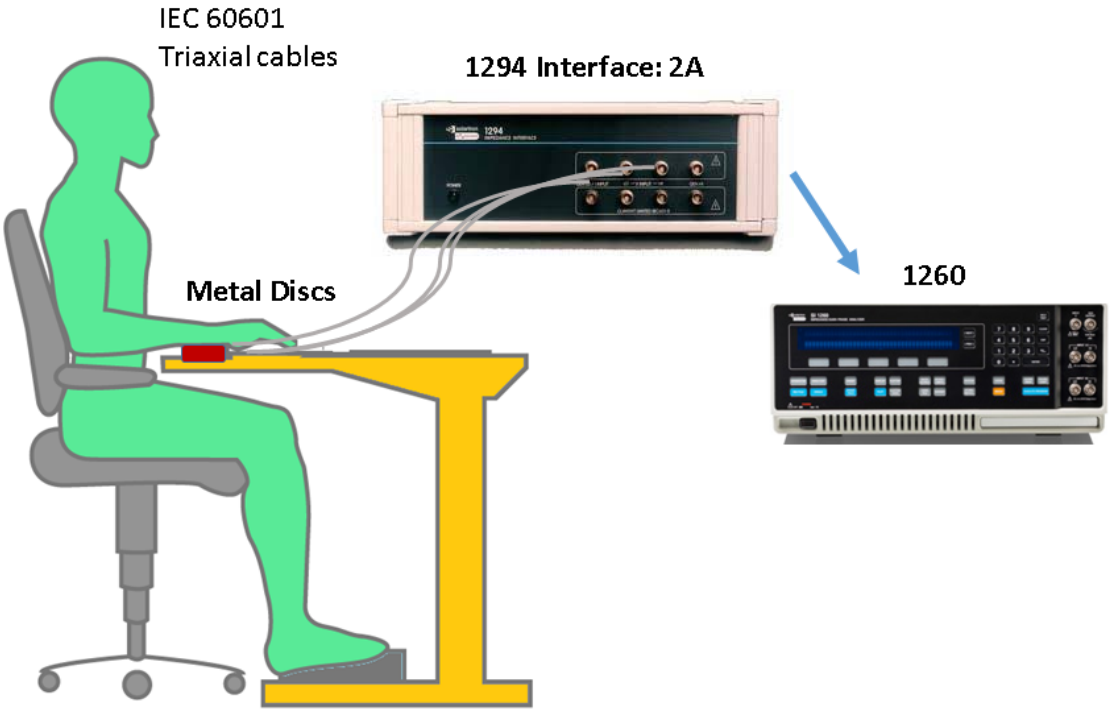


Figure 4.30: The measurement setup of dry sensor - skin interface bioimpedance.Two metal discs were used in contact with adult's wrists.

Figure 4.31 shows the impedance of the skin-metal plates dry interface before and after the skin preparation (log scale) within the frequency of 1 Hz to 100 KHz. As expected, the skin preparation decreased the impedance significantly at the low frequency (ECG bandwidth). The impedance of the interface was 7.89 MΩ at 1 Hz, and after the skin preparation, it dropped by more than a half to 3.97 MΩ at 1 Hz. Similar to Warburg model of Ag/AgCl electrodes, the measured resistivity of the dry skin interface was frequency dependent as well. In order to simulate the skin interface layer in the dry contact accurately, the parallel capacitors and resistors of the dry contact model should be substituted as frequency dependent variables using the experimental measurement points.

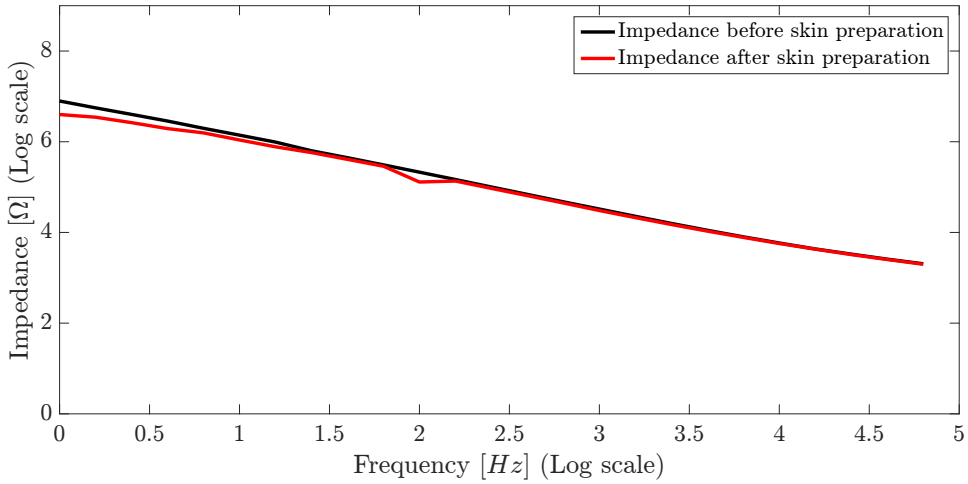


Figure 4.31: Impedance measurements of dry contact skin interface before and after skin preparation, using the experimental setup shown in Figures 4.30 and 3.14.

4.7.3 Impedance Measurements of The Dielectric Materials

In order to understand the reasons for the different materials behaviour during the capacitive coupling of the ECG sensors, the impedance of these materials were investigated theoretically and experimentally. As shown in the literature review, the dielectric material layer is generally modelled as parallel impedance and capacitor. In the capacitive contact, the impedance model includes the dry contact model discussed in the previous section, in addition to the capacitive material layer as shown in Figure 4.32, where R_m and C_m represent the dielectric material's layer. In this section, the electrical characteristics of cotton material are discussed along with polyethylene and vinyl plastic bags in order to complete the capacitive contact model. The impedance of these dielectric materials was measured separately without skin contact because of the devices accuracy limitation. The capacitance of cotton, vinyl and polyethylene plastic bags were calculated theoretically using the electrical characteristics of the material in the literature review and compared to the measured impedances.

Theoretical Capacitance of Cotton, Vinyl and Polyethylene

The capacitance of the dielectric materials is calculated using: the dielectric constants of the materials, the area of the sensor, and the thickness of the used plastic and cotton sheets, using the equation:

$$C = \varepsilon(A/d) \tag{4.1}$$

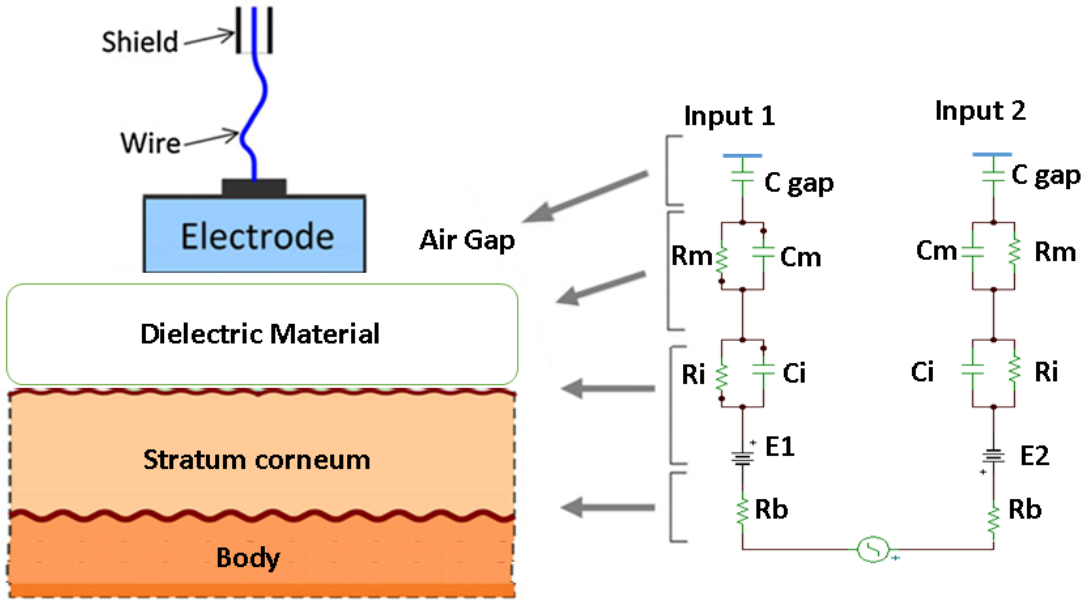


Figure 4.32: The capacitive contact model of the skin-sensor interface in capacitive contact, including body layer, Stratum corneum interface and the dielectric material (cotton or plastic sheet). R_i and C_i represent the interface resistor and capacitor, R_m and C_m represent the dielectric material's layer, while R_b represents the body resistor. The skin interface equivalent model has been used [56].

where:

$$\varepsilon = \varepsilon_0 * \kappa \tag{4.2}$$

As shown in Figure 4.33: A is the area of the plates overlap, d: is the distance between the plates, ε is the absolute permittivity of the material, ε_0 is the permittivity of vacuum and κ is the relative permittivity of the material.

The cotton material's relative permittivity is in the range of $2.3 - 3.18$ [124, 125], however, the dielectric constant of the cotton material increases significantly when the fabric is moist [126]. When substituting cotton dielectric constant ($\kappa = 3.18$), the area of the sensors $= 1.54\,cm^2$ and the cotton towel and two sheets thicknesses:

$$C_{towel} = \frac{\varepsilon * 3.18 * 1.54\,cm^2}{2000\,\mu m} = 25.77\,nF \tag{4.3}$$

$$C_{254um} = \frac{\varepsilon * 3.18 * 1.54\,cm^2}{254\,\mu m} = 137\,nF \tag{4.4}$$

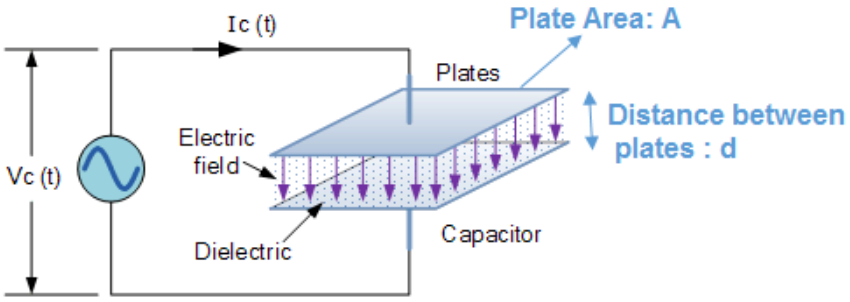


Figure 4.33: The capacitance representation of dielectric materials [123].

$$C_{355um} = \frac{\varepsilon * 3.18 * 1.54\,cm^2}{355\,\mu m} = 122.1\,nF \tag{4.5}$$

The vinyl plastic bag was made of Ethylene-vinyl Acetate (EVA) and its dielectric constant, relative permittivity, of 2.65 [127]. The second type of plastic bag, polyethylene bag, was made of Low-Density polyethylene (LDPE) which has a dielectric constant of 2.25 [128].

When substituting $d = 10$ μm as the thickness of the plastic sheets, the area of the sensors $= 1.54\,cm^2$ and $\kappa = 2.25$ and 2.65: the capacitors are:

$$C_{vinyl} = \frac{\varepsilon * 2.65 * 1.54\,cm^2}{10\,\mu m} = 36.1\,nF \tag{4.6}$$

$$C_{poly} = \frac{\varepsilon * 2.25 * 1.54\,cm^2}{10\,\mu m} = 30.7\,nF \tag{4.7}$$

The calculated capacitance are shown in Figures 4.35 and 4.36 in comparison with the experimental impedance measurements from the next section.

Experimental Impedance Measurements of Cotton, Vinyl and Polyethylene

In order to determine the impedance of the cotton and plastic bags which were used during ECG capacitive coupling in this Chapter, 1260 impedance analyser and 1294 normal interface were used (non-bio part). As mentioned in the previous section, when the 1260 Solartron impedance analyser is used combined with 1294 interface, they can measure up to 1 GΩ $\pm$10%. Figure 4.34 shows the setup for measuring the

impedance of the materials experimentally within the bandwidth of 1Hz to 1MHz. The experimental impedance of the plastic bags are shown in log scale in Figure 4.35. The calculated capacitance, using dielectric constants, are also shown in the same figure as dashed lines. As shown in the figure, the experimental measurements of the plastic bags correlate with the calculated capacitance. This means that the impedance of the plastic bags is dominated by the capacitance, within the bandwidth of the measurement (1 Hz to 1 MHz). That is because the resistive component of these plastic bags is very high compared to the capacitance, which makes the overall parallel impedance mainly reflects the capacitance of the material.

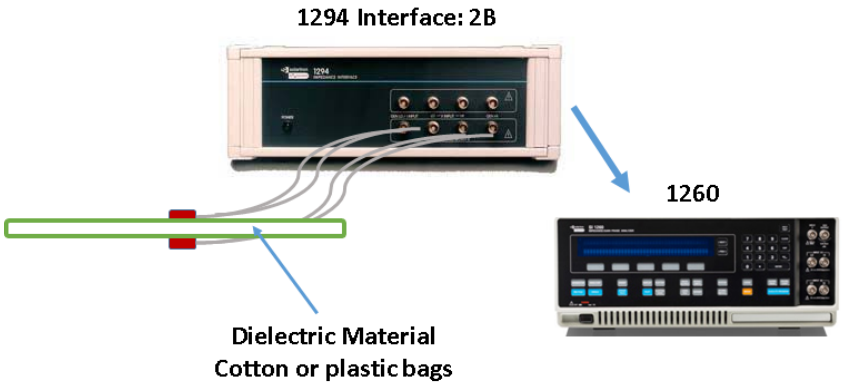


Figure 4.34: The impedance measurements setup of plastic bags, cotton towel and cotton sheets.

It is also seen that the measured impedance of the polyethylene bag is bigger than the vinyl. The difference is significant within the ECG signal bandwidth (1 Hz - 50 Hz). At 1 Hz the impedance of the polyethylene's bag is 688 MΩ while the vinyl bag is only 409 MΩ, which explains why the vinyl plastic bag had better coupling than the polyethylene's when recording the ECG signal from adult volunteers.

On the other hand, the cotton towel impedance was not measured, because it was bigger than the devices limit (the limit is 1GΩ). The impedance of the cotton sheets was measured and shown in Figure 4.36, along with the calculated capacitance of the cotton towel. The measured cotton impedance was dominated by the resistive component at (1 Hz to 100 Hz) bandwidth. Unlike the plastic bags, the capacitance of cotton material is very high compared to the resistance at the low frequencies. The capacitance starts to affect the overall impedance after 100Hz. The capacitance contributes to the ECG bandwidth only if the cotton sheet is very thin; about less than 50 μm. Other papers have referred to the fact that the ECG capacitive coupling through cotton clothing is mainly dominated by the resistive component because the

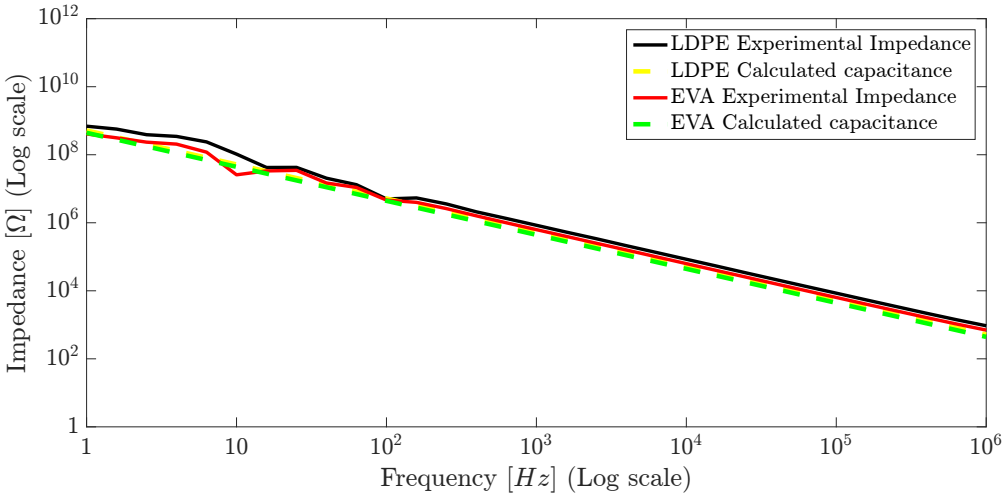


Figure 4.35: Impedance measurements of vinyl bag made of Ethylene vinyl Acetate (EVA) and polyethylene bag made of Low Density polyethylene (LDPE) compared to the calculated capacitance.

capacitance of the cotton shirts is so high in general with a typical fabric thickness of 200 μm [129] [126].

As expected, the impedance of the thicker cotton sheet of 355 μm is more than the impedance of 254 μm sheet, which is illustrated in Figure 4.36. At the 1 Hz, the impedance of the 355 μm cotton is 501 MΩ, while for the 254 μm the impedance is 316 MΩ. The thicker sheet with higher impedance attenuates the ECG signal more than the thinner sheet, and this is the reason behind the bad coupling through the thick cotton sheets from adult volunteers.

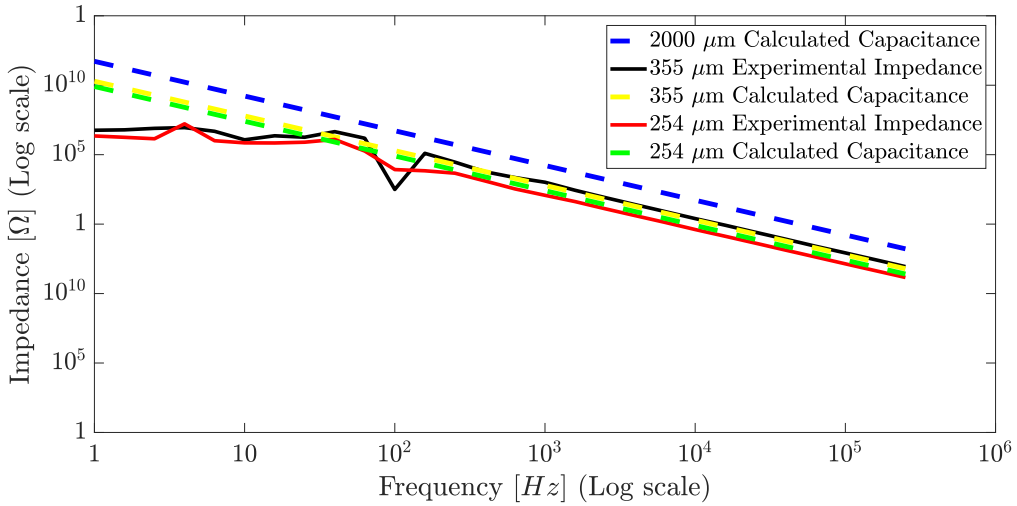


Figure 4.36: Impedance measurements of cotton fabrics are compred to the calculated capacitance. Fabrics' thicknesses are: 2000 μm, 355 μm and 254 μm. The impedance of 2000 μm cotton towels is not shown because it was bigger than the analyser maximum.

4.8 The Simulation of Dry And Capacitive Models

The dry contact impedance model from the previous section was used to simulate the ECG signal coupling by EPIC sensors. The model was combined with the dielectric materials to simulate ECG coupling 254um cotton sheet and the vinyl plastic bag in order to compare them with the collected results. The models were simulated by TINA-TI software. The generated ECG signal shown in Figure 4.37 was as an input to the model after being mixed with 20 μV of 50 Hz frequency noise. The simulation does not include digital filtering and processing part of the system, and the 50 Hz noise could be seen in the output of the simulation.

The input resistor and capacitor of the sensors have the values of 20 GΩ and 15 pF according to EPIC datasheet [22]. The values of the impedance model at 10 Hz were used in the simulation. The 10 Hz represents the peak of QRS complex power in the frequency domain for adult ECG signal, as shown in Chapter Two, Figure 2.10. For the fetal ECG signal, the QRS complex is typically found within the region of $10-15$ Hz, as shown in Figure 4.38 [130]. As the QRS complex was the main feature that was used to extract the HR, the values of the impedance at 10 Hz was used in the simulation.

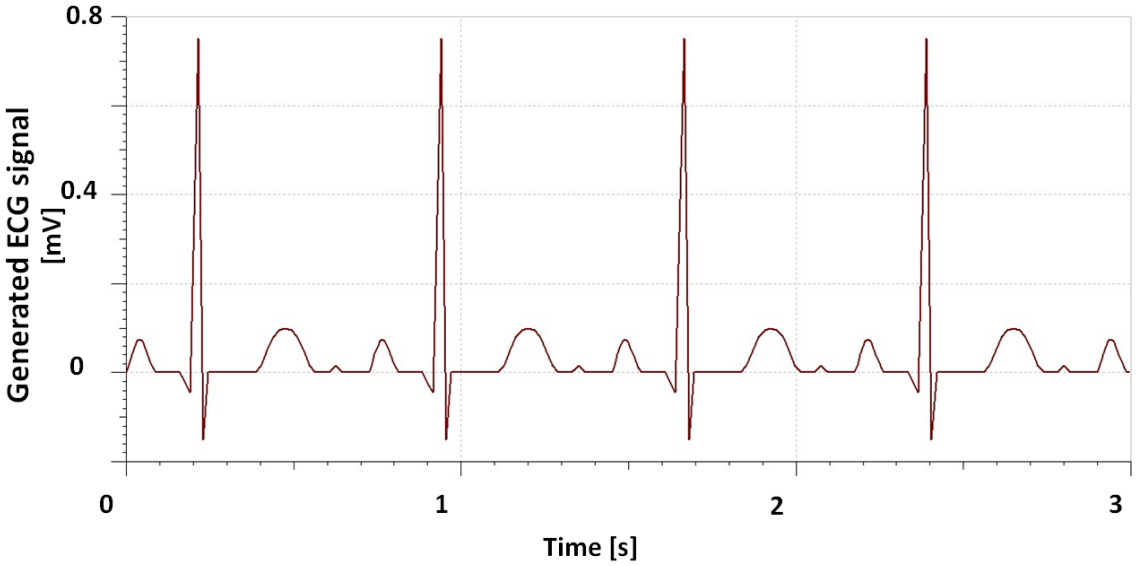


Figure 4.37: Sample of the generated ECG signal that was used as an input for the simulation.

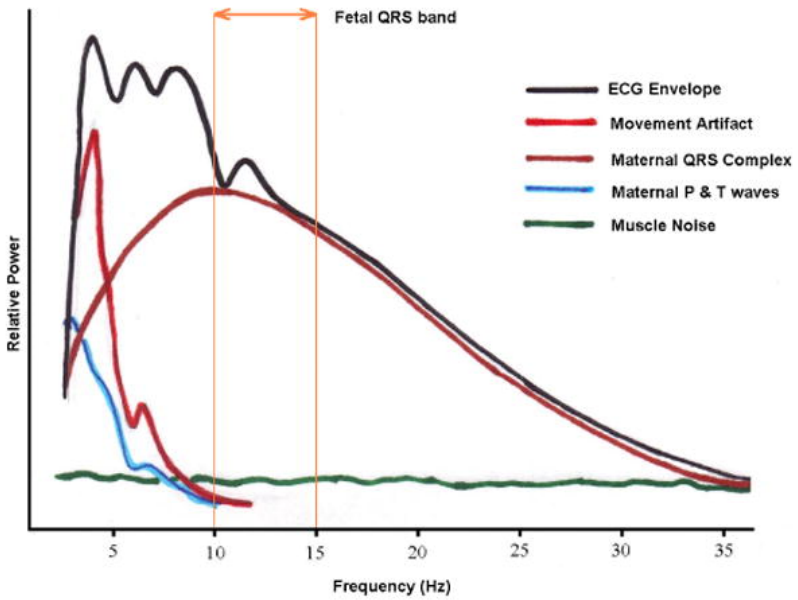


Figure 4.38: A general representation of the noise and artefacts present in the fetal QRS in the frequency domain [130].

4.8.1 Simulation Results

The output of the dry contact model simulation is shown in Figure 4.39. The skin interface resistor and capacitor values were both frequency dependent, but the values at 10 Hz were used for the simulation. As shown in the previous figure, the output of the model has the same morphology of the input signal, similar to the experimental results of the dry contact output. This ECG will e used to compare the tow capacitive ECG signals through cotton and plastic bags.

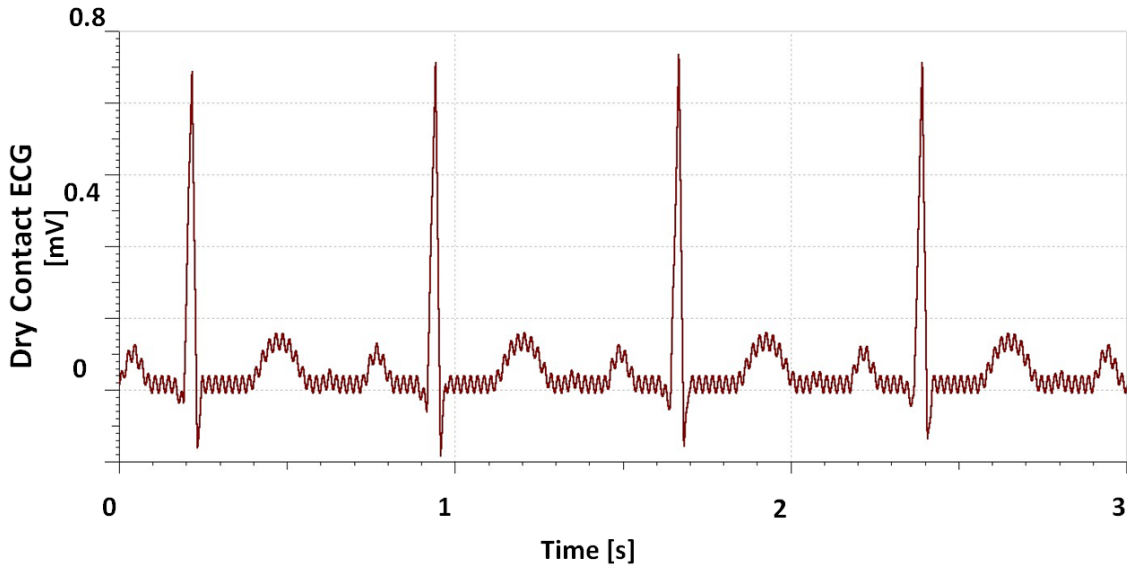


Figure 4.39: The output ECG of the dry contact model simulation. The impedance measurement at 10 Hz was used with the impedance model shown in Figure 4.29.

The capacitive interface model includes the dry contact interface with an additional layer of cotton and plastic was used for the capacitive simulation. The impedance of the cotton material, as discussed above, was dominated by the resistive component while the plastic material's impedance was dominated by the capacitive component, which affects the ECG signal differently. Additional coupling capacitor was added to the capacitive impedance model to represent the air gap of the coupling. This capacitor was assigned the value of 1 pF for the plastic coupling and 5 pF to the cotton coupling. The skin interface resistor and capacitor values were both frequency dependent, but the values at 10 Hz were used for the simulation.

The output of the capacitive coupling ECG through the cotton sheet with 254 μm is shown in Figure 4.40.

The morphology of the ECG signal was distorted in the output ECG compared to the original signal, and the R-S segment has changed because of the effect of the

air gap capacitor discharging. A similar effect has been noticed in the experimental results, and it increased in the thicker cotton sheet. The R peak was attenuated significantly compared to the dry; the amplitude's decrease was about $\approx 50\%$. In the experimental results, the decrease of the R peak amplitude of the capacitive ECG through cotton was $\approx 25\%$, which had significantly affected the QRS detection and hence the HR calculation accuracy.

On the other hand, the output of the capacitive coupling ECG through the vinyl bag is shown in Figure 4.40. The coupling capacitor was set to be 5 pF to simulate the air gap into the skin fabric interface and the fabric sensor interface. Normally the range of 1 pF to 1 nF is used in the literature papers with Cotton ECG coupling.

The output of the cotton ECG was less distorted than the plastic ECG shown in Figure 4.41. The capacitive coupling of the plastic in the simulation model was set to 5 PF to simulate the air gap between the skin/plastic interface and the plastic/sensor interface. As shown in the figure, the amplitude of the R peak was further attenuated, and the decrease was about $\approx 75\%$. The QRS complex morphology was distorted as well, and the QS segment became wider than the capacitive ECG through the cotton sheet. In the experimental results, some of the collect signals through the vinyl bag were not recognisable, and they were heavily distorted by the artefacts. The friction and motion artefacts were not simulated. Hence, there was a difference between the experimental and simulation results.

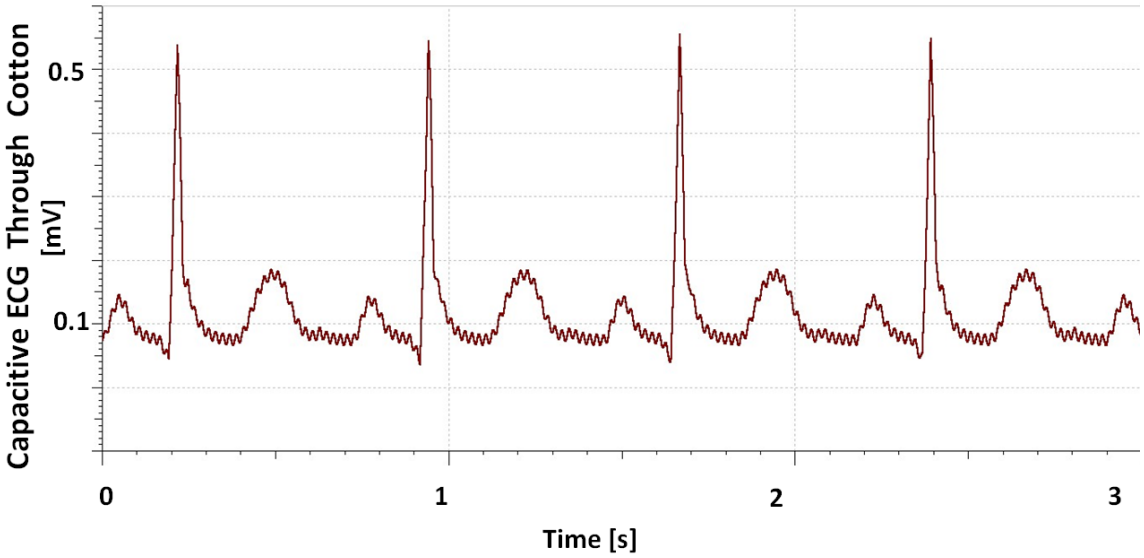


Figure 4.40: The output ECG of the capacitive contact model simulation through $254um$ cotton sheet. The impedance measurement at 10 Hz were used with the impedance model shown in Figure 4.32.

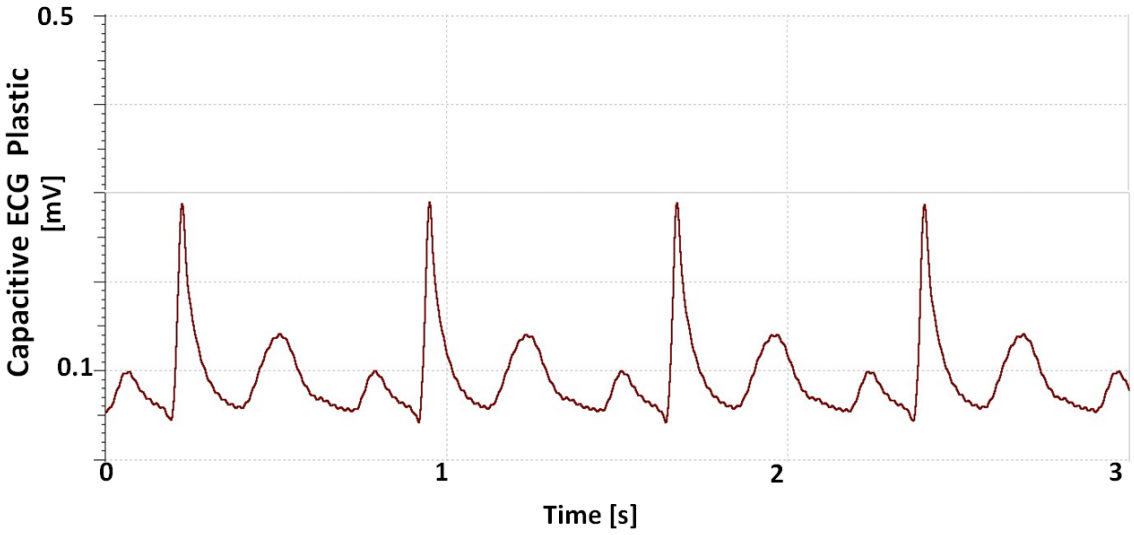


Figure 4.41: The output ECG of capacitive contact interface simulation through the vinyl plastic bag. The impedance measurement at 10 Hz were used with the impedance model is shown in Figure 4.32.

4.9 Conclusion

The objective of this Chapter was to investigate the possibility of using the capacitive ECG sensors of EPIC PS25101 to collect ECG signals through the cotton towels and plastic bags- which are typically used to wrap babies during the resuscitation in the delivery room. The collected ECG would be used to extract the HR allowing medical staff to monitor the heart rate continuously while resuscitating. Many papers in the literature review have tested the use of EPIC sensors to couple ECG signals in dry contact and through cotton shirts and sweaters, and some has claimed that the sensors have successfully coupled capacitive ECG signal through 2.37mm of cotton thickness [13, 120, 121, 131]. As illustrated in the previous sections, five experiments were performed on adult and baby volunteers to collect ECG signals in dry and capacitive setups. The objective of the first experiment was to evaluate the ability of the capacitive sensors to couple ECG signal without applying the conductive gel or preparing the skin. Good quality ECG signals were collected from adult volunteers, with average QRS accuracy detection of 99.8%. However, the quality of the ECG coupled from the babies was lower than adults' ECG because of the introduced motion artefacts; on average, 89.3% of the babies ECG was detectable by the QRS algorithm.

The second experiment was conducted to test the ability of EPIC sensors to collect an ECG signal through the materials that are typically used for swaddling the babies in the delivery room. The sensors were not able to couple any detectable ECG signal through the cotton towel or the polyethylene bag, but the ECG was coupled from five adults through the vinyl plastic bag. Based on the performance of the EPIC sensors in this experiment, it is unlikely to be applicable for the delivery room applications.

An additional experiment was performed to collect ECG signals from the volunteers through cotton sheets with thicknesses of 254 μm and 355 μm. The QRS detection accuracy of the adult ECG signal through the cotton sheets were 99.71% and 93.3%. The ECG signal of the babies was only detectable through the 254 μm cotton sheet with QRS accuracy of 73.4%. The results of this experiment and the dry contact suggest that the capacitive sensors could be applicable for the NICU applications. The initial proposal of the array system was used to couple the ECG signals from fully clothed adult volunteers; on average, 92.5% of these capacitive ECG signals were detectable. Finally, the impedance of skin interface impedance was measured along with the impedance of the dielectric materials to model the interface of the dry and capacitive ECG signal. The output of the simulation had correlated with the experimental findings.

The success rate of QRS detection in adults' ECGs was higher than the babies' in all types of coupling, as illustrated in Table 4.5. The babies ECGs have more motion artefacts because the babies were crying, moving their limbs and trying to roll over on their backs. The older babies had more muscles and tended to move more, and hence, their ECG signals were more distorted. The stratum corneum of the full term baby is 30% thinner than the adult's [132], which means that the resistivity of the baby's skin is smaller than the adult's. On the other hand, the amplitude of the babies' ECG is typically smaller than adults'.

The ECG signals recorded in dry contact have better quality than the capacitive ECG signals in terms of robustness against motion artefacts, distortion, general signal morphology and signal to noise ratio. Referring to Table 4.5, this has translated into higher QRS detection rate for the dry contact signals from both adults and babies. The QRS detection was processed using a Matlab code based on Pan and Tompkins algorithm, which is discussed in Chapter Three, 3.5. The average success rate of the QRS detection from the dry contact ECG signals was 98.3% for adults volunteers and 89.3% for babies, as shown in Table 4.5. According to the skin impedance model, the dry contact was expected to have less coupling impedance and less air gap than the capacitance model.

For the capacitive ECG signals coupled through cotton fabrics, when the fabric gets thicker, the QRS accuracy became lower, as shown in Table 4.5. No ECG signal was detected from any volunteer through cotton towels of 2000 μm thickness. The adults' ECG was coupled capacitively through the two cotton sheets of 254 μm and 355 μm thickness. While the babies ECG was only coupled through the thinnest sheet of 254 μm thickness. The QRS detection accuracy decreased as the fabric thickness increased because the impedance of cotton sheets is dominated by the resistive component within the ECG bandwidth. The thicker the fabric, the bigger the impedance and hence, more attenuated ECG. The capacitive component of cotton affects the ECG signal when the thickness of the cotton sheet is less than 50 μm.

On the other hand, the QRS detection accuracy of plastic bag capacitive coupling was very low. No ECG signals were coupled from the baby volunteers through any of the plastic bags. Moreover, only five adults recognisable ECG signals were coupled through the vinyl bag, and none of them was coupled through the polyethylene. In contrary to the cotton material, the plastic bags impedance is dominated by the capacitive component, because the parallel resistivity is very high compared to the capacitance, and also because they were very thin (10 μm) compared to cotton sheets. Both bags have the same thickness, but they were made of different materials with

Coupling type	# Volunteers /group	Detected ECG	QRS detection success rate
Dry coupling	7 adults	7	99.84%
	3 babies	3	89.3%
2000 μm Cotton towel	7 adults	0	–
	3 babies	0	–
Vinyl plastic	7 adults	5	66.26%
	3 babies	0	–
Polyethylene plastic	7 adults	0	–
	3 babies	0	–
254 μm Cotton sheet	7 adults	7	99.71%
	3 babies	3	73.45%
355 μm Cotton sheet	7 adults	7	93.3%
	3 babies	0	–
Multiple layers of cotton clothing	7 adults	7	92.5%

Table 4.5: Average accuracy of the QRS detection among dry and capacitive coupled ECG signals from adult and baby volunteers.

different dielectric constant, as shown in Section 4.7.2 above. It has been illustrated from the experimental impedance measurements and calculated capacitance, that the capacitance of the vinyl plastic bag is less than the polyethylene's within the ECG bandwidth. The adults average QRS detection rate through the vinyl was 66.26%, which is significantly lower than the rate of dry and capacitive coupling ECG through cotton sheets. In the simulation, the coupling capacitor was assigned to the value of 5 pF, which simulates the air gap created between the skin/plastic bag/sensor.

The simulated Impedance model and results are shown in Section 4.7 does not fully represent the actual coupling system. The skin components are frequency dependent, but their values at 10 Hz was used in the simulation. Also, the model of the capacitive interface was measured in two different steps: (1) skin dry contact impedance measurements, (2) dielectric material impedance measurements. The impedance of the dielectric materials was measured without the skin contact because the 1260 Solartron analyser used in the experiments can only measure up to 1 G Ω. Separating the measurements in two steps decreases the accuracy of the full model. The dry and capacitive models in this chapter have illustrated the difference between the used setups and gave insights about why one material was better than the other, although those models were only based on adult bioimpedance measurements, not babies.

In conclusion, the accuracy of dry contact ECG recorded from baby volunteers was of 89.3%, and it is expected to be higher for newborns due to their weak muscles and hence, limited movement. The ECG was also coupled through the cotton sheet with a thickness of 254 μm. On average, 73.4% of the baby volunteers ECG through the cotton sheet was detectable. These results suggest that the EPIC non-contact ECG sensors could not be used to monitor the heart rate by capacitively coupling the ECG signals from babies during the resuscitation. The sensors might be used in dry contact by making holes in the towel or plastic bags to accommodate the sensors.

On the other hand, the capacitive sensors can be applied for the dry contact ECG in the neonatal intensive care unit, where the babies are put almost naked inside the incubators in the supine position. An array of sensors could be fit in the incubators' mattresses to record the ECG signal for heart rate monitoring purpose. Because of these results, another method was proposed to record the ECG in the delivery room HR monitoring. The fabric sensors were proposed to couple the ECG in dry contact from the newborns in the delivery room. Unlike the non-contact EPIC sensor, fabric sensors are flexible and could be used to record the ECG in dry contact from the exposed parts of babies such as forehead and forearms. This method is discussed in the next Chapter.

Chapter 5

Fabric Sensors: Results and Discussion

5.1 Overview

As shown in the literature review, many papers have concluded that the ECG signal has the best accuracy for extracting the heart rates of the newborn babies over other widely used methods [8,9,32,34,55,118]. However, the risk of skin scarring associated with the standard AG/AgCl electrodes has compromised the use of the ECG signal during resuscitation in the delivery room. In this research, fabric and non-contact ECG sensors were proposed to eliminate the scaring risk.

The non-contact sensors were firstly investigated as a potential method to record the ECG signal capacitively during resuscitation. Chapter Four reviewed the possibility of coupling capacitive ECG signal using EPIC sensors by Plessey through cotton sheets and plastic bags. However, the sensors were shown to only couple capacitive ECG through a very thin cotton sheet (254 μm). The dry contact ECG from baby volunteers had a QRS detection accuracy of 89.3% but was not detectable through cotton towels, vinyl or polyethylene. This is significant as the babies are often swaddled in plastic bags or cotton sheets at birth to prevent dehydration and hypothermia. After this conclusion, fabric sensors have been proposed as another potential method of recording the ECG in the delivery room with more flexibility. The babies in the delivery room have their faces exposed when they are wrapped in either plastic bags or cotton towels. The exposed skin-face and forearms could be accessed for dry contact using more flexible sensors like fabric sensors. Some papers have used the fabric sensors to record ECG signal from babies in the Neonatal intensive care unit (NICU) where the fabrics are applied on baby's back and chest as part of wearable jackets [16, 81, 133]. A small number of papers in the literature review

had discussed collecting ECG signal from the forehead. They were mostly attached to helmets to monitor cyclists' heart rates. Some of them used Ag/AgCl electrodes [89, 134], others used dry sensors [90, 91] and some of them have used fabric sensors [92]. In addition, a few papers discussed recording ECG from mastoids with hearing aids or earplugs [95–97]. However, most of the literature review discussing ECG signal acquisition from the head was associated with filtering the ECG out of EEG, EOG and EMG signals [135–137] as shown in Chapter Two, section 2.6. No published work was found about fabric sensors applied on the forehead for the application of neonatal ECG monitoring in general.

The objective of this chapter was to investigate the possibility of placing fabric ECG sensors on the newborn's forehead and forearm to record ECG signals for heart rate monitoring during resuscitation. In this research, the proposed fabric sensors placements on babies in the delivery room are shown in Figure 5.1, where a babies' hat would be used to hold the forehead sensor, and another band would be placed on the forearm to hold the forearm sensor and the driven right leg. In this proposed placement, the hat will work as a fabric sensor holder, and would provide warmth to baby at the same time. The conductive fabric acts as an efficient metal plate on dry skin, with the attachment very secured due to fabric's flexibility and bendiness. The flexibility of the fabric makes it an excellent option for wrist and forehead placement in newborn babies.

In this Chapter, three different conductive fabric materials were initially reviewed to perform as ECG fabric sensors on newborn babies in the delivery room. The performance of these fabric sensors was tested in dry contact with babies' skin without applying conductive gel or any kind of skin preparation. These materials were further discussed in Chapter three, Section 3.3.3, and their images are shown in Figure 5.2. (1) Medtex P130 Silver plated knitted fabric made of 78% Nylon + 22% Elastomer by Statex Company, Bremen, Germany [107].

(2) SP31 smart textiles for medical applications, made of 20% stainless steel and 80% polyester fibres by Footfalls and Heartbeats Company, Nottingham, Uk [109,110].

(3) Laird 3080–500 Stretchable conductive fabric for athletic, smart wear development and general use, made of 78% Nylon and 22% Spandex by Laird Company, Missouri, United States [108].

Five experiments were conducted in this chapter to evaluate the performance of these fabric sensors for HR detection in the delivery room. All the ECG recordings using fabric sensors were collected without any skin preparation. Three experiments were performed on adult volunteers to test these fabric sensors' setups and placements

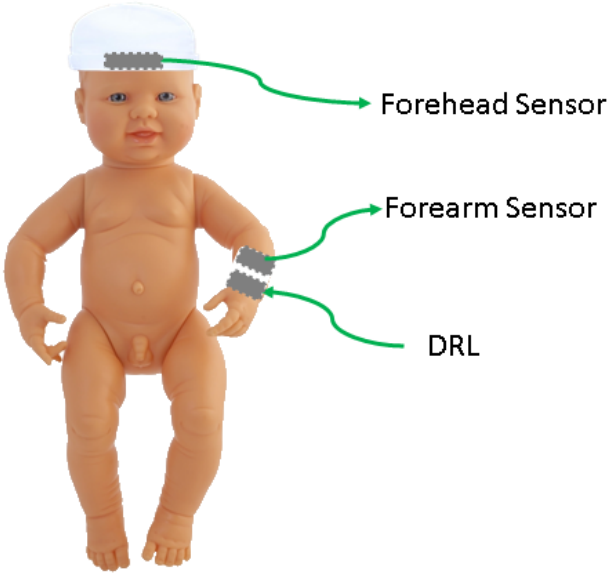


Figure 5.1: Proposed fabric placements on newborn babies in the delivery room. The hat is used to hold the forehead sensor, and additional band to hold the forearm sensor and DRL.

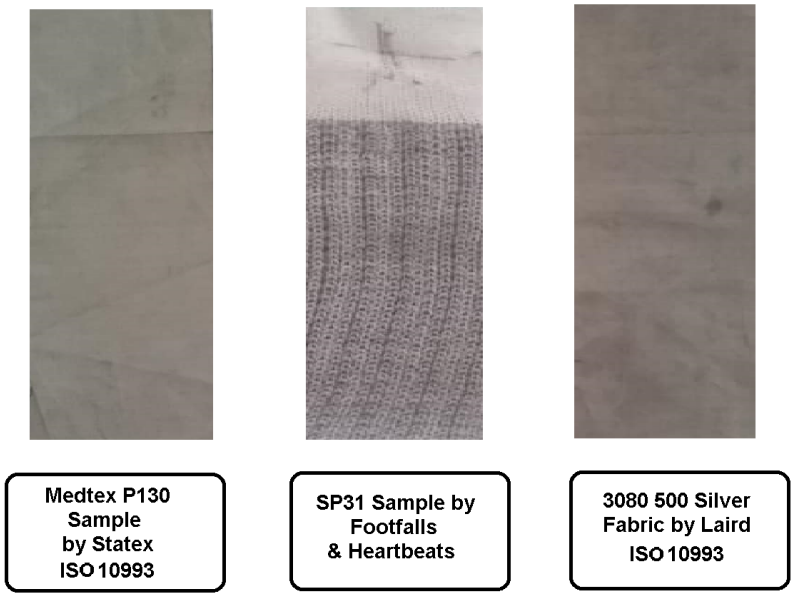


Figure 5.2: Three samples of the conductive fabrics that used in this research.

before being used with baby volunteers. The materials were tested on adult volunteers in different setups to find out the best arrangement for babies. In the first experiment, three stretchy bands were used to hold three fabric sensors for ECG signal collection. The ECG signals were collected using two sensors' arrangements; to compare between their signals. In the first arrangement, the sensors were placed on the right arm(RA), left arm (LA) and left leg (LL); and in the second arrangement, the sensors were placed on the forehead (FH) and left forearm (LFA). The ECG signals of this experiment were collected using a wireless ECG recorder made within the research team at the University of Nottingham [111]. The functionality of this ECG recorder is to input two sensors,generate the filtered digital ECG and transmit it over Bluetooth to a computer. Two of the fabrics had coupled good quality ECG from forehead and forearm with a DRL electrode placed on left leg.

The second and third experiments were designed to find a suitable arrangement of the fabric sensors regarding the babies body size. The fourth experiment was conducted on babies to collect the ECG signal from the forehead and forearm using the fabric sensors. Finally, the fifth experiment was conducted to measure the dry skin interface using conductive fabric materials.

5.2 Experiment One: Three Fabric Materials Test

5.2.1 Experimental Setup

Two pieces of each fabric were used as ECG sensors, and an additional fabric piece was used as a driven right leg (DRL). The sensors were a rectangular shape with area of $3cm * 2.5cm$, and were connected to the wireless ECG recording system shown in Figure 5.3. The fabric sensors were attached to stretchy bands using Velcro tape and placed on adult volunteers in two different arrangements as shown in Figure 5.4.

The first arrangement represented the typical ECG sensor placements of Lead I where the ECG sensors are placed on RA and LA setup. On the other hand, the second arrangement represented the sensor placements on the accessible skins of the newborns in the delivery room (FH and LFA). The distance between the DRL and forearm sensor was set to be 30cm. The two arrangements were used on four adult volunteers to record ECG signals using three conductive fabric materials: SP31, Medtex P130 and Laird 3080–500. The recorded ECG is shown and discussed in the next section.

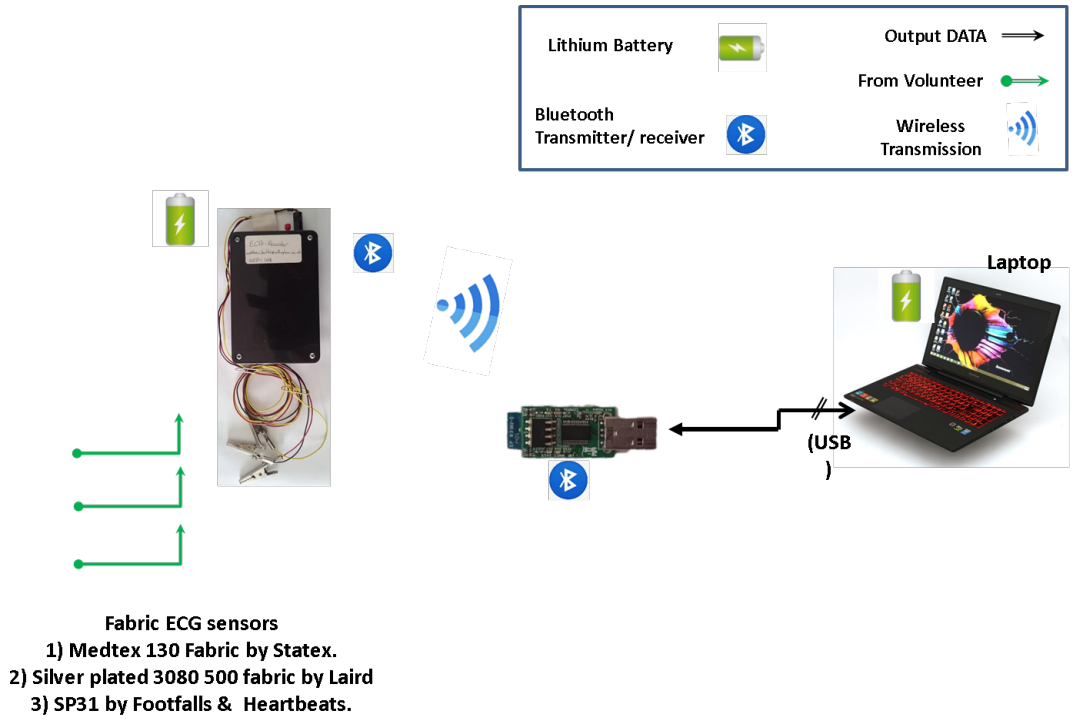


Figure 5.3: The system used to collect ECG signals over Bluetooth from adult volunteers using fabric sensors in the setups shown in Figure 5.4.

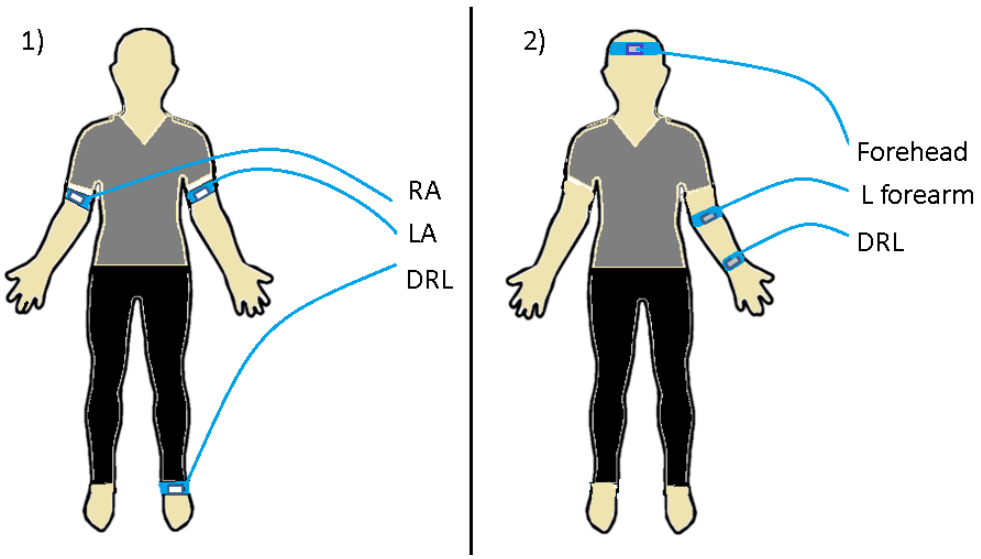


Figure 5.4: Fabric sensors placement arrangements on adult volunteers: (1) Left arm and right arm while the DRL was connected to left leg, and (2) Left forearm and forehead, while the DRL was connected to left wrist.

5.2.2 Results

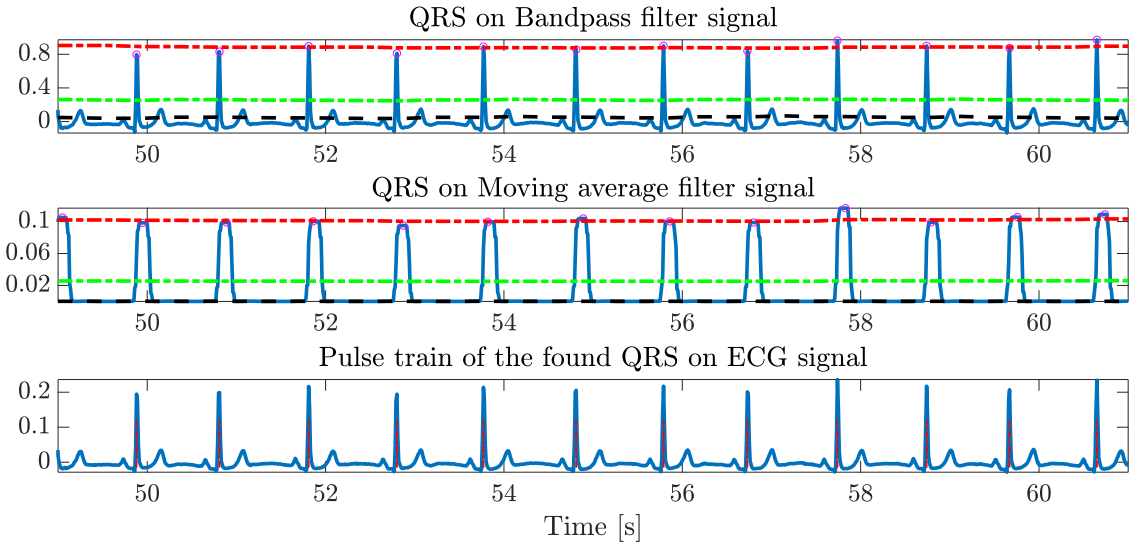
The conductive fabrics coupled the ECG signals with good quality from adult volunteers using the arrangements of LA, RA and LL in setup (1). The ECG morphology was recognisable before additional digital processing. The ECGs collected from the ECG recorders using Sp31, Medtex P130 and Laird 3080–500 were processed to extract the heart rate using the QRS detection based on Pan and Tompkins's algorithm discussed in Chapter Three, Section 3.5. The QRS detection accuracy was 100% among the ECGs collected by Medtex P130 and Laird 3080–500 fabrics. Samples of the processed signals of an adult volunteer ECG by Medtex and Laird are shown in Figure 5.5a and 5.5b. The ECG signals collected from the forehead and forearm had almost the same quality as the previous setup. The QRS detection accuracy was $\simeq$ 100% by Medtex P130 and Laird 3080–500 as shown in Table 5.1. Samples of the processed signals of an adult volunteer ECG by Medtex and Laird are shown in Figure 5.6b and 5.6a.

On the other hand, the ECG signals collected using SP31 fabric were distorted and noisy in both arrangements. The heart rate extraction was not applicable because the signal artefacts were similar to R peaks, as shown in Figure 5.7a and Figure 5.7b. The summary of the QRS detection accuracy of these different setups is shown in Table 5.1.

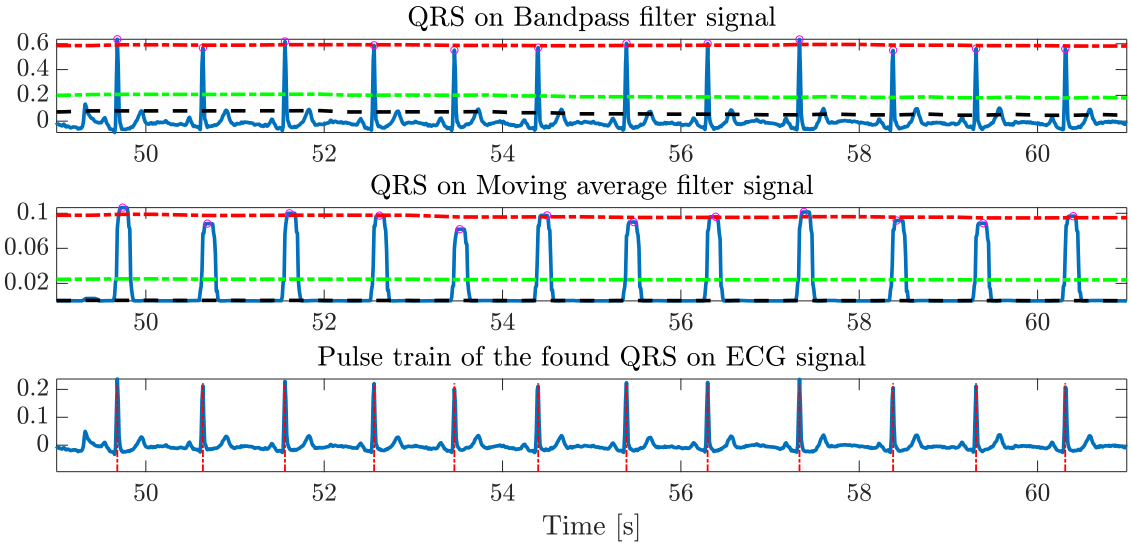
Based on these results, Medtex P130 made by Statex and Laird 3080–500 made by Laird Tech were considered for further experiments on both adult and baby volunteers. Both fabrics are certified to be used with medical devices, according to ISO 10993. Statex company had provided an additional certificate to prove that their fabric is classified as class I product by OEKO-TEX® ®standard 100 established for baby articles and the inspection was done according to ISO 17050-1. All these certificates were included in Appendix A.

The SP31 fabric had been withdrawn from further experiments because of the poor quality of collected ECG signals and because Footfalls and Heartbeats company did not provide additional fabric samples to produce different sized sensors. Moreover, Footfalls and Heartbeats did not make it clear that they had safety certificates enabling the fabrics to be tested on babies.

This experiment confirmed that the ECG signal could be collected from adults' forehead and forearm using the conductive fabric sensors made of Medtex P130 and Laird 3080–500 bio-compatible materials. Unlike the other types of ECG dry sensors, the fabric was very flexible and could be easily bent around the forehead and arm without creating dis-bonds or air gaps. The QRS detection was high in all the ECGs

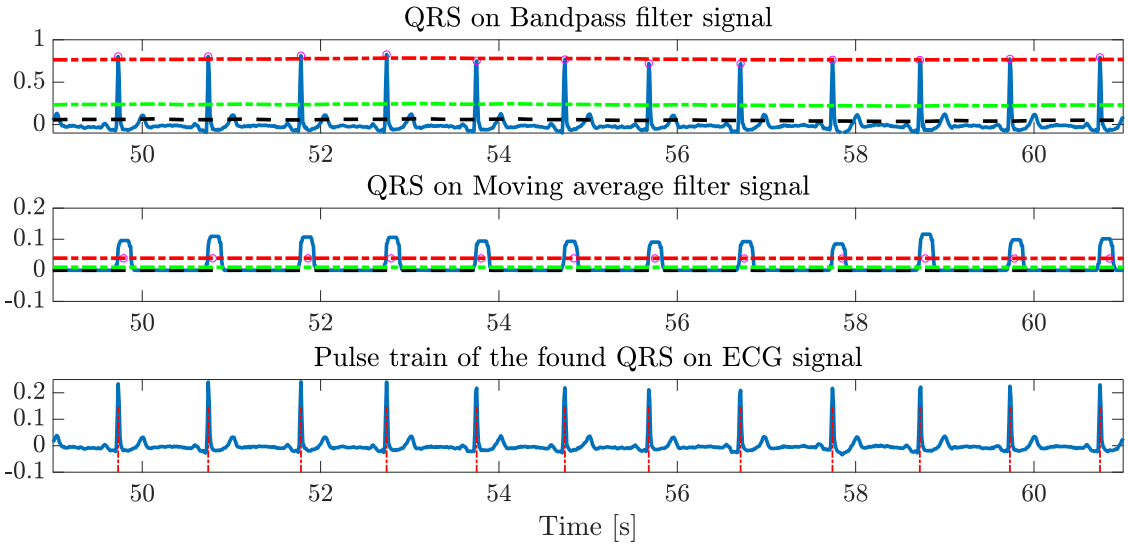


(a) Medtex P130 Fabric.

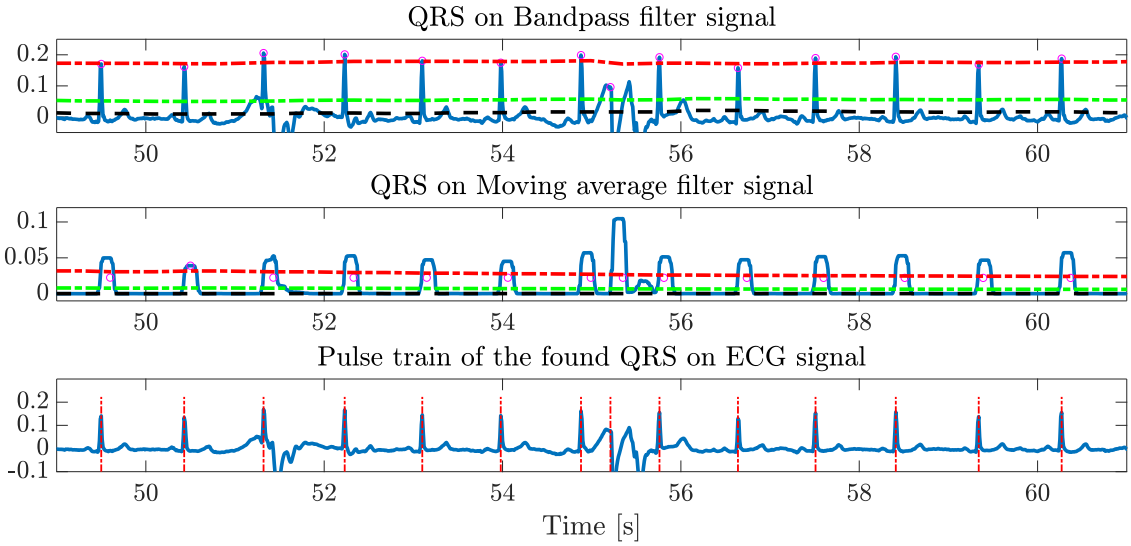


(b) Laird 3080–500 Fabric.

Figure 5.5: Sample of QRS detection on adult ECG signals recorded from (LA, RA, LL DRL). It shows the detected QRS on bandpass, moving average raw ECG signals with noise level (Black), signal level (Red) , adaptive threshold (Green) and the QRS detection (Pulse train).

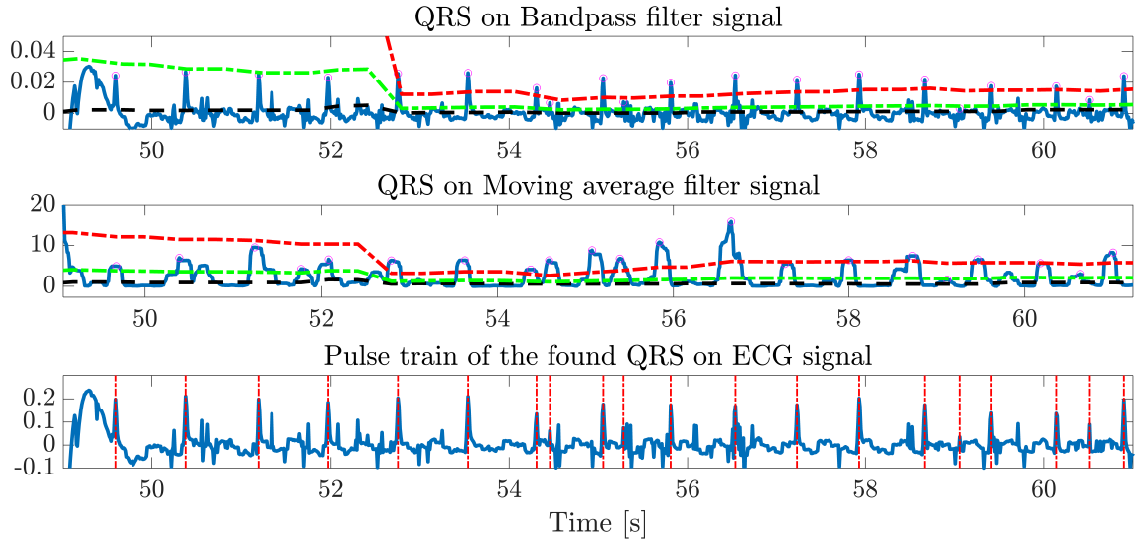


(a) Medtex P130 Fabric.

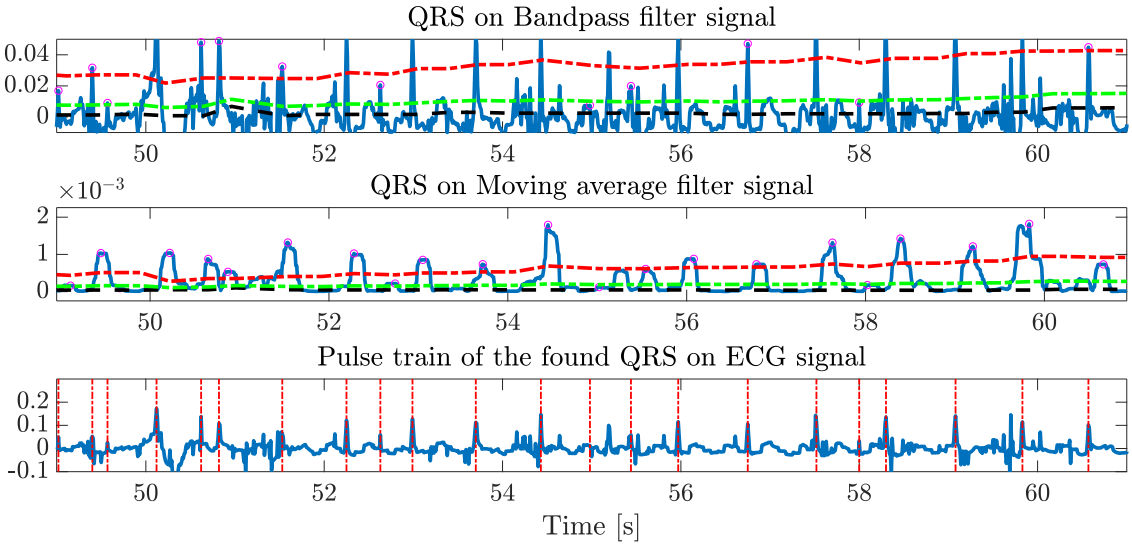


(b) Laird 3080–500 Fabric.

Figure 5.6: Sample of QRS detection on adult ECG recorded from (Left forearm, Forehead, Wrist DRL). It shows the detected QRS on bandpass, moving average raw ECG signals with noise level (Black), signal level (Red) , adaptive threshold (Green) and the QRS detection (Pulse train).



(a) LA,RA and LL DRL by SP31



(b) Left forearm,Forehead and Wrist DRL by SP31

Figure 5.7: Sample of QRS detection on adult ECG recorded using SP31 fabric. It shows the detected QRS on bandpass, moving average raw ECG signals with noise level (Black), signal level (Red) , adaptive threshold (Green) and the QRS detection (Pulse train)..

Gender/age/ placement of volunteers	SP31 by Footfalls and Heartbeats	Laird 3080–500 by Laird Tech	Medtex P130 by Statex
Male 25Y LA, RA	NA	100%	100%
Male 25Y LA, Forehead	NA	99.5%	100%
Male 29Y LA, RA	NA	100%	100%
Male 29Y LA, Forehead	NA	100%	99.2%
Female 27Y LA, RA	NA	99.3%	100%
Female 27Y LA, Forehead	NA	99.2%	99.0%
Male 29Y LA, RA	NA	100%	100%
Male 29Y LA, Forehead	NA	98.7%	99.1%

Table 5.1: The QRS detection accuracy of adult ECG signals collected by wireless ECG recorder using three types of fabric sensors. Samples of the yellow colour row data was shown in this Chapter.

collected from arms or the forehead, as shown in Table 5.1. Based on these findings, Medtex P130 and Laird fabrics were further tested in the next experiment with a certified ECG monitor (GE B450) instead of the wireless ECG recorder. The next experiment was designed to determine if the DRL and the left arm sensor can be fit together within the size of a newborn forearm.

5.3 Fabric Sensors With GE B450 ECG/PPG Monitor

In the first experiment explained above, three types of conductive fabrics were applied to volunteers in order to test the ability of these fabrics to collect ECG signals from using forehead and forearm sensors. Medtex P130 and Laird 3080–500 sensors had

coupled good quality ECG from volunteers with high SNR that allowed accurate QRS detection and heart rate extraction with more than 99% accuracy. The ECG signals collected by SP31 fabric were dominated by noise and motion artefacts, and hence, this fabric was excluded from further experiments. Both Medtex P130 fabric Laird 3080–500 fabrics were certified by the compatibility standard of ISO 10993 to be used with medical devices. These fabrics were used to couple ECG signals in the next three experiments, two of the experiments were applied on adults, and the third experiment was applied to babies. The adult's experiments were designed to investigate the best sensors placement, which would be suitable for the newborn size.

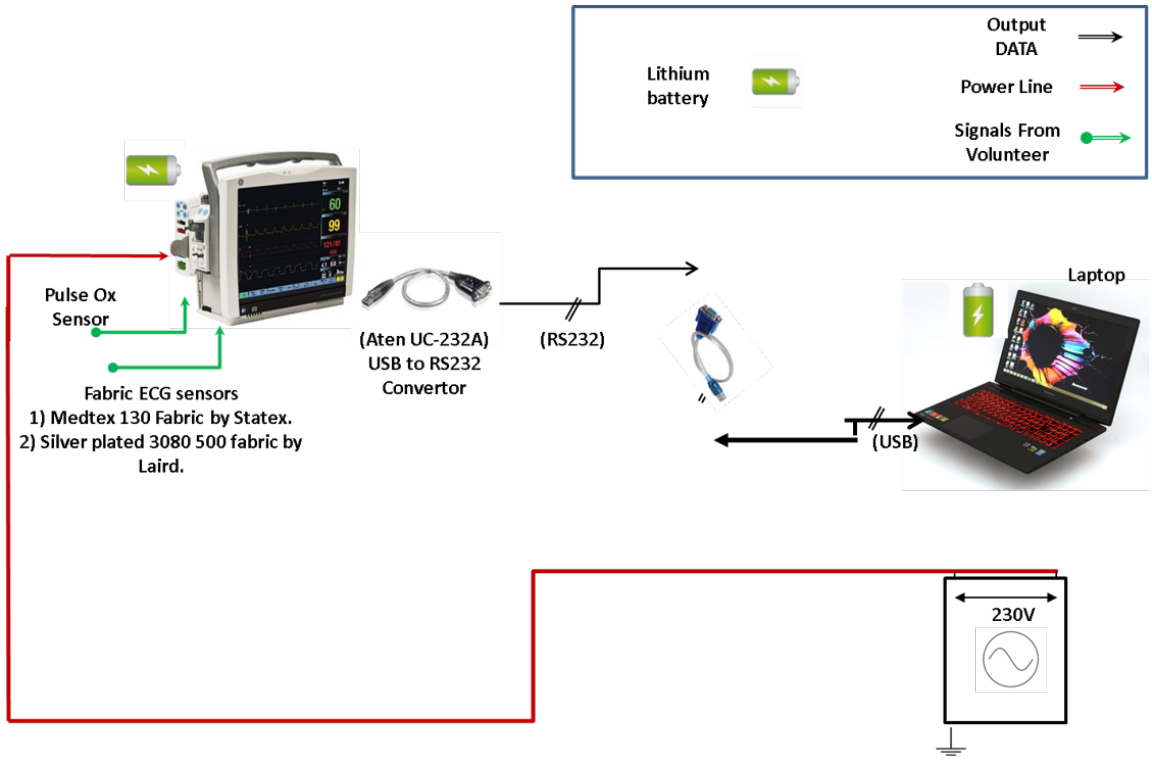


Figure 5.8: The setup of the system that used to record ECG signals from adult and babies volunteers using GE B450 monitor. GE monitor could be powered by either the mains power or Lithium batteries.

During these experiments, the fabric sensors were connected to a certified ECG/PPG monitor GE-B450 to collect ECG signals from foreheads and forearms of volunteers. The GE B450 unit is typically used in the hospitals to monitor the heart rate and the oxygen saturation levels of the patients by collecting the ECG and PPG signals. The schematic design of the GE B450 differential monitor was not published by the vendors and is considered intellectual property. The ECG/PPG acquisition system shown in Figure 5.8, was connected to fabric sensors for the ECG recording and a

pulse oximeter for PPG recording, as a comparator. The sensors were held to stretchy cotton bands using Velcro tape and were strapped around forearms and foreheads of the volunteers. The fabric sensors were connected to the GE450 unit using the press stud cables, as shown in Figure 5.9. The different setups of ECG experiments using GE B450 monitor are discussed in the next sections.

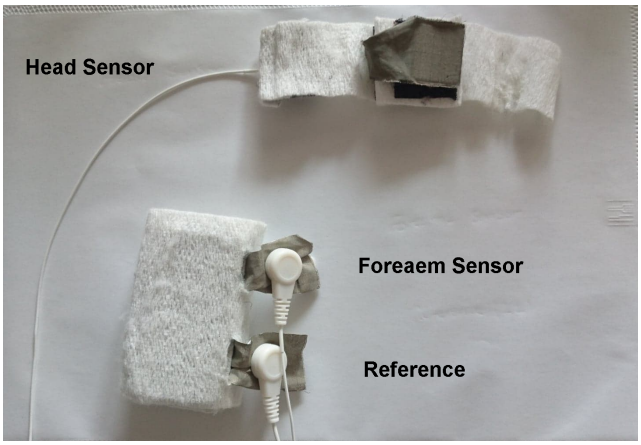


Figure 5.9: The fabric sensors were connected to GE B450 unit using press studs cables while the sensors were attached to stretchy bands.

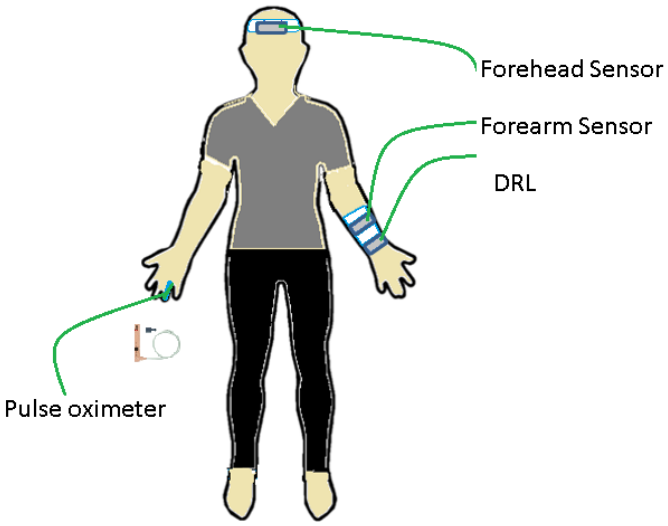


Figure 5.10: The GE B450 setup that used to record ECG and PPG signals from adult volunteers using the conductive fabric sensors (silver plated) and the pulse oximeter.

5.4 Experiment Two: GE B450: Sensors' Placement

5.4.1 Experimental Setup

As shown in the previous section, Medtex P130 and Laird 3080–500 were used successfully to record ECG signals from adult volunteers with a QRS detection accuracy of more than 90%. The next experiment aimed to optimise the sensor's placement for the average newborn size. GE B450 monitor was used to collect ECG signals from adult volunteers using fabric sensors as discussed in the previous section. PPG signals were also collected from the adult right index finger, simultaneously with ECG.

In order to optimise the placement of the sensor, two factors should be determined: (1) The size of the sensors to be applied for babies which are restricted by newborns' wrist circumferences, and (2) The size of armband which should hold the forearm sensor and DRL which is restricted by newborns' forearm length. The area of the ECG sensor has been linked to the introduced noise in the literature, where the noise is inversely proportional to the square of the ECG sensors' area [58]. On the other hand, the area of the sensor was restricted by the size of newborn babies and their measurements (wrist circumferences and forearm length). Chapter Three, Section 3.3.2 has discussed the placements of the fabric sensors on babies and concluded that according to newborn babies measurements restrictions, the sensor width should not exceed five centimetres. Also, the length of newborns forearm band which will be used to hold the forearm and DRL shall not exceed six centimetres, which is the average length of babies' forearms. Otherwise, two bands are needed to place the DRL and the ECG sensor.

This experiment was designed to find out the possibility of placing the DRL the forearm ECG sensor and hence using a single armband for both sensors. The function of Driven Right Leg is to reduce the power-line interference of 50 Hz coupled in the common mode of bio-potential amplifiers and is used widely to increase ECG signal to noise ratio especially in smart textiles applications [138, 139]. However, when the amplifiers are isolated, the DRL could increase the differential mode interference or affect it in an unpredictable way [100].

Three different ECG sensors arrangements were applied to adult volunteers in order to compare the DRL placement with the DRL absence in terms of signal quality. The ECG quality was compared by measuring the SNR of each setup outputs.

These different arrangements are shown in Figure 5.11, where the same sensor' size was used with different DRL placements. In the first setup in Figure 5.11 (a), the DRL was eliminated, and only two sensors were applied on forehead and forearm

with the size of 2.5cm×3cm. In setup (b), the DRL was placed on the wrist of the volunteers, five cm away from the forearm sensor. In setup (c), the DRL was placed one centimetre away from the forearm sensor.

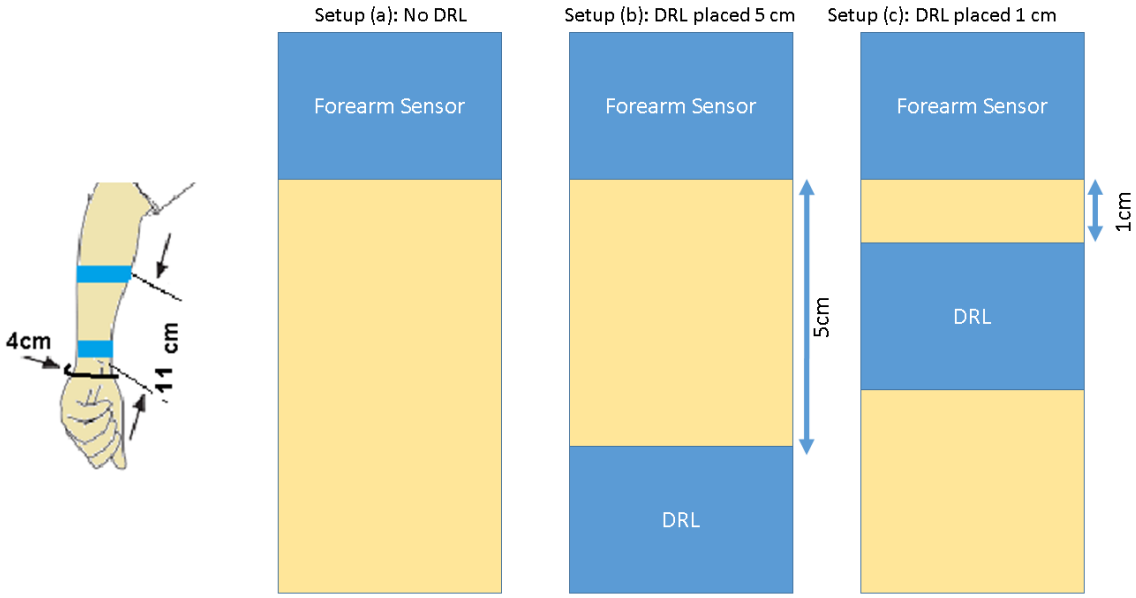


Figure 5.11: Three different arrangements of the DRL placements on the adult volunteers forearms. The size of each of the senors was 2.5cm×3cm

The GE B450 monitor was used to record ECG and PPG signals from adults while it was connected to the main power. The laptop used to collect the data from the monitor was working on batteries during the ECG recording to minimise the effect of 50 Hz interference. The GE B450 data was collected by Labview software and processed by Matlab. The three setups in this experiment were applied to ten different adult volunteers using Medtex P130 and Laird 3080–500 fabrics. The signal to noise ratios were calculated from the sixty ECG signals In order to find out the setup that achieved the highest SNR.

The signal to noise ratio was calculated after filtering the ECG signal with a high pass filter and IIR notch filter. The cut off frequency of the high pass filter was set to 0.05 Hz in order to preserve the ECG signal morphology. The high pass filter cut off frequency is recommended not to exceed the 0.05 Hz limit for ECG signal processing [68]. The IIR notch filter was used to remove the 50 Hz noise with a bandwidth of

1.4 Hz. The SNR is calculated in dB from the filtered and raw ECG signal as follows:

ECG_{raw} Raw ECG signal;

$ECG_{filtered}$ Filtered ECG signal;

The noise in the signal is calculated from the difference between the raw and filtered signals:

$$Noise = ECG_{raw} - ECG_{filtered} \tag{5.1}$$

Then the signal and noise RMS were calculated according to Equations 5.2 and 5.3:

$$RMS_{signal} = \sqrt{(mean(ECG^2_{filtered}))} \tag{5.2}$$

$$RMS_{noise} = \sqrt{(mean(Noise^2))} \tag{5.3}$$

And the SNR was calculated as the ratio between the signal and noise RMS values, and it is converted to dBs as follows:

$$SNR_{dB} = 20 * \log_{10} \frac{RMS_{signal}}{RMS_{noise}} \tag{5.4}$$

5.4.2 Results

5.4.2.1 DRL Placement Setups

The ECG in this section were recorded from ten different adults, while sitting on a chair in a lab full of electrical equipment. The medically approved GE B450 monitor used for the ECG recording, was powered by mains power. The three setups shown in Figure 5.11 were used to record the ECG for five minutes from each volunteer. Sixty ECG signals were recorded in total from ten adults, three different setups and using two different types of fabrics.

The ECG signals collected in setup (b), when the DRL was placed 5 cm away from the forearm sensor, had the best quality and the highest signal to noise ratio among the three setups for all the volunteers. Moreover, unexpectedly setup (c), where the DRL was placed 1 cm away from the forearm sensor, provided the ECG signals with the lowest SNR. Typically, the DRL is designed to decrease the main power interference, but in this experiment, the DRL placement increased the interference compared to the DRL absence. Samples of ECG signals that were recorded from one

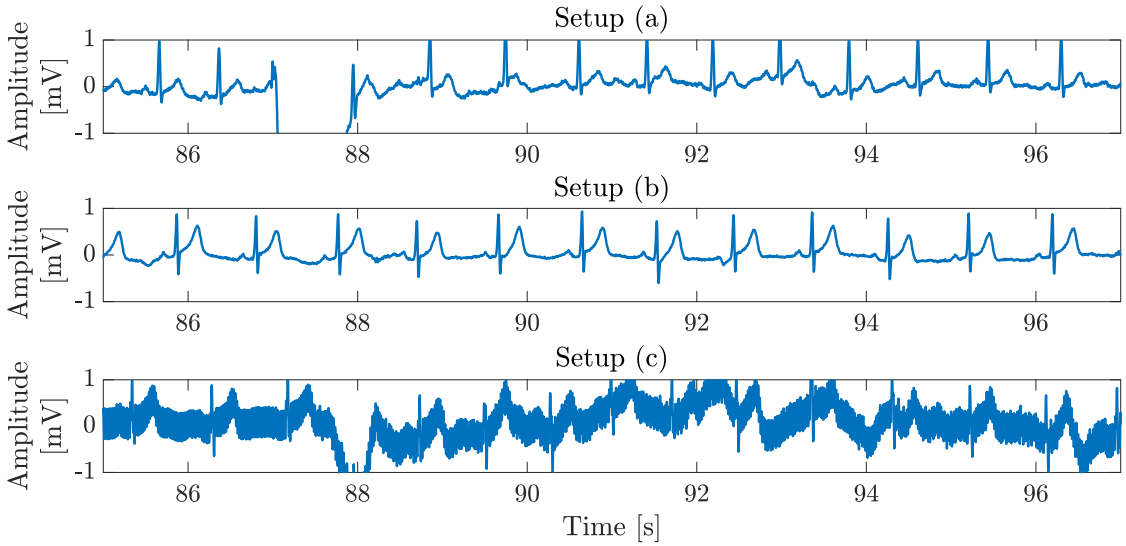


Figure 5.12: ECG samples collected from an adult volunteer using three different arrangements of Laird 3080–500 fabric sensors. (a) No DRL, (b) DRL was placed 5cm from forearm sensor, and (c) DRL was placed 1 cm from forearm sensor.

volunteer in the three setups using Laird 3080–500 and Medtex P130 are shown in Figure 5.12 and 5.13. The 50 Hz power is the highest in signals recorded in setup (c) and the lowest among the signals recorded in setup (b). The DRL sensor had a clear negative impact on the differential mode signal when it was placed closer to one of the sensors. The average of the SNR for these different setups is shown in Table 5.2. In the next experiments, the DRL placement was repeated on the volunteers while the ECG monitor was working on batteries for better understanding of the effect.

It could also be seen that Medtex P130 fabric had coupled ECG signals with higher SNR than Laird 3080–500. Bioimpedance measurements were conducted using the two fabrics in order to find out the interface impedance for Medtex and Laird fabrics.

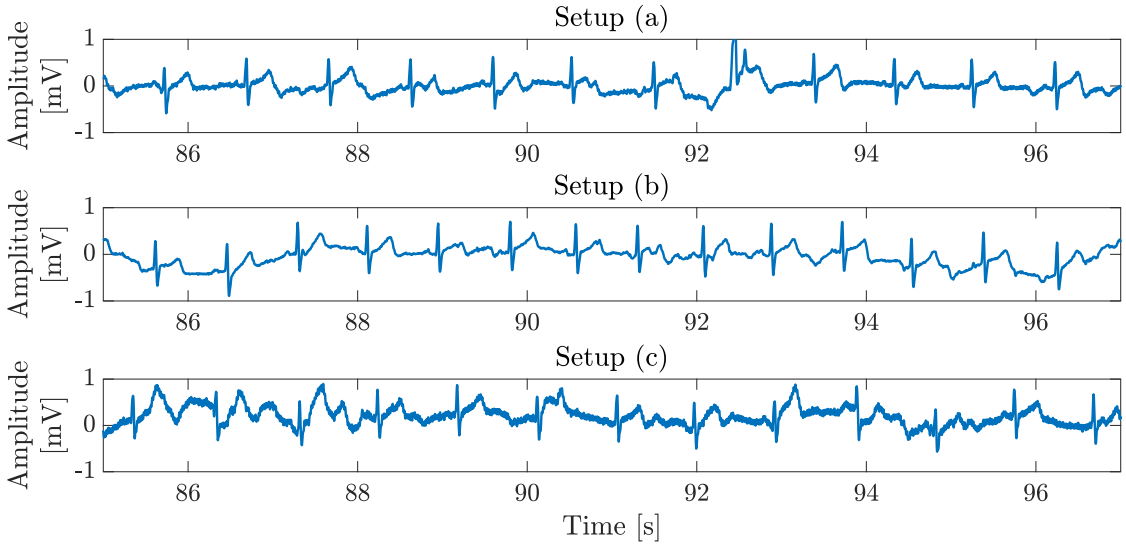


Figure 5.13: ECG samples collected from an adult volunteer using three different arrangements of Medtex P130 fabric sensors. (a) No DRL, (b) DRL was placed 5 cm from forearm sensor, and (c) DRL was placed 1 cm from forearm sensor.

Sensors' Setup	**SNR of Laird 3080–500 (dBs)**	**SNR of Medtex P130 (dBs)**
No DRL	29.02	30.83
DRL placed 5 cm from forearm sensor	32.17	35.32
DRL placed 1 cm from forearm sensor	20.77	27.47

Table 5.2: The average signal to noise ratio of ECG signals that were collected from ten adult volunteers in three different setups shown in Figure 5.11. The GE B450 monitor was connected to the main power during the recording.

5.4.3 PPG Comparison to ECG

As mentioned earlier, the PPG signal was collected simultaneously with the fabric ECG to test the robustness of the collected ECG signal. The two signals were compared for the HR detection in terms of fast coupling and robustness to motion artefacts. The PPG signal took a few seconds at the beginning of the recording before showing the signal, while the ECG signal started immediately from the adult volunteers, as shown in Figure 5.14.

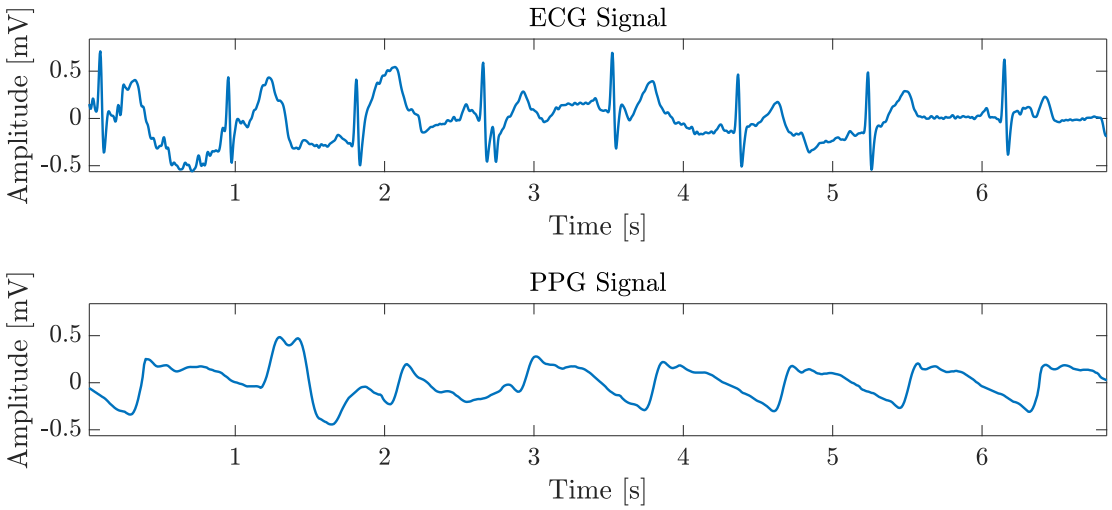


Figure 5.14: The PPG signal took time to start at the beginning of recording, while the ECG signal started immediately.

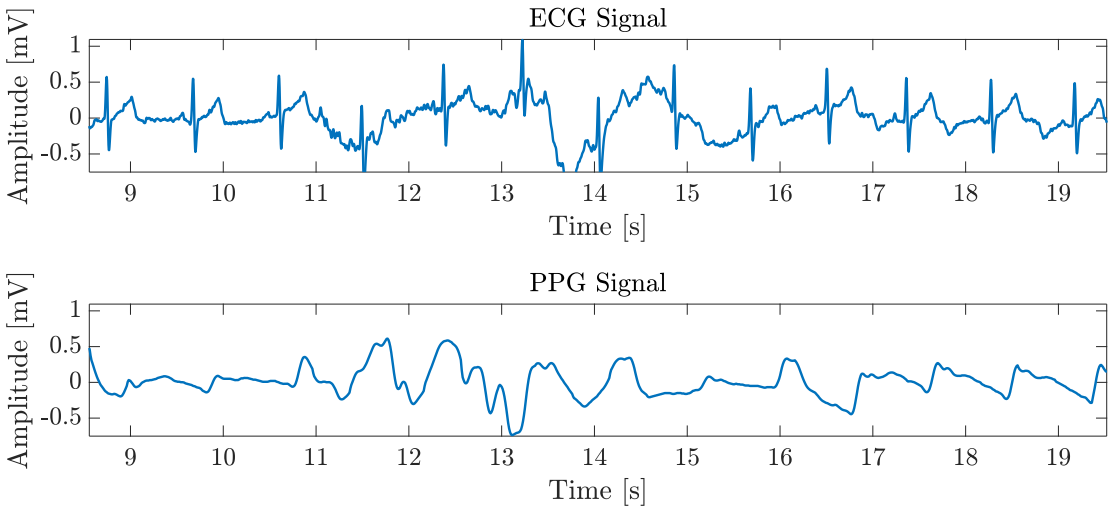


Figure 5.15: The ECG signal was more robust to mild movements, while the PPG signal was affected.

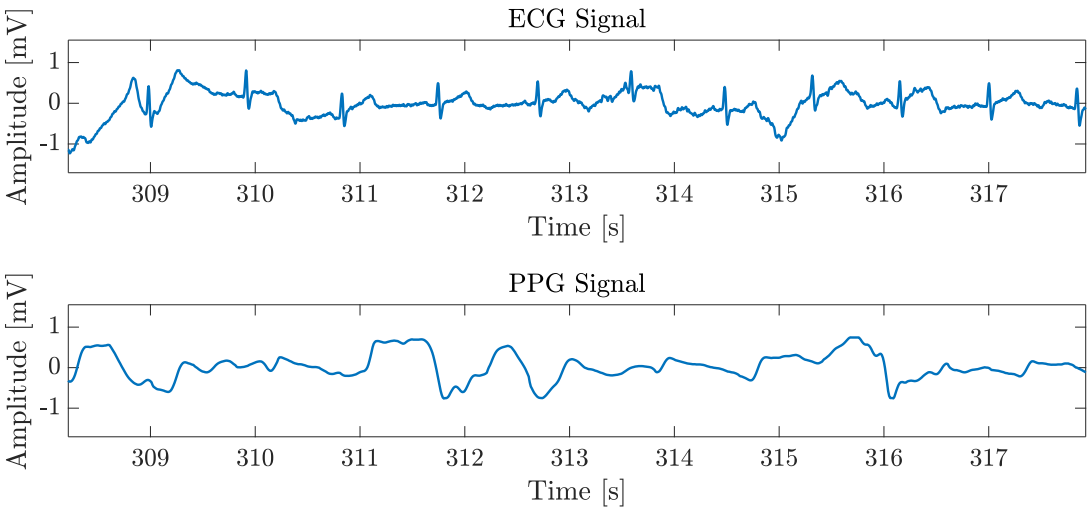


Figure 5.16: The PPG signal was completely distorted by motion artefacts, while the ECG signal was still detectable.

The ECG signal was more robust to motion artefacts and friction, as shown in Figures 5.15 and 5.16. The PPG signal gets easily distorted when the volunteer moves the arms or the forehead slightly. One minute of the PPG/ECG recordings using Medtex and Laird's fabrics are available in Appendix C. In order to quantify the comparison, the ECG signals were processed by the QRS detection algorithm in order to quantify the accuracy of the detection. The percentage of the detectable PPG signals were calculated visually by calculating by subtracting the duration where the PPG signal was entirely distorted by movement artefacts. This analysis was performed on the sixty collected PPG signals, and the summary is shown in Table 5.3.

Sensor and system	Signal type	# Recordings	Average percentage of detectable Signal
Medtex P130 fabric, GE B450	ECG	30	99.3%
Laird 3080–500 fabric, GE B450	ECG	30	98.6%
GE pulse oximeter, GE B450	PPG	60	91.2%

Table 5.3: The average percentage of the detectable ECG and PPG signals collected of 5 minutes recordings.

5.5 Experiment Three : DRL Placement Effect

In the previous experiment, when the DRL was placed on the adult volunteer wrist 1cm from forearm sensor, the signal quality deteriorated even when compared with no DRL at all. This means the close placement of DRL had coupled 50 Hz noise in differential mode. There are a few studies in the literature that have discussed that the DRL can adversely impact an ECG signal quality if the device used is isolated according to the safety standards. Gomez in 2011 [100] have concluded that the DRL can couple 50 Hz noise in the differential mode, in an unpredictable way, when the isolated device is connected to the power lines. In order to investigate the matter of DRL placement, the following experiment was designed to be carried out on adult volunteers.

5.5.1 Experimental Setup

In this experimental setup, the GE B450 unit was used to collect the ECG signal from adult volunteers using Medtex P130 fabric. The objective of the experiment was to investigate the effect of placing DRL close to forearm sensors when the GE B450 was powered by battery, and when it was powered by mains power. The area of Medtex P130 sensors used in this experiment, in contact with the skin, was 2.5cm×3cm.

Two setups were used in this experiment, as shown in Figure 5.17. In the first setup, no DRL was used, and in the second setup, a DRL was placed only 1 cm further from the forearm sensor. These two setups were used to record ECG signals

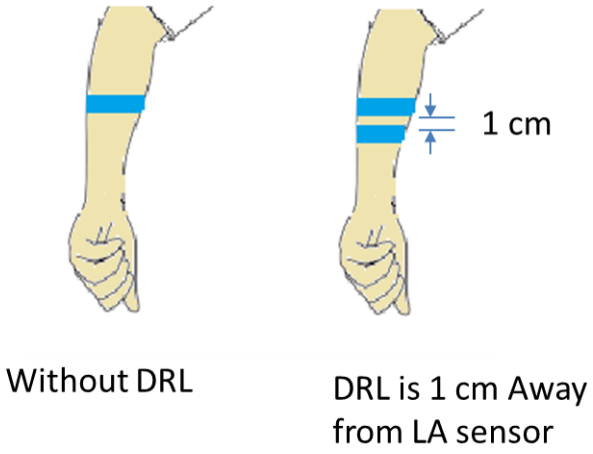


Figure 5.17: Setup of ECG recording with and without DRL. The DRL was placed 1 cm from the forearm sensor.

from adult volunteers when the GE B450 was connected to the power lines and when it was working on batteries. The laptop used to collect the signals was disconnected from mains power to minimise the interference effect. This experiment was applied to four adults and recorded four ECG signals from each volunteer for five minutes.

5.5.2 Results

Sixteen ECG signals were collected in total, from four adult volunteers in different four setups. Samples of ECG signals which were collected when the GE B450 monitor was connected to the mains power are shown in 5.18. While samples of the ECG collected when the monitor was on the battery are shown in 5.19. When the GE monitor was connected to the mains power, the DRL placement decreased the SNR of the ECG. On the other hand, when GE monitor was working on batteries, the DRL placement increased the SNR and enhanced the signal in general. Table 5.4 shows the average SNR calculated for all four setups.

As a conclusion for this experiment and the previous one, the DRL would be applied 5cm or more from the forearm sensor to prevent increasing the interference in the differential mode. Since the average forearm length of the newborns is 62mm [106], then the DRL and the sensor would not be fit in the forearm together. The ECG sensor should be placed on the left arm instead of the forearm, and the DRL should be placed on the wrist.

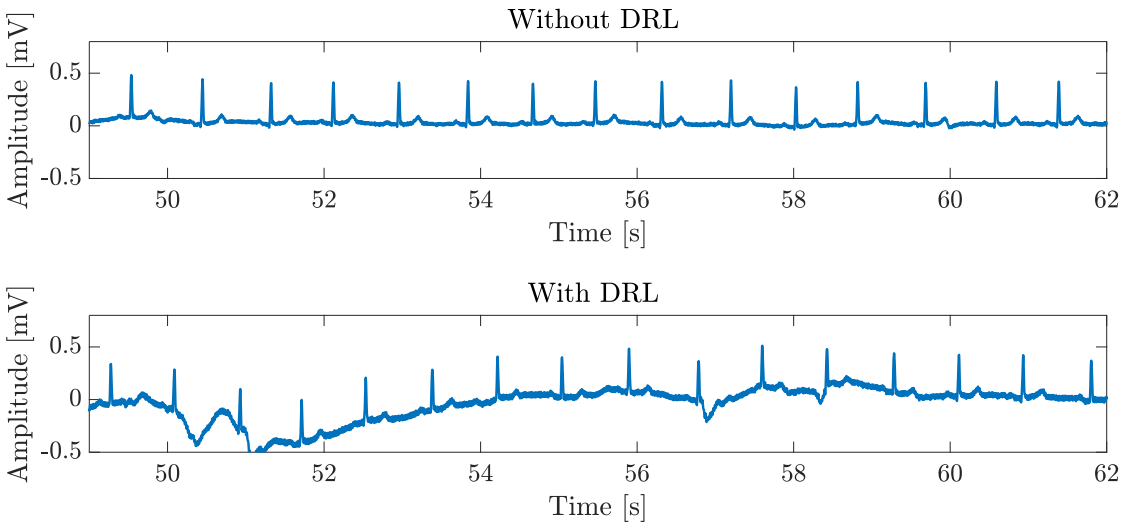


Figure 5.18: ECG samples collected from adult volunteer by GE B450 when the monitor was powered by the mains power.

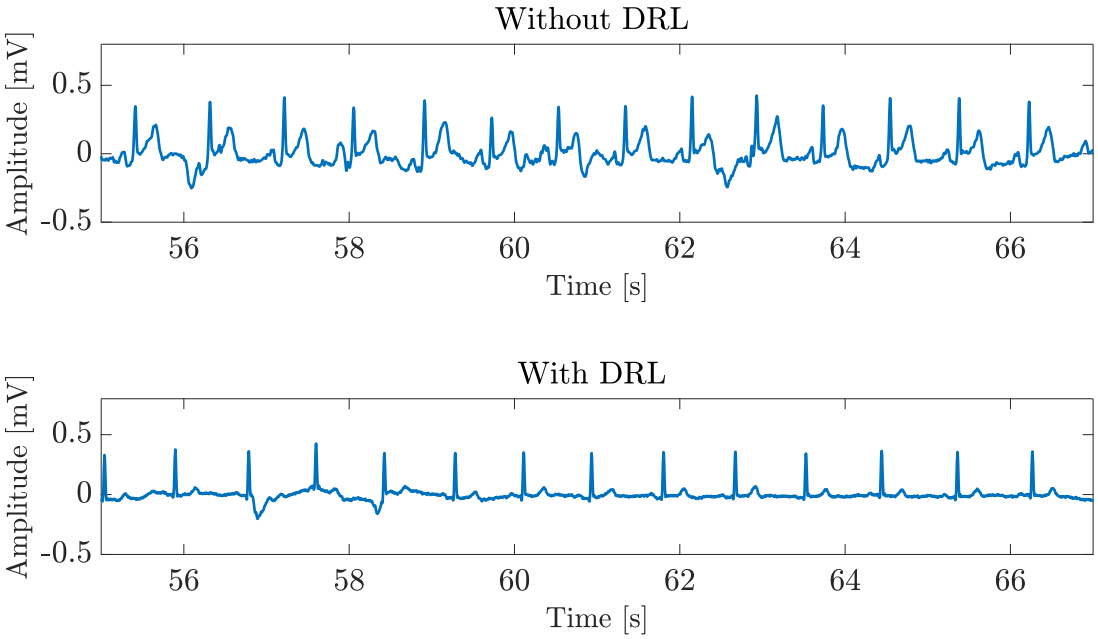


Figure 5.19: ECG samples collected from adult volunteer by GE B450 when the monitor was powered by Lithium battery.

Setup	Average SNR without DRL	Average SNR with DRL
Mains power	29.3	25.6
Battery	31.5	34.7

Table 5.4: The signal to noise ratio (dBs) of ECG signals that were collected using GE B450 monitor. Four different combinations were used from placing the DRL and changing the power source of the ECG monitor.

5.6 Experiment Four: Fabric ECG Sensors on Babies

5.6.1 Experimental Setup

The aim of the previous adult experiments using the GE B450 ECG monitor was to investigate the best placement of ECG sensors. The outcome of these experiments suggested that the DRL should be placed further from the forearm sensor. For the babies experimental setup, three bands were used to hold the sensor: headband for the forehead sensor, armband for the arm sensor and wrist band for the DRL as shown in Figure 5.20. The left arm was used because the right arm is usually used to place the pulse oximeter during the delivery room resuscitation [140, 141]. The setup was applied to four babies of $9 - 34$ weeks of age.

The ECG signals were collected using the GE B450 from four different babies using two types of fabric sensors, Medtex P130 and Laird 3080–500. The sensors were sewn on a headband to hold the forehead sensor, a stretchy armband to hold the arm sensor, and additional wrist band to hold the DRL as shown in Figure 5.20. The gender and age of the babies at the time of the experiment were: Female 9 weeks, Female 20 weeks, Male 27 weeks and Female 34 weeks. Another volunteer of the age of 65 weeks had been eliminated from the results because she had more motion artefacts due to bigger muscle and better movement abilities.

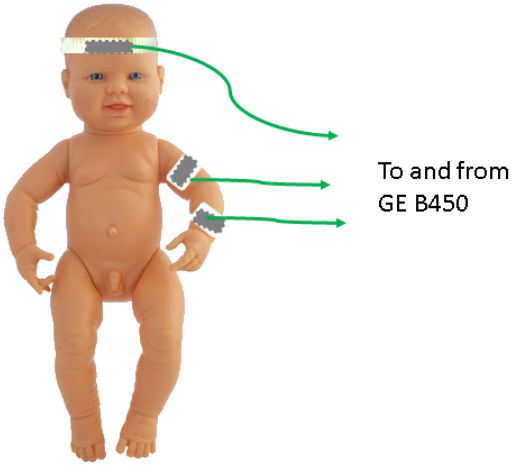


Figure 5.20: Proposed fabric placements on newborn babies in the delivery room. The headband used to hold the forehead sensor, while the armband used to hold the arm sensor, and the wrist band was used to hold the DRL.

5.6.2 Results

The experiment was initially planned to use a pulse oximeter on the right wrists of the babies as a comparator but was later withdrawn in order to make the experiment more comfortable to the babies. Samples of ECG recordings using both types of fabrics: Medtex P130 and Laird 3080–500 are shown in Figure 5.21. The figure shows that the ECG signal was successfully collected from the forehead and arm of the babies using the GE B450 monitor with both types of fabric sensors-Medtex P130 and Laird 3080–500. Table 5.5 shows the QRS detection accuracy of the ECG signals collected from the four volunteer babies. As the baby gets older, his motor skills improve, which affects the dry contact of the fabric sensors negatively. The detectable ECG signal decreases with age as the motion artefacts increase. The above results indicate that, in general, the ECG signals collected using Medtex P130 had better quality than ECGs recorded using Laird 3080–500. In order to investigate this, another experiment was carried out to understand the skin interface impedance of both types of fabrics. A bio-impedance experiment, discussed in the next section, was designed to measure the dry contact impedance to a better understanding of the results obtained from the baby and adult volunteers.

One of the babies was excluded from these calculations; she was much older than other babies (65 weeks), and the motion artefacts were significant in her signals. Figure 5.22 shows sample of the artefacts. only 28% of her ECG signal was detectable due to her active movements during the data collection.

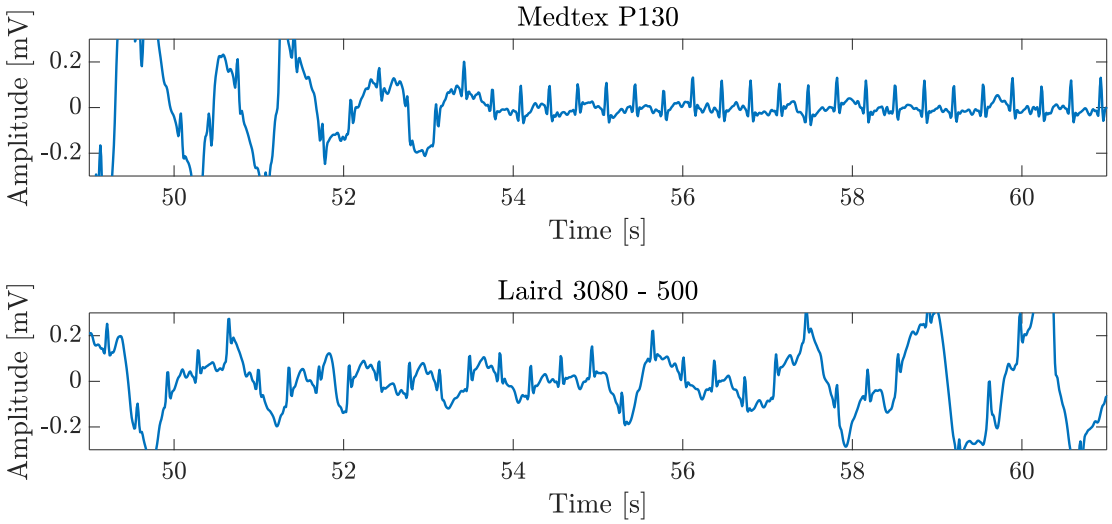


Figure 5.21: Samples of ECG recordings from babies using Medtex P130 and Laird 3080–500 fabrics.

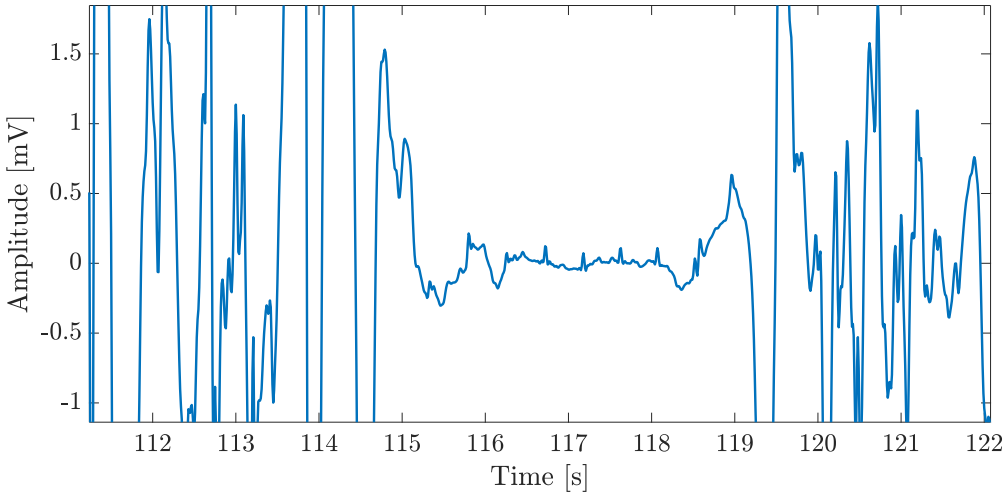


Figure 5.22: Sample of ECG recorded from 65 weeks baby. The signal was heavily affected by the baby's movements.

Baby Gender/age	**QRS accuracy (Medtex P130)**	**QRS accuracy (Laird 3080–500)**
Female 9W	97.5% 621/637	95.5% 625/654
Female 20W	95.9% 589/614	93.2% 567/608
Male 29W	94.2% 541/574	94.6% 556/588
Female 34W	92.7% 502/542	88.7% 492/554
Average	95.1%	93%

Table 5.5: The QRS accuracy of ECG signals that were collected from four babies by GE B450 monitor connected to mains power using Medtex P130 and Laird 3080–500 as ECG fabric sensors. Samples of the yellow colour row data were shown in this chapter.

5.7 Experiment Five: Bioimpedance measurements on Adults

The ECG results from baby volunteers in the previous section indicated that both Medtex P130 and Laird 3080–500 fabrics sensors had successfully collected ECG signals from forehead and arm. However, the ECGs collected by Medtex P130 from both adult and babies had higher SNR and better QRS detection. The resistivity of both fabrics are almost the same according to their data sheet; both of the fabrics' resistors are less than 2 Ω/square. In order to understand the reason behind this slight difference, the skin interface for both fabrics has been investigated.

As discussed in the previous Chapter, Section 4.7.2, the interface between the dry contact ECG electrodes and the skin could be modelled by a half cell with a parallel resistor and capacitor. The dry interface impedance measured from the adult's wrists in the previous chapter was 7.89 MΩ at 1 Hz. In this section, a bioimpedance measurement experiment has been carried out on an adult volunteer to find out the interface impedance of the Medtex P130 and Laird 3080–500 from the forehead and left arm. Solartron impedance analyser (1260) was used with the bio-impedance interface (1294) to measure the skin impedance interface using Medtex P130 and Laird fabrics, as shown in Figure 5.23.

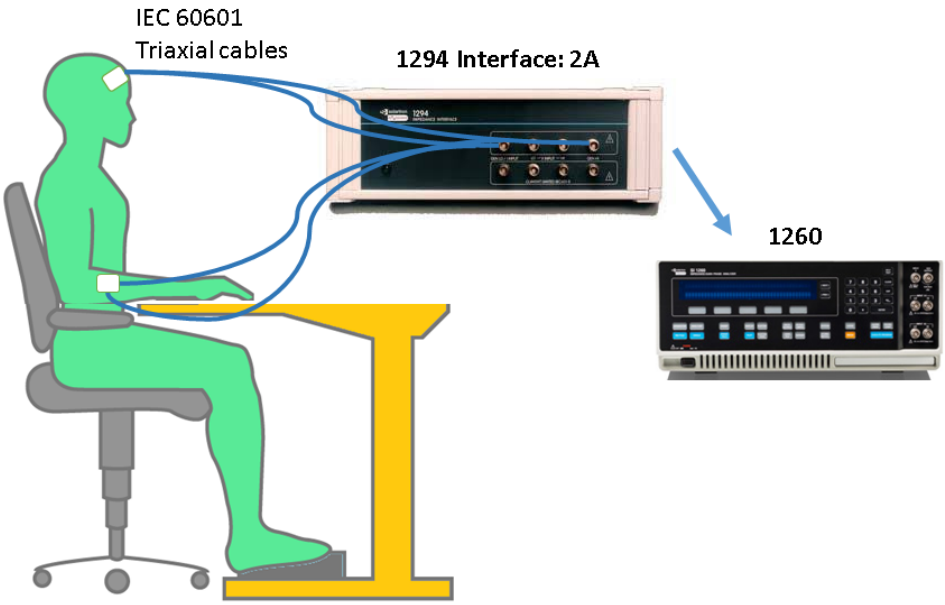


Figure 5.23: The fabric sensors with area of 2.5cm*3cm were applied on adult volunteer head and forearm to measure the skin interface bio-impedance.

The fabric sensors with the area of 2.5cm×3cm were attached to the forehead and forearm of the adult volunteer using stretchy bands. The sensors were connected to the bio-impedance measurement system using triaxial cables which were manufactured according to IEC 60601 safety standards. The system analysed the skin/sensor interface impedance in the frequency domain. The first experiment was to measure the interface bio-impedance of fabric Medtex P130 and then the experiment was repeated using Laird 3080–500. The impedance measurement system was discussed in further detail in Chapter three, Section 3.4, and shown in Figure 3.14.

The bio-impedance measurements of Medtex P130 and Laird 2080-500 fabrics are shown in Figure 5.24. The figure shows that the interface impedance of Medtex P130 was lower than Laird 3080–500, which explains the slight difference in the quality of collected ECG signals. The impedance at 1 Hz is 418 kΩ for Medtex P130 and 740 kΩ for Laird 3080–500.

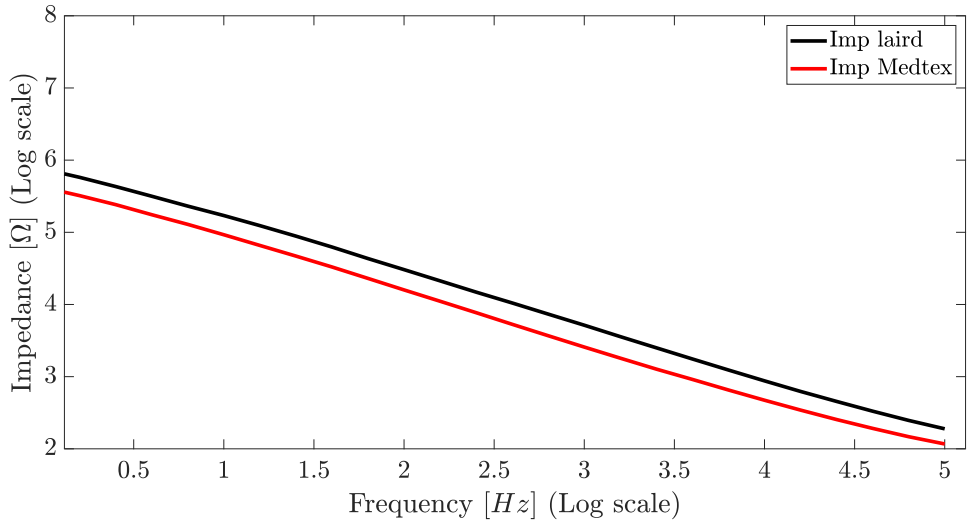


Figure 5.24: The Impedance of Laird vs Medtex P130.

The measurements of the interface impedance were very low compared to the dry contact impedance of MΩs in the previous chapter. In the literature, it was reported that the bio-impedance from the head is typically low compared to other parts of the body such as chest, legs and arms [134].

5.8 Fabric Sensors Results Summary and Discussion

5.8.1 Overview

In Chapter Four, capacitive ECG sensors, EPIC PS 25101, were investigated as a possible method of heart rate monitoring in the delivery room. The EPIC sensors did not work well on babies when used capacitively through thick cotton sheets and plastic bags that used to wrap babies in the delivery room.

This Chapter discussed the use of conductive fabric sensors in dry contact for the delivery room HR monitoring. These sensors are flexible and can be easily attached to the exposed and accessible skin area of the wrapped babies (forehead and forearms). Three experiments were performed on adult volunteers, as illustrated in the previous sections, to test the performance of fabric sensors when collecting ECG signals from the forehead and forearms in different arrangements. The sensors were placed on four babies of age 9-34 weeks, where the ECG signals were successfully coupled from forehead and arm. The flow chart of this chapter experiments is shown in Figure 5.25, where three experiments were carried out on adults, green boxes, and one experiment on babies, orange box.

5.8.2 Results Summary

Table 5.6 summarises the five experiments performed in this chapter. The first row shows the results for the first experiment, where an in-house wireless ECG recorder was used to record ECG signals. The second, third and fourth experiments were performed using an approved ECG/PPG monitor (GE B450). The fifth experiment was to measure the bioimpedance of the fabrics skin interface using impedance analyser 1260 by Solartron and 1294 bioimpedance interface.

The first experiment has tested the possibility of detecting the ECG signal from the forehead and forearm and compared the results to the conventional arms' ECG (lead I). Medtex P130 and Laird 3080–500 have successfully coupled ECG signals from the adult volunteers with high QRS detection of more than 99%, using an in-house ECG recorder. However, SP31 fabric recorded poor quality ECG signals and was excluded from the rest of the chapter experiments.

In the second experiment, the GE B450 ECG monitor was used with the fabric sensors to record the ECG from adult volunteers in three different setups. This experiment aimed to find out the best sensor placements within the restriction of newborns body size. The average measurement of newborns forearm is 62 mm, restricting the distance between the wrist DRL and forearm sensor. After analysing the collected

Sensor placement	Experiment aim	Materials	Volunteers	Findings
LA, FH (Wrist DRL)	Will fabric sensor collect ECG from FH and LFA?	Medtex, Laird and SP31	4 adults	Good ECG by Medtex and Laird, poor ECG by SP31
LFA, FH (wrist DRL)	DRL placement and ECG/PPG comparison	Medtex, Laird and PO	10 adults	Setup of DRL placed further, has the highest SNR, Medtex was better than Laird, ECG was better than PPG
LFA, FH (3 DRL placements)	Should DRL be used when the monitor is connected to mains power?	Medtex	4 adults	Close DRL placement reduces SNR when connected to mains power
LA, FH (wrist DRL)	ECG from babies	Medtex and Laird	4 babies	Medtex is better than Laird
LFA, FH	Measure the bioimpedance of skin-fabric interface	Medtex and Laird	one adult	Medtex interface impedance is less than laird's

Table 5.6: Summary of Chapter Five experiments, where: LA is left arms, LFA is Left forearm, LL is Left Leg and FH is Forehead.

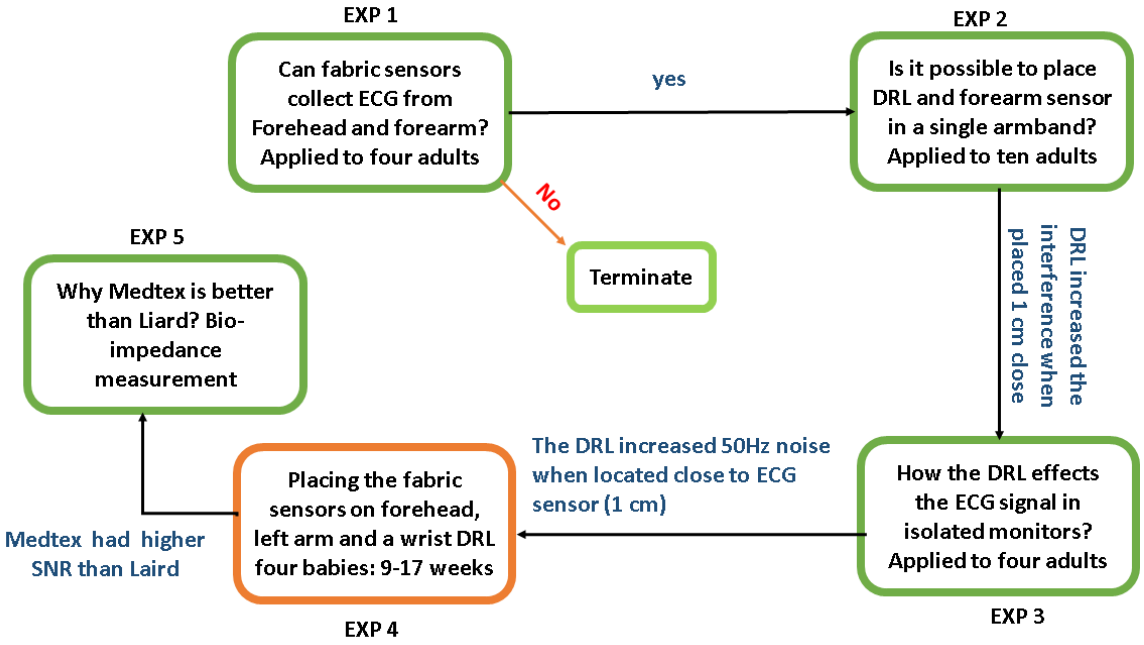


Figure 5.25: Diagram shows the experiments' flow chart; four experiments were conducted on adults (green) and one experiment on babies (orange).

signals, it appeared that the DRL placement had decreased the SNR of the signal when applied close to the forearm sensor (1 cm). However, the placement of DRL has increased the SNR when applied 5 cm from the forearm sensor.

In order to further investigate the DRL placement issue, a third experiment was designed to study the effect of DRL placement on the interference when the monitor was connected to mains power and when it was working on batteries. The results showed that the close placement of DRL reduced the SNR of the ECG when the monitor was connected to mains power. However, when the monitor is working on batteries, the DRL placement increased the SNR. This behaviour means that the DRL have coupled 50 Hz noise in the differential mode of the ECG differential amplifier. In the literature, the DRL was effective and necessary when the biomedical devices were not isolated, but with the current safety standards, many papers have discussed the undesirable effect from the DRL especially when using dry contact sensors [142–144]. One of the literature review papers [100] had concluded that the DRL could couple 50 Hz noise in the differential mode in an unpredictable way when that amplifier is isolated for safety standards.

The PPG signal was collected from the adult volunteers for comparison. The ECG signal was more robust to the introduced motion artefacts than the PPG signal as shown in the previous samples and the recordings in Appendix C. On average, 91%

of the PPG signal was detectable, and the rest of the signal was heavily affected by the motion artefacts. On the other hand, 99.3% of the Medtex ECG and 98.6% of Laird ECG were detected by the QRS algorithm.

From the above results, the arm sensor and the DRL should not be placed close to each other, and hence, the proposed placement was changed to left arm sensor instead of the forearm, and the DRL was placed on the wrist. The sensors were applied on four babies of age 9-34 weeks and recorded good quality ECG signal from babies with an average QRS detection accuracy of 95.1% by Medtex and 93% by Laird. The last experiment was designed to find out the skin interface measurement of both fabrics. The impedance of Medtex P130 was less than Lairds despite that both of them were silver plated. The lower impedance enabled better signal coupling and less attenuation. The reason for the interface impedance might be caused by the difference in the fabric base components, Elastomer in Medtex P130 and Spandex in Laird.

To conclude these experiments, there was evidence from the adults ECG recordings that the DRL has coupled more 50 Hz noise to ECG signal when placed closer to the forearm sensor. Therefore, the conductive fabric sensors were placed on the forehead and the arm of the babies, with the DRL placed on the wrist. Medtex and Laird fabrics had coupled good quality ECG signal with QRS detection percentage of 95% and 93% respectively. The fabric ECG was robust to motion artefacts when compared to the PPG signal. Medtex P130 fabric is recommended to be used over Laird 3080–500 fabric because Medtex has lower skin interface impedance and coupled ECG signals with a higher signal to noise ratio and higher QRS detection accuracy.

Chapter 6

Conclusions

6.1 Overview

Medical guidelines advise medical staff to assess the HR of the newborns immediately after birth. Around 10% of the newborns need an intervention in the first few minutes of life, where the staff should perform a resuscitation to help them breathe. A heart rate re-assessment is needed every 30 seconds during the resuscitation procedure in order to evaluate the process [1], and the assessment is usually done by palpation or auscultation. In the recent neonatal resuscitation guidelines [1,27], the ECG has been introduced as another potential method for HR assessment with more measurement accuracy. However, the standard ECG sensors available in the hospitals can scar the fragile skin of the newborns, especially the preterms. Additionally, a relatively long time is needed for skin preparation before the application of wet ECG sensors [19]. Therefore, this research has investigated two technologies for the application of newborns HR monitoring in the delivery room, namely, the EPIC capacitive sensors and the conductive fabric sensors.

6.2 Capacitive Sensors

The first part of the research has evaluated the performance of EPIC PS25101 capacitive sensors when coupling the ECG signal through the cotton towels and plastic bags, which are typically used for swaddling the newborns. The initial proposal of capacitive sensors placement was to be arranged as an array of eight sensors and embedded in the mattress of the resuscitation table in order to cover the baby's back area. This arrangement would collect four ECG signals, process them and choose the best signal, which increases the detection accuracy and efficiency. A pair of EPIC sensors were used in a pilot stage to record one ECG signal from adults wrists (seven volunteers)

and babies backs (three volunteers) in dry contact, and capacitively through: cotton towels of 2000 μm, vinyl plastic bag of 10 μm and polyethylene plastic bag of 10 μm. It has also been noticed that the capacitive ECG took five to ten seconds, in the beginning, to settle in, due to the high pass filter effect of the capacitive sensors. The bandwidth characteristics of the EPIC capacitive sensors are similar to a high-pass filter with a low cutoff frequency of 0.2 Hz. The dry contact ECG was successfully coupled without any skin preparation from all the adult and baby volunteers with different qualities. On average, the QRS detection accuracy was 99.8% of adult dry ECG signals and 89% of babies'. That is because parts of babies signals were highly affected by the motion artefacts; especially to older babies. On the other hand, the capacitive ECG signal was only coupled through the vinyl plastic bags from five adult volunteers, and no capacitive ECG was collected from the newborns through any of these three materials.

Additional experiments were conducted to test if the EPIC sensors could couple capacitive ECG signals through thinner cotton layers of clothing. These tests were performed to look at capacitive ECG applications in neonatal intensive care (NICU), where the babies are placed inside the incubators; either without clothing or with thin layers of cotton clothing in order to control their body heat [19].

In these experiments, a pair of EPIC sensors were used to collect ECG signals capacitively through a cotton sheet of 254 μm and a cotton sheet of 355 μm. The adults' ECG was successfully coupled through the two cotton sheets, but the babies' ECG was only coupled through the thinner sheet. Pan and Tompkins's algorithm was used to detect the QRS complex of the collected ECG signals, the accuracy of the detection was calculated by visually counting the missed QRS peaks and the duration where the ECG is undetectable. The average QRS detection accuracy of the adult capacitive ECG was 99.4% through 254 μm and 93.3% through the 355 μm sheet. On the other hand, the average QRS detection accuracy of the babies' ECG was 73.4% through the 254 μm sheet.

An additional experiment was performed to test the array arrangements on adult volunteers while they were fully clothed. Eight EPIC sensors were used to couple four ECG signals from the backs of seven adult volunteers through cotton clothing of different layers. The eight sensors were distributed in a yoga mat where the volunteers were asked to lay down with their back. Four ECG signals were collected from the shoulders, mid-back, waist and lower back. The ECG signals were successfully coupled from the upper part of the body; shoulders, mid-back and waist of the volunteers, who were wearing one or two cotton layers. However, no ECG signals were collected

from the lower back where the volunteers were wearing thicker layers of clothing. On average, 92.5% of the ECG signals were detectable from the shoulders, mid-back and waist.

Bioimpedance measurements were performed in order to understand the dry and capacitive contact setups. The 1260 Impedance/gain-phase analyser by Solartron was used with 1294 bioimpedance interface to measure the dry interface between the skin and electrodes in the frequency range of 1 Hz to 100 kHz. They were also used to measure the impedance of the different materials that were used in the above experiments. The cotton towel impedance was out of the limits of the device, and therefore, was not measured. The impedance of the polyethylene was higher than the vinyl's, which explains why some of the adults ECG signals were coupled capacitively through the vinyl, and none of them was coupled through the polyethylene. Both of the plastic bag's impedances were mainly capacitive through the measurement frequency range. The parallel resistivity component of the plastic is very high compared to the capacitance, and thus, it worked as an open circuit. Moreover, the calculated capacitance of the plastic bags using their dimensions and materials characteristics have correlated with the impedance measurements, emphasising that the plastic bags were mainly capacitive.

On the other hand, the impedance of cotton sheets (254 μm and 355 μm) was dominated by the resistive component of the impedance in the low frequencies ($<$100 Hz). The capacitive component of the typical cotton fabrics is relatively large compared to the cotton resistive component. The cotton capacitance does not contribute within the ECG bandwidth unless the fabric is very thin $<$50 μm. As a result, the thicker cotton fabrics have a higher impedance, which explains why the babies ECG signal was not coupled through the thicker sheet.

The interface impedance measurement at 10 Hz was used to simulate the electrical model of the acquisition system of two EPIC sensors input in dry and capacitive contact. The 10 Hz point was chosen because it represents the peak of the power of the QRS complex that was used for HR detection. The output of the dry contact model was similar to the dry contact ECG recordings. The morphology did not change, and the amplitude of the QRS was about 0.8 mV. The output of the capacitive simulation using cotton sheets values was also similar to the measured ECG signal. The signal amplitude was attenuated by $\approx$ 50% of the output of the simulation, but it was reduced by $\approx$ 25% of the recorded ECG signal. The QRS complex of the simulated and recorded ECG were both distorted with wider R–S segment. This distortion was

caused by the air gap capacitive effect, which was simulated as 5 pF, as suggested in the literature [68].

The output of the plastic bag model was further attenuated with QRS amplitude reduction of $\approx 75\%$. In the ECG recordings, the reduction of the QRS amplitude in adult's ECG signals was $\approx 25\%$. The output of the plastic model was more distorted than the cotton model output. The R–S segment was wider, which was noticed in the recorded ECG signal through the vinyl bag. Generally, the capacitive ECG signal through the vinyl plastic was affected by the motion artefacts and friction, which was not simulated or modelled.

To conclude, the findings suggest that EPIC capacitive sensors do not work through the delivery room materials that are used for swaddling the baby. For this reason, another technology was investigated for this application in the second part of the research, the fabric sensors. However, the capacitive coupling might be applicable for the NICU applications, where the baby is kept naked or in thin clothing most of the time.

6.3 Fabric Sensors

In the second part of the research, the conductive fabric sensors were tested to couple the ECG for the application of the newborns' HR monitoring in the delivery room. The fabric sensors are flexible and could be attached to the forehead and arm of the newborns. The initially proposed placement of fabric sensors was to attach three pieces of the conductive fabric to the newborns using a hat and an armband.

Three types of conductive fabrics were firstly tested on adults to collect ECG signals from the forehead and left arm using an in-house wireless ECG system. Two of the fabrics (Medtex P130 by Statex Company and Laird 3080–500 by Laird Tech Company) enabled the collection of high-quality signals. The third fabric (SP31 by footfalls and heartbeats) was much less effective and therefore was withdrawn from further experiments. Medtex P130 and Laird 3080–500 fabrics were used to collect ECG signals from adult volunteers (forehead and left forearm) using the clinically approved ECG monitor (GE B450).

Three setups were tested on ten volunteers in order to decide if one armband is enough to fit the sensor and the DRL: (1) No DRL was placed, (2) The DRL was placed 5 cm away from the forearm sensor, and (3) DRL was placed 1 cm away from the forearm sensor. The ECG collected from the second setup, where the DRL was placed five cm from the forearm sensor had the highest SNR compared to the other two

setups. The signals collected in the first and third setup had a significant contribution of 50 Hz interference. Additional tests were performed for a better understanding of the effect of the DRL. In these tests, the DRL placement was studied when the GE B450 monitor was connected to the mains power and when it was working on batteries. It was found that when the monitor was powered by the mains, the 50 Hz interference increased by placing the DRL 1 cm from the ECG sensor. However, when the monitor is working on batteries, the interference decreased by placing the DRL 1 cm from the ECG sensor. From these results, it was concluded that, when the DRL is placed very close to the forearm sensor (1 cm), it can increase the 50 Hz noise. And when the DRL was placed further (5 cm), the 50 Hz interference was decreased. Accordingly, the sensors arrangement was changed, enabling the longer distance between the DRL and the sensor.

The PPG signal was collected using a pulse oximeter simultaneously in the previous experiment. The PPG recordings were collected as a comparison to the fabric dry contact ECG signals in terms of robustness against the motion artefacts. On average, 91.2% of the PPG signal was detectable, and the rest of the signal was severely distorted by the motion artefacts. On the other hand, the QRS detection accuracy of the ECG signals, simultaneously recorded, was 99.3% for Medtex P130 fabric , and 98.6% for Laird fabric. This experiment has shown that the dry ECG signals collected by the fabric sensors in the dry contact were more robust to the motion artefacts than the pulse oximeter PPG.

Medtex P130 and Laird 3080–500 fabrics were then applied to four baby volunteers to collect the ECG signals using a forehead sensor and left arm sensor, with the DRL placed on the wrist. The ECG signals collected from the babies were of good quality, and the average of detected QRS was >93%, and the signals collected by Medtex P130 were of better quality than Laird's in terms of SNR and QRS detection. Hence, additional bioimpedance measurements were conducted to understand the skin fabric interface. The 1260 Impedance/gain-phase analyser by Solartron was used with 1294 bioimpedance interface to measure the dry interface between the skin and conductive fabrics. Medtex P130 fabric was found to have lower electrode impedance than Laird's, and this explains the slightly better signals obtained using Medtex P130 fabric.

6.3.1 Future Work

The capacitive sensors are recommended to be applied for the NICU applications, where the babies are usually naked or minimally clothed inside their incubators. The

dry contact ECG is more practical for the delivery room, but the active dry contact sensors are usually bulky compared to the standard wet sensors, which makes it harder to maintain their physical attachment to the baby's skin.

The fabric sensors tested in this research when placed on the forehead and arm, and they produced good quality ECG signals from adults and babies. Their flexibility makes them easy to strap and bend around the body contours. Also, they were easily attached to standard clinical ECG monitors using the same leads and press studs that are typically used with wet sensors. Because of these advantages, the conductive fabrics are recommended for further investigation and clinical trial. The forehead fabric sensor can be sewn on the babies hat, and the arm sensor and DRL can be sewn to arm and wrist bands. Figure 6.1 shows a model of the newborn's hat that was designed by SurePulse Company for PPG measurements incorporating Medtex P130 fabric sensor. This figure shows a proposed placement for a clinical trial where both of the forehead PPG sensor by SurePulse and forehead ECG fabric sensor are fit into the baby's hat together.

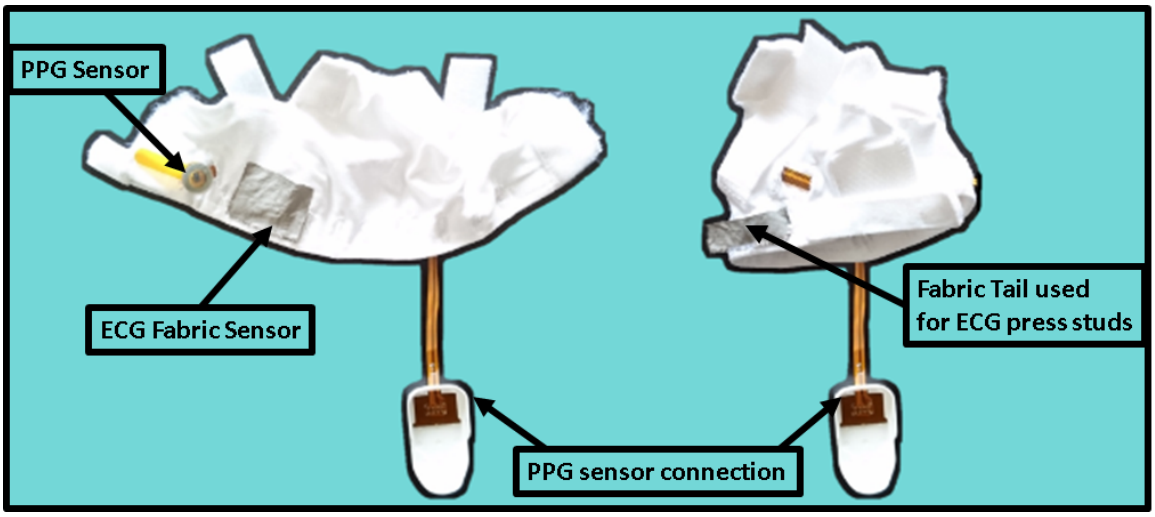


Figure 6.1: Newborn's hat designed by SurePulse company for PPG measurements. MedteX P130 fabric ECG sensor was fit into the hat for a clinical setup.

Bibliography

[1] J. M. Perlman, J. Wyllie, J. Kattwinkel, M. H. Wyckoff, K. Aziz, R. Guinsburg, H.-S. Kim, H. G. Liley, L. Mildenhall, W. M. Simon *et al.*, "Part 7: neonatal resuscitation: 2015 international consensus on cardiopulmonary resuscitation and emergency cardiovascular care science with treatment recommendations," *Circulation*, vol. 132, no. 16_suppl_1, pp. S204–S241, 2015.

[2] J. P. Nolan, J. Soar, D. A. Zideman, D. Biarent, L. L. Bossaert, C. Deakin, R. W. Koster, J. Wyllie, B. Böttiger *et al.*, "European resuscitation council guidelines for resuscitation 2010 section 1. executive summary," *Resuscitation*, vol. 81, no. 10, pp. 1219–1276, 2010.

[3] R. Chitkara, A. K. Rajani, J. W. Oehlert, H. C. Lee, M. Epi, and L. P. Halamek, "The accuracy of human senses in the detection of neonatal heart rate during standardized simulated resuscitation: implications for delivery of care, training and technology design," *Resuscitation*, vol. 84, no. 3, pp. 369–372, 2013.

[4] E. Phillipos, A. L. Solevåg, G. Pichler, K. Aziz, S. van Os, M. O"Reilly, P.-Y. Cheung, and G. M. Schmölzer, "Heart rate assessment immediately after birth," *Neonatology*, vol. 109, no. 2, pp. 130–138, 2015.

[5] M. Butler, J. Crowe, B. Hayes-Gill, and P. Rodmell, "Motion limitations of non-contact photoplethysmography due to the optical and topological properties of skin," *Physiological measurement*, vol. 37, no. 5, p. N27, 2016.

[6] M. Grubb, B. Hayes-Gill, J. Crowe, D. Sharkey, N. Marlow, and N. Miles, "Towards forehead reflectance photoplethysmography to aid delivery room resuscitation in newborns," in *4th European Conference of the International Federation for Medical and Biological Engineering*. Springer, 2009, pp. 1053–1056.

[7] M. Grubb, J. Carpenter, J. A. Crowe, J. Teoh, N. Marlow, C. Ward, C. Mann, D. Sharkey, and B. R. Hayes-Gill, "Forehead reflectance photoplethysmography

to monitor heart rate: preliminary results from neonatal patients," *Physiological measurement*, vol. 35, no. 5, p. 881, 2014.

[8] A. Katheria, W. Rich, and N. Finer, "Electrocardiogram provides a continuous heart rate faster than oximetry during neonatal resuscitation," *Pediatrics*, vol. 130, no. 5, pp. e1177–e1181, 2012.

[9] H. Mizumoto, S. Tomotaki, H. Shibata, K. Ueda, R. Akashi, H. Uchio, and D. Hata, "Electrocardiogram shows reliable heart rates much earlier than pulse oximetry during neonatal resuscitation," *Pediatrics International*, vol. 54, no. 2, pp. 205–207, 2012.

[10] R. Lemke, M. Farrah, and P. Byrn, "Use of a new doppler umbilical cord clamp to measure heart rate in newborn infants in the delivery roomlow perceived social support is associated to cd8+ cd57+ lymphocyte expansion and increased," *E-Journal of Neonatology Research*, vol. 1, pp. 83–88, 2011.

[11] S. C. Mukhopadhyay, "Wearable sensors for human activity monitoring: A review," *IEEE sensors journal*, vol. 15, no. 3, pp. 1321–1330, 2014.

[12] M. A. Yokus, R. Foote, and J. S. Jur, "Printed stretchable interconnects for smart garments: design, fabrication, and characterization," *IEEE Sensors Journal*, vol. 16, no. 22, pp. 7967–7976, 2016.

[13] S. Mukherjee, R. Breakspear, and S. D. Connor, "Wireless, non-contact driver's ecg monitoring system," in *Proceedings of the conference on Wireless Health*. ACM, 2012, p. 16.

[14] O. Aziz and S. N. Robinovitch, "An analysis of the accuracy of wearable sensors for classifying the causes of falls in humans," *IEEE transactions on neural systems and rehabilitation engineering*, vol. 19, no. 6, pp. 670–676, 2011.

[15] W. Chen, S. Bouwstra, S. B. Oetomo, and L. Feijs, "Intelligent design for neonatal monitoring with wearable sensors," in *Intelligent and Biosensors*. InTech, 2010.

[16] S. Bouwstra, W. Chen, L. Feijs, and S. B. Oetomo, "Smart jacket design for neonatal monitoring with wearable sensors," in *2009 Sixth International Workshop on Wearable and Implantable Body Sensor Networks*. IEEE, 2009, pp. 162–167.

[17] Y. Furusawa, A. Ueno, H. Hoshino, S. Kataoka, H. Mitani, and Y. Ishiyama, "Low invasive measurement of electrocardiogram for newborns and infants," in *IEEE EMBS Asian-Pacific Conference on Biomedical Engineering, 2003.* IEEE, 2003, pp. 256–257.

[18] T. Kato, A. Ueno, S. Kataoka, H. Hoshino, and Y. Ishiyama, "An application of capacitive electrode for detecting electrocardiogram of neonates and infants," in *2006 International Conference of the IEEE Engineering in Medicine and Biology Society.* IEEE, 2006, pp. 916–919.

[19] L. Atallah, A. Serteyn, M. Meftah, M. Schellekens, R. Vullings, J. Bergmans, A. Osagiator, and S. B. Oetomo, "Unobtrusive ecg monitoring in the nicu using a capacitive sensing array," *Physiological measurement*, vol. 35, no. 5, p. 895, 2014.

[20] R. B. Knobel, J. E. Wimmer, and D. Holbert, "Heat loss prevention for preterm infants in the delivery room," *Journal of Perinatology*, vol. 25, no. 5, pp. 304–308, 2005.

[21] S. Çağlar, D. Gözen, and Z. İnce, "Heat loss prevention (help) after birth in preterm infants using vinyl isolation bag or polyethylene wrap," *Journal of Obstetric, Gynecologic, & Neonatal Nursing*, vol. 43, no. 2, pp. 216–223, 2014.

[22] http://www.plesseysemiconductors.com/, "Plessey."

[23] C. H. Robert Prance, "Electric potential sensor," 2006.

[24] G. R. Polglase, S. L. Miller, S. K. Barton, A. A. Baburamani, F. Y. Wong, J. D. Aridas, A. W. Gill, T. J. Moss, M. Tolcos, M. Kluckow *et al.*, "Initiation of resuscitation with high tidal volumes causes cerebral hemodynamic disturbance, brain inflammation and injury in preterm lambs," *PloS one*, vol. 7, no. 6, p. e39535, 2012.

[25] G. R. Polglase, S. L. Miller, S. K. Barton, M. Kluckow, A. W. Gill, S. B. Hooper, and M. Tolcos, "Respiratory support for premature neonates in the delivery room: effects on cardiovascular function and the development of brain injury," *Pediatric research*, vol. 75, no. 6, p. 682, 2014.

[26] A. B. te Pas and F. J. Walther, "A randomized, controlled trial of delivery-room respiratory management in very preterm infants," *Pediatrics-English Edition*, vol. 120, no. 2, pp. 322–329, 2007.

[27] J. Wyllie, J. Bruinenberg, C. C. Roehr, M. Rüdiger, D. Trevisanuto, and B. Urlesberger, "European resuscitation council guidelines for resuscitation 2015: Section 7. resuscitation and support of transition of babies at birth," 2015.

[28] J. Kattwinkel, S. Niermeyer, V. Nadkarni, J. Tibballs, B. Phillips, D. Zideman, P. Van Reempts, and M. Osmond, "Ilcor advisory statement: Resuscitation of the newly born infant an advisory statement from the pediatric working group of the international liaison committee on resuscitation," *Circulation*, vol. 99, no. 14, pp. 1927–1938, 1999.

[29] K. G. Voogdt, A. C. Morrison, F. E. Wood, R. M. van Elburg, and J. P. Wyllie, "A randomised, simulated study assessing auscultation of heart rate at birth," *Resuscitation*, vol. 81, no. 8, pp. 1000–1003, 2010.

[30] C. O. F. Kamlin, C. P. O'Donnell, N. J. Everest, P. G. Davis, and C. J. Morley, "Accuracy of clinical assessment of infant heart rate in the delivery room," *Resuscitation*, vol. 71, no. 3, pp. 319–321, 2006.

[31] C. J. Owen and J. P. Wyllie, "Determination of heart rate in the baby at birth," *Resuscitation*, vol. 60, no. 2, pp. 213–217, 2004.

[32] J. Dawson, A. Saraswat, L. Simionato, M. Thio, C. Kamlin, L. Owen, G. Schmölzer, and P. Davis, "Comparison of heart rate and oxygen saturation measurements from masimo and nellcor pulse oximeters in newly born term infants," *Acta paediatrica*, vol. 102, no. 10, pp. 955–960, 2013.

[33] C. O. F. Kamlin, J. A. Dawson, C. P. O'donnell, C. J. Morley, S. M. Donath, J. Sekhon, and P. G. Davis, "Accuracy of pulse oximetry measurement of heart rate of newborn infants in the delivery room," *The Journal of pediatrics*, vol. 152, no. 6, pp. 756–760, 2008.

[34] J. J. Van Vonderen, S. B. Hooper, J. K. Kroese, A. A. Roest, I. C. Narayen, E. W. Van Zwet, and A. B. te Pas, "Pulse oximetry measures a lower heart rate at birth compared with electrocardiography," *The Journal of pediatrics*, vol. 166, no. 1, pp. 49–53, 2015.

[35] C. O. F. Kamlin, C. P. O'Donnell, N. J. Everest, P. G. Davis, and C. J. Morley, "Accuracy of clinical assessment of infant heart rate in the delivery room," *Resuscitation*, vol. 71, no. 3, pp. 319–321, 2006.

[36] J. Rohana, W. Khairina, N. Y. Boo, and I. Shareena, "Reducing hypothermia in preterm infants with polyethylene wrap," *Pediatrics international*, vol. 53, no. 4, pp. 468–474, 2011.

[37] N. B. S. T. O. C. N. D. A. P. inNeonatology, "Nottingham neonatal service - clinical guidelines," *nottingham childrens hospital*, 2015.

[38] T. Cordaro, A. G. Phalen, and K. Zukowsky, "Hypothermia and occlusive skin wrap in the low birth weight premature infant: an evidentiary review," *Newborn and Infant Nursing Reviews*, vol. 12, no. 2, pp. 78–85, 2012.

[39] M. Watkinson, "Temperature control of premature infants in the delivery room," *Clinics in perinatology*, vol. 33, no. 1, pp. 43–53, 2006.

[40] J. Allen, "Photoplethysmography and its application in clinical physiological measurement," *PHYSIOLOGICAL MEASUREMENT*, 2007.

[41] J. May, P. Kyriacou, and A. Petros, "Development of an optoelectronic sensor for the investigation of photoplethysmographic signals from the anterior fontanel of the newborn," in *Engineering in Medicine and Biology Society, EMBC, 2011 Annual International Conference of the IEEE.* IEEE, 2011, pp. 18–21.

[42] C. P. O'Donnell, C. O. F. Kamlin, P. G. Davis, and C. J. Morley, "Feasibility of and delay in obtaining pulse oximetry during neonatal resuscitation," *The Journal of pediatrics*, vol. 147, no. 5, pp. 698–699, 2005.

[43] C. O. F. Kamlin, J. A. Dawson, C. P. O'Donnell, C. J. Morley, S. M. Donath, J. Sekhon, and P. G. Davis, "Accuracy of pulse oximetry measurement of heart rate of newborn infants in the delivery room," *The Journal of pediatrics*, vol. 152, no. 6, pp. 756–760, 2008.

[44] A. Thuring, K. J. Bränström, T. Jansson, and K. Maršál, "Audio spectrum analysis of umbilical artery doppler ultrasound signals applied to a clinical material," *Acta obstetricia et gynecologica Scandinavica*, vol. 93, no. 12, pp. 1320–1324, 2014.

[45] S. Shakespeare, J. Crowe, B. Hayes-Gill, K. Bhogal, and D. James, "The information content of doppler ultrasound signals from the fetal heart," *Medical and Biological Engineering and Computing*, vol. 39, no. 6, pp. 619–626, 2001.

[46] D. Hutchon, "Technological developments in neonatal care at birth," *J Nurs Care*, vol. 3, no. 218, pp. 2167–1168, 2014.

[47] S. Goenka, "Precordial doppler ultrasound achieves earlier and more accurate newborn heart rates in the delivery room," in *2013 AAP National Conference and Exhibition*. American Academy of Pediatrics, 2013.

[48] R. P. Lemke and M. F. BMET, "Use of a new doppler umbilical cord clamp to measure heart rate in newborn infants in the delivery room," *EJ Neonatol Res*, vol. 1, pp. 83–8, 2011.

[49] J. A. C. Cardiol, "Recommendations for the standardization and interpretation of the electrocardiogram," *Journal of the American College of Cardiology, JACC*, 2007.

[50] M. AlGhatrif and J. Lindsay, "A brief review: history to understand fundamentals of electrocardiography," *Journal of community hospital internal medicine perspectives*, vol. 2, no. 1, p. 14383, 2012.

[51] R. Klabunde, "Electrocardiogram standard limb leads (bipolar)," 2008.

[52] C. J. S. S. O. Lonneke A.M.Aartsa, VincentJeanneb, "Non-contact heart rate monitoring utilizing camera photoplethysmography in the neonatal intensive care unit — a pilot study," *Early Human Development*, vol. 89, pp. 943–948, 2013.

[53] M. M. Baharestani, "An overview of neonatal and pediatric wound care knowledge and considerations." *Ostomy/wound management*, vol. 53, no. 6, pp. 34–6, 2007.

[54] F. Afsar, "Skin care for preterm and term neonates," *Clinical and experimental dermatology*, vol. 34, no. 8, pp. 855–858, 2009.

[55] K. G. Voogdt, A. C. Morrison, F. E. Wood, R. M. van Elburg, and J. P. Wyllie, "A randomised, simulated study assessing auscultation of heart rate at birth," *Resuscitation*, vol. 81, no. 8, pp. 1000–1003, 2010.

[56] L. A. Geddes, *Principles of applied biomedical instrumentation*. John Wiley & Sons, 1975.

[57] A. Searle and L. Kirkup, "A direct comparison of wet, dry and insulating bioelectric recording electrodes," *Physiological measurement*, vol. 21, no. 2, p. 271, 2000.

[58] E. Huigen, A. Peper, and C. Grimbergen, "Investigation into the origin of the noise of surface electrodes," *Medical and biological engineering and computing*, vol. 40, no. 3, pp. 332–338, 2002.

[59] A. Baba and M. Burke, "Measurement of the electrical properties of ungelled ecg electrodes," *International journal of biology and biomedical engineering*, vol. 2, no. 3, pp. 89–97, 2008.

[60] A. Lopez and P. C. Richardson, "Capacitive electrocardiographic and bioelectric electrodes," *IEEE Transactions on Biomedical Engineering*, no. 1, pp. 99–99, 1969.

[61] B. A. Taheri, R. T. Knight, and R. L. Smith, "A dry electrode for eeg recording," *Electroencephalography and clinical neurophysiology*, vol. 90, no. 5, pp. 376–383, 1994.

[62] Y. M. Chi and G. Cauwenberghs, "Wireless non-contact eeg/ecg electrodes for body sensor networks," in *Body Sensor Networks (BSN), 2010 International Conference on.* IEEE, 2010, pp. 297–301.

[63] F. Padmadinata, J. Veerhoek, G. Van Dijk, and J. Huijsing, "Microelectronic skin electrode," *Sensors and Actuators B: Chemical*, vol. 1, no. 1-6, pp. 491–494, 1990.

[64] C. Lagow, K. Sladek, and P. Richardson, "Anodic insulated tantalum oxide electrocardiograph electrodes," *IEEE Transactions on Biomedical Engineering*, no. 2, pp. 162–164, 1971.

[65] P. Cartlidge, P. Fox, and N. Rutter, "The scars of newborn intensive care," *Early human development*, vol. 21, no. 1, pp. 1–10, 1990.

[66] L. Geddes, "Electrodes and the measurement of bioelectric events," *Chicester: Interscience*, 1972.

[67] A. Van Oosterom and J. Strackee, "The solid angle of a plane triangle," *IEEE transactions on Biomedical Engineering*, no. 2, pp. 125–126, 1983.

[68] Y. M. Chi, T.-P. Jung, and G. Cauwenberghs, "Dry-contact and noncontact biopotential electrodes: Methodological review," *IEEE reviews in biomedical engineering*, vol. 3, pp. 106–119, 2010.

[69] M. Fernandez and R. Pallas-Areny, "A simple active electrode for power line interference reduction in high resolution biopotential measurements," in *Proceedings of 18th Annual International Conference of the IEEE Engineering in Medicine and Biology Society*, vol. 1. IEEE, 1996, pp. 97–98.

[70] S. Lobodzinski, "Ecg instrumentation: Applicationand design," *Comprehensive Electrocardiology*, pp. 427–480, 2010.

[71] N. Meziane, J. Webster, M. Attari, and A. Nimunkar, "Dry electrodes for electrocardiography," *Physiological measurement*, vol. 34, no. 9, p. R47, 2013.

[72] M. Lopez-Gordo, D. Sanchez-Morillo, and F. Valle, "Dry eeg electrodes," *Sensors*, vol. 14, no. 7, pp. 12 847–12 870, 2014.

[73] P. Griss, P. Enoksson, H. Tolvanen-Laakso, P. Merilainen, S. Ollmar, and G. Stemme, "Spiked biopotential electrodes," in *Micro Electro Mechanical Systems, 2000. MEMS 2000. the Thirteenth Annual International Conference on.* IEEE, 2000, pp. 323–328.

[74] C. Chang and J. Chiou, "Surface-mounted dry electrode and analog-front-end systems for physiological signal measurements," in *Life Science Systems and Applications Workshop, 2009. LiSSA 2009. IEEE/NIH.* IEEE, 2009, pp. 108–111.

[75] A. Ueno, Y. Akabane, T. Kato, H. Hoshino, S. Kataoka, and Y. Ishiyama, "Capacitive sensing of electrocardiographic potential through cloth from the dorsal surface of the body in a supine position: A preliminary study," *IEEE Transactions on biomedical engineering*, vol. 54, no. 4, pp. 759–766, 2007.

[76] R. Matthews, N. J. McDonald, P. Hervieux, P. J. Turner, and M. A. Steindorf, "A wearable physiological sensor suite for unobtrusive monitoring of physiological and cognitive state," in *Engineering in Medicine and Biology Society, 2007. EMBS 2007. 29th Annual International Conference of the IEEE.* IEEE, 2007, pp. 5276–5281.

[77] S. Heuer, D. R. Martinez, S. Fuhrhop, and J. Ottenbacher, "Motion artefact correction for capacitive ecg measurement," in *2009 IEEE Biomedical Circuits and Systems Conference*. IEEE, 2009, pp. 113–116.

[78] J. Ottenbacher and S. Heuer, "Motion artefacts in capacitively coupled ecg electrodes," in *World Congress on Medical Physics and Biomedical Engineering, September 7-12, 2009, Munich, Germany*. Springer, 2009, pp. 1059–1062.

[79] M. S. Chavan, R. Agarwala, and M. Uplane, "Suppression of baseline wander and power line interference in ecg using digital iir filter," *International journal of circuits, systems and signal processing*, vol. 2, no. 2, pp. 356–365, 2008.

[80] M. Oehler, M. Schilling, and H. Esperer, "Novel multichannel capacitive ecg-system for cardiac diagnostics beyond the standard-lead system," in *4th European Conference of the International Federation for Medical and Biological Engineering*. Springer, 2009, pp. 30–33.

[81] P. Perego, G. Andreoni, R. Zanini, and R. Bellù, "Wearable biosignal monitoring system for newborns," in *2014 4th International Conference on Wireless Mobile Communication and Healthcare-Transforming Healthcare Through Innovations in Mobile and Wireless Technologies (MOBIHEALTH)*. IEEE, 2014, pp. 271–274.

[82] R. Aviles-Espinosa, E. Rendon Morales, Z. Luo, H. Dore, O. Anton, H. Rabe, and R. J. Prance, "Neo-sense: a non-invasive smart sensing mattress for cardiac monitoring of babies," in *2019 IEEE Sensors Applications Symposium*. Institute of Electrical and Electronics Engineers, 2019.

[83] G. Boxwell, *Neonatal intensive care nursing*. Routledge, 2010.

[84] W. Chen, J. Hu, S. Bouwstra, S. B. Oetomo, and L. Feijs, "Sensor integration for perinatology research," *IJSNet*, vol. 9, no. 1, pp. 38–49, 2011.

[85] J. Werth, L. Atallah, P. Andriessen, X. Long, E. Zwartkruis-Pelgrim, and R. M. Aarts, "Unobtrusive sleep state measurements in preterm infants–a review," *Sleep medicine reviews*, vol. 32, pp. 109–122, 2017.

[86] G. Lu, J.-S. Brittain, P. Holland, J. Yianni, A. L. Green, J. F. Stein, T. Z. Aziz, and S. Wang, "Removing ecg noise from surface emg signals using adaptive filtering," *Neuroscience letters*, vol. 462, no. 1, pp. 14–19, 2009.

[87] H.-J. Park, J.-M. Han, D.-U. Jeong, and K.-S. Park, "A study on the elimination of the ecg artifact in the polysomnographic eeg and eog using ar model," in *Proceedings of the 20th Annual International Conference of the IEEE Engineering in Medicine and Biology Society. Vol. 20 Biomedical Engineering Towards the Year 2000 and Beyond (Cat. No. 98CH36286)*, vol. 3. IEEE, 1998, pp. 1632–1635.

[88] F. Abtahi, F. Seoane, K. Lindecrantz, and N. Löfgren, "Elimination of ecg artefacts in foetal eeg using ensemble average subtraction and wavelet denoising methods: a simulation," in *XIII Mediterranean Conference on Medical and Biological Engineering and Computing 2013*. Springer, 2014, pp. 551–554.

[89] Y. S. Kim, J. M. Choi, H. B. Lee, J. S. Kim, H. J. Baek, M. S. Ryu, R. H. Son, and K. S. Park, "Measurement of biomedical signals from helmet based system," in *2007 29th Annual International Conference of the IEEE Engineering in Medicine and Biology Society*. IEEE, 2007, pp. 359–362.

[90] A. L. Bleda, R. Maestre, B. Schmitz, C. Hofmann, J. M. Nacenta, G. Santa, S. Pellicer, and V. Melcher, "Electrical cardiac monitoring in the head for helmet applications," in *2015 Computing in Cardiology Conference (CinC)*. IEEE, 2015, pp. 413–416.

[91] W. von Rosenberg, T. Chanwimalueang, D. Looney, and D. P. Mandic, "Vital signs from inside a helmet: A multichannel face-lead study," in *2015 IEEE International Conference on Acoustics, Speech and Signal Processing (ICASSP)*. IEEE, 2015, pp. 982–986.

[92] W. von Rosenberg, T. Chanwimalueang, V. Goverdovsky, and D. P. Mandic, "Smart helmet: monitoring brain, cardiac and respiratory activity," in *2015 37th Annual International Conference of the IEEE Engineering in Medicine and Biology Society (EMBC)*. IEEE, 2015, pp. 1829–1832.

[93] W. von Rosenberg, T. Chanwimalueang, V. Goverdovsky, N. S. Peters, C. Papavassiliou, and D. P. Mandic, "Hearables: Feasibility of recording cardiac rhythms from head and in-ear locations," *Royal Society Open Science*, vol. 4, no. 11, p. 171214, 2017.

[94] K. Silvadorai, T. Anwar, and M. Jamaludin, "Stimulus based algorithm for extracting electrocardiogram signal from the head for eyewear devices," in *2017*

6th ICT International Student Project Conference (ICT-ISPC). IEEE, 2017, pp. 1–5.

[95] T.-W. Shen, T. Hsiao, Y.-T. Liu, and T.-Y. He, "An ear-lead ecg based smart sensor system with voice biofeedback for daily activity monitoring," in *Tencon 2008-2008 IEEE Region 10 Conference*. IEEE, 2008, pp. 1–6.

[96] D. Da He, E. S. Winokur, and C. G. Sodini, "An ear-worn vital signs monitor," *IEEE Transactions on Biomedical Engineering*, vol. 62, no. 11, pp. 2547–2552, 2015.

[97] ——, "A continuous, wearable, and wireless heart monitor using head ballistocardiogram (bcg) and head electrocardiogram (ecg)," in *2011 Annual International Conference of the IEEE Engineering in Medicine and Biology Society*. IEEE, 2011, pp. 4729–4732.

[98] A. Flasterstein, "Voltage fluctuations of metal-electrolyte interfaces in electrophysiology," *Medical and Biological Engineering and Computing*, vol. 4, no. 6, pp. 583–588, 1966.

[99] C. Gondran, E. Siebert, S. Yacoub, and E. Novakov, "Dry electrode based on nasicon ceramic for surface biopotential measurements: skin-electrode impedance and noise," *Innovation et technologie en biologie et médecine*, vol. 16, pp. 113–118, 1995.

[100] J. Gomez-Clapers, E. Serrano-Finetti, R. Casanella, and R. Pallas-Areny, "Can driven-right-leg circuits increase interference in ecg amplifiers?" in *2011 Annual International Conference of the IEEE Engineering in Medicine and Biology Society*. IEEE, 2011, pp. 4780–4783.

[101] T. Tang, W. L. Goh, L. Yao, J. H. Cheong, and Y. Gao, "An integrated multichannel neural recording analog front-end asic with area-efficient driven right leg circuit," *2017 39th Annual International Conference of the IEEE Engineering in Medicine and Biology Society (EMBC)*, pp. 217–220, 2017.

[102] R. Bogue, "Plessey launches range of unique electric field sensors," *Sensor Review*, vol. 32, no. 3, pp. 194–198, 2012.

[103] R. Prance, S. Beardsmore-Rust, P. Watson, C. Harland, and H. Prance, "Remote detection of human electrophysiological signals using electric potential sensors," *Applied Physics Letters*, vol. 93, no. 3, p. 033906, 2008.

[104] P. Semiconductors, "Datasheet ps25251 epic ultra high impedance ecg sensor."

[105] M. Tipple, "Interpretation of electrocardiograms in infants and children," *Images in paediatric cardiology*, vol. 1, no. 1, p. 3, 1999.

[106] E. Pomeroy, J. T. Stock, T. J. Cole, M. O'Callaghan, and J. C. Wells, "Relationships between neonatal weight, limb lengths, skinfold thicknesses, body breadths and circumferences in an australian cohort," *PloS one*, vol. 9, no. 8, p. e105108, 2014.

[107] https://www.shieldextrading.net/wp-content/uploads/2018/08/1150902130 Medtex-P130.pdf, "statex company, bremen, germany."

[108] https://pm.lairdtech.com/sites/default/files/2018 11/EMI-DS-FOF-3080-500%200214.pdf, "laird company, missouri, united states."

[109] https://www.footfallsandheartbeats.com/, "Footfalls& heartbeat company, nottingham, uk."

[110] C. Isaia, D. McNally, S. A. McMaster, and D. T. Branson, "Investigation of changes in the electrical properties of novel knitted conductive textiles during cyclic loading," in *2016 38th Annual International Conference of the IEEE Engineering in Medicine and Biology Society (EMBC)*. IEEE, 2016, pp. 6058–6061.

[111] M. J. Butler, "Motion artefact reduction for reflection-mode photoplethysmography. phd thesis, university of nottingham," Ph.D. dissertation, UK Campuses > Faculty of Engineering, The address of the publisher, 7 2018.

[112] https://www.gehealthcare.com/en/products/patient-monitoring/patient-monitors/carescape-monitor b450, "Ge healthcare."

[113] S. Analytical, "1260 impedance/gain-phase analyzer," *Operating Manual*, 2005.

[114] H. I. I. Solartron, "1294 operating manual," *Frequency Response Analyzer*, vol. 1255, 2001.

[115] M. Elgendi, B. Eskofier, S. Dokos, and D. Abbott, "Revisiting qrs detection methodologies for portable, wearable, battery-operated, and wireless ecg systems," *PloS one*, vol. 9, no. 1, p. e84018, 2014.

[116] A. Goutas, Y. Ferdi, J.-P. Herbeuval, M. Boudraa, and B. Boucheham, "Digital fractional order differentiation-based algorithm for p and t-waves detection and delineation," *ITBM-RBM*, vol. 26, no. 2, pp. 127–132, 2005.

[117] J. Pan and W. J. Tompkins, "A real-time qrs detection algorithm," *IEEE Trans. Biomed. Eng*, vol. 32, no. 3, pp. 230–236, 1985.

[118] A. Katheria, W. Rich, and N. Finer, "Electrocardiogram provides a continuous heart rate faster than oximetry during neonatal resuscitation," *Pediatrics*, vol. 130, no. 5, pp. e1177–e1181, 2012.

[119] R. Bloss, "Numerous recent shows highlight the latest in sensor innovations," *Sensor Review*, vol. 32, no. 2, pp. 101–105, 2012.

[120] T. Torfs, Y.-H. Chen, H. Kim, and R. F. Yazicioglu, "Noncontact ecg recording system with real time capacitance measurement for motion artifact reduction," *IEEE transactions on biomedical circuits and systems*, vol. 8, no. 5, pp. 617–625, 2014.

[121] I. D. Castro, R. Morariu, T. Torfs, C. Van Hoof, and R. Puers, "Robust wireless capacitive ecg system with adaptive signal quality and motion artifact reduction," in *2016 IEEE International Symposium on Medical Measurements and Applications (MeMeA)*. IEEE, 2016, pp. 1–6.

[122] T. M. A. T. R. J. R. Chenggang Yu, Zhenqiu Liu, "A method for automatic identification of reliable heart rates calculated from ecg and ppg waveforms," *Journal of the American Medical Informatics Association*, 2006.

[123] Z. Kappassov, J.-A. Corrales, and V. Perdereau, "Tactile sensing in dexterous robot hands," *Robotics and Autonomous Systems*, vol. 74, pp. 195–220, 2015.

[124] F. S. C. Mustata and A. Mustata, "Dielectric behaviour of some woven fabrics on the basis of natural cellulosic fibers," *Advances in Materials Science and Engineering*, vol. 2014, 2014.

[125] J. Leśnikowski, "Dielectric permittivity measurement methods of textile substrate of textile transmission lines," *Przegląd elektrotechniczny*, vol. 88, no. 3a, pp. 148–151, 2012.

[126] M. Pourova, R. Zajicek, L. Oppl, and J. Vrba, "Measurement of dielectric properties of moisture textile," in *Microwave Techniques, 2008. COMITE 2008. 14th Conference on.* IEEE, 2008, pp. 1–4.

[127] https://www.azom.com/article.aspx?ArticleID=410.

[128] Plastic bags, May 2019, [Online; accessed 8. May 2019]. [Online]. Available: http://www.packagingknowledge.com/plastic_bags.asp

[129] R. Matthews, N. J. McDonald, H. Anumula, J. Woodward, P. J. Turner, M. A. Steindorf, K. Chang, and J. M. Pendleton, "Novel hybrid bioelectrodes for ambulatory zero-prep eeg measurements using multi-channel wireless eeg system," in *International Conference on Foundations of Augmented Cognition.* Springer, 2007, pp. 137–146.

[130] R. Sameni and G. D. Clifford, "A review of fetal ecg signal processing; issues and promising directions," *The open pacing, electrophysiology & therapy journal*, vol. 3, p. 4, 2010.

[131] A. A. Uvarov, I. A. Lezhnina, K. Overchuk, A. Starchak, S. D. Akhmedov, and I. A. Larioshina, "Study of the properties of plessey's electrocardiographic capacitive electrodes for portable systems," in *Journal of Physics: Conference Series*, vol. 671, no. 1. IOP Publishing, 2016, p. 012032.

[132] G. N. Stamatas, J. Nikolovski, M. A. Luedtke, N. Kollias, and B. C. Wiegand, "Infant skin microstructure assessed in vivo differs from adult skin in organization and at the cellular level," *Pediatric dermatology*, vol. 27, no. 2, pp. 125–131, 2010.

[133] R.-K. Chang, "Ecg leads system for newborn ecg screening," Feb. 25 2014, uS Patent 8,660,630.

[134] J. J. Almasi and O. H. Schmitt, "Systemic and random variations of ecg electrode system impedance," *Annals of the New York Academy of Sciences*, vol. 170, no. 2, pp. 509–519, 1970.

[135] A. G. Correa, E. Laciar, H. Patiño, and M. Valentinuzzi, "Artifact removal from eeg signals using adaptive filters in cascade," in *Journal of Physics: Conference Series*, vol. 90, no. 1. IOP Publishing, 2007, p. 012081.

[136] J. Sijbers, J. Van Audekerke, M. Verhoye, A. Van der Linden, and D. Van Dyck, "Reduction of ecg and gradient related artifacts in simultaneously recorded human eeg/mri data," *Magnetic resonance imaging*, vol. 18, no. 7, pp. 881–886, 2000.

[137] G. Srivastava, S. Crottaz-Herbette, K. Lau, G. Glover, and V. Menon, "Ica-based procedures for removing ballistocardiogram artifacts from eeg data acquired in the mri scanner," *Neuroimage*, vol. 24, no. 1, pp. 50–60, 2005.

[138] J. Coosemans, B. Hermans, and R. Puers, "Integrating wireless ecg monitoring in textiles," *Sensors and Actuators A: Physical*, vol. 130, pp. 48–53, 2006.

[139] A. Wong, K.-P. Pun, Y.-T. Zhang, and C.-S. Choy, "An ecg measurement ic using driven-right-leg circuit," in *2006 IEEE International Symposium on Circuits and Systems*. IEEE, 2006, pp. 4–pp.

[140] M. H. Wyckoff, K. Aziz, R. Guinsburg, H.-S. Kim, H. G. Liley, L. Mildenhall, W. M. Simon, E. Szyld, M. Tamura, and S. Velaphi, "Part 7: neonatal resuscitation," *Circulation*, vol. 132, no. 1, pp. S204–S241, 2015.

[141] V. Sundaram, D. Louis, S. S. Saini, and P. Kumar, "Pulse oximetry sensor application for neonates during resuscitation," *Cochrane Database of Systematic Reviews*, no. 7, 2016.

[142] U. Imtiaz, L. Bartolomeo, Z. Lin, S. Sessa, H. Ishii, K. Saito, M. Zecca, and A. Takanishi, "Design of a wireless miniature low cost emg sensor using gold plated dry electrodes for biomechanics research," in *2013 IEEE International Conference on Mechatronics and Automation*. IEEE, 2013, pp. 957–962.

[143] S. Consul-Pacareu, R. Mahajan, B. I. Morshed *et al.*, "Neuromonitor: a low-power, wireless, wearable eeg device with drl-less afe," *IET Circuits, Devices & Systems*, vol. 11, no. 5, pp. 471–477, 2017.

[144] R. Mahajan and B. I. Morshed, "Performance analysis of a drl-less afe for battery-powered wearable eeg," *Measurement*, vol. 90, pp. 583–591, 2016.

Appendix A

Materials Datasheets and Certificates

Study Information Sheet

Conductive Fabric ECG System: Experiment on limitations

Participants:

Number of participants: 30

Participant type: Healthy males/females, age 18+.

Recruitment: **Staff/students within the department via research group bulk e-mail or via a recruitment poster.** The e-mail will contain a brief description of the study and the 'Participant Information Sheet' (without reference number) as an attachment.

Payment: None.

Activities:

Number of activities: six.

Activity duration: 55 minutes (10 mins introduction+15 mins between the activity+ 30 mins actual experiment).

Equipment and Procedure:

Equipment:

1. University computer (networked or stand-alone).
2. ECG monitor B450 (PO and ECG).
3. Three fabric pieces (2.5cm*2cm) of Medtex P130 (Biocompatible fabric).
4. Three fabric pieces (2.5cm*2cm) of Laird (Biocompatible fabric).

Procedure:

1. Re-iterate information provided in the 'Participant Information Sheet' to make sure the volunteers and the babies' parents understand what is being asked of them. Explain the study in more detail if the participant does not understand any terms or the procedures.
2. Ask them to sign the 'Participant Consent Form'.
3. Allocate a unique, random, seven-digit number to the participant as a reference number.
4. Ask the participant to sit down in a chair, while three fabric sensors from Medtex fabric will be applied using starchy bands around the head, left forearm and left wrist (5 cm apart) as shown in Fig 1 and Fig 2(b). The volunteer ECG signal will be recorded for 5 minutes. The pulse oximeter is applied on the right index finger and is used only to get reference signals in order to compare them to the signal from the sensors under test.
5. The left forearm sensors will be rearranged, and the distance will only be 1cm between them as shown in Fig 2(C). Then, the volunteer ECG signal will be recorded for 5 minutes.
6. After that, the fabric sensor around the wrist will be removed as shown in Fig 2(a) and the ECG will be collected for an additional 5 mins.
7. The steps 9, 10, 11 will be repeated for Laird fabric sensors.
8. The total ECG recording will be saved to a USB flash memory drive under a directory titled with the participants' reference number. Collected Data:

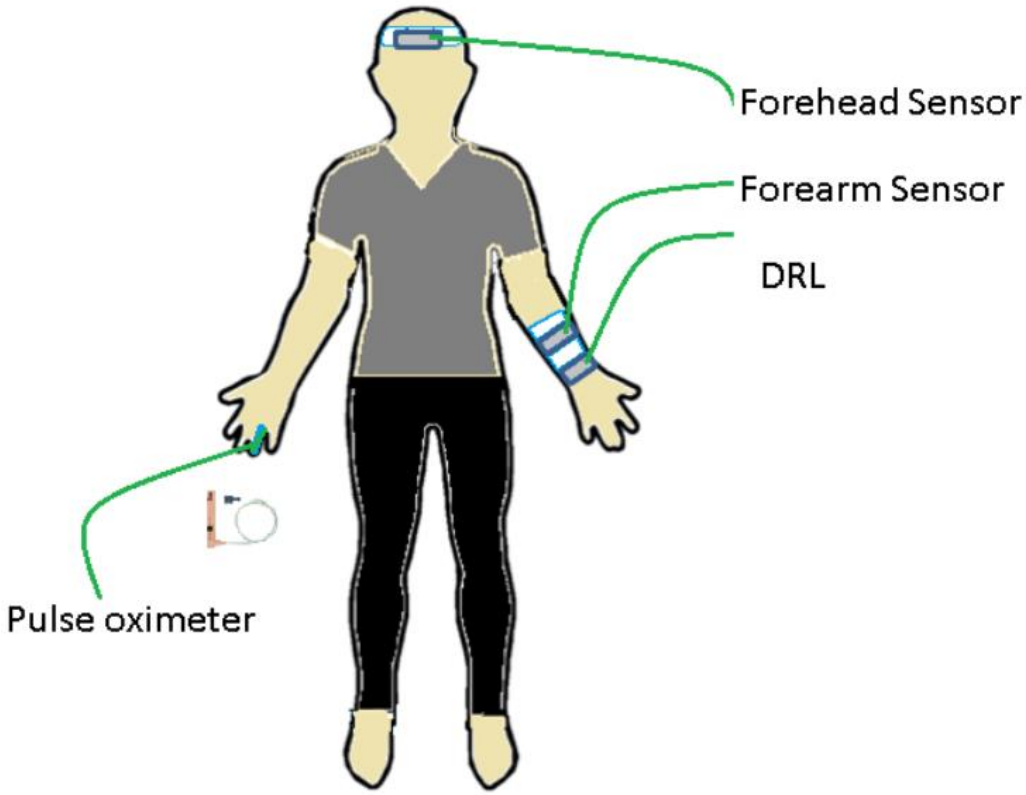


Figure 1: ECG sensors placement on forehead, forearm and wrist. Pulse oximeter is placed on the right hand index.

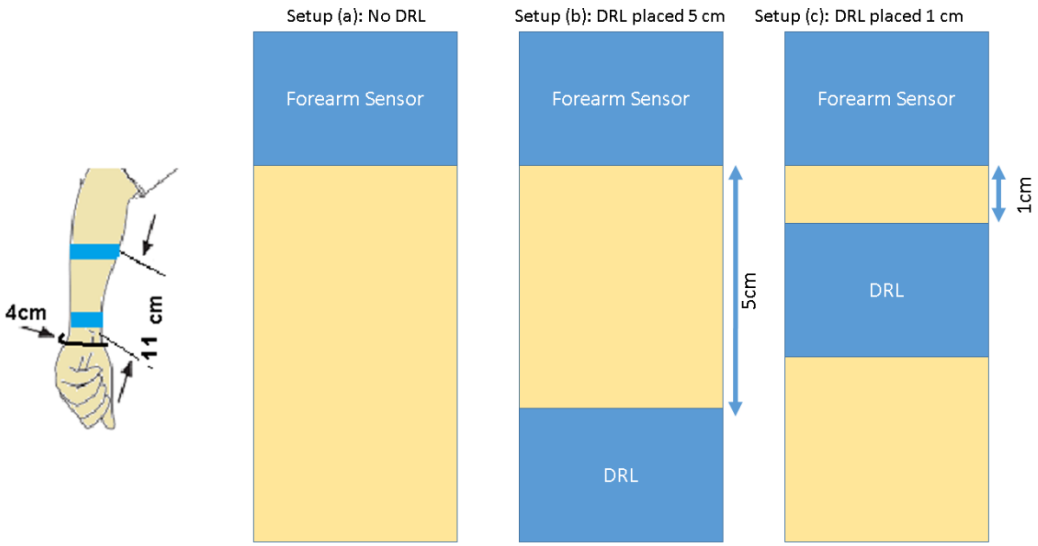


Figure 2: Placement of the sensors on the left forearm.

Collected data

- Consent form containing name, date and signature which no one could associate with the collected ECG recording data.

- Thirty minutes of ECG recording and the age of the participant.

Ensuring confidentiality: No personal information will be collected about the participants (Name*, address, etc.) Only the age and sex will be required. Each participant will be given a unique, random, seven digit number that is used to link the participant to the collected data.

- The student conducting the study will not contact the participants after the study has ended.
- The participants may contact the student conducting the study (using the reference number to identify the particular participant) if they should wish for their data to be deleted.

* Each participant will sign a consent form which will contain their name and signature, but not the reference number (i.e. the reference number and name are not linked).

Storage method: Original data will be stored directly to a portable flash memory drive (all participants' data will be stored on the same drive, under different directories). Digital copies of the data will be stored on the University's network (requiring a username and password to login-to) for processing and analysis. The student conducting the study will have direct access to the data. The consent forms will be stored separately in safe cabin within the university.

Data usage: After the data (ECG recordings) have been collected, it will be analysed and the data will be presented in the student's PhD thesis and one or more journal publications. The presentable data will be in the form figures or graphs (to demonstrate the collection method) and the processed data. The consent forms data will not be published or used in any type of publication outside or inside the university.

Identifying individuals: It will **not** be possible to identify a participant by the data that has been collected from them.

After the study: The collected ECG data will be stored securely for seven years; then deleted (copies too). The hard copies of the consent forms will be destroyed appropriately after 7 years. Data will be passed on to a supervisor if/when the student leaves the university.

Participant Consent Form

Conductive Fabric ECG System: Experiment on limitations

	Please initial
I confirm that I have read and understand the information sheet for the above study:	☐
I have had the opportunity to consider the information, ask questions and have had these answered satisfactorily:	☐
I understand that my participation is voluntary and that I am free to withdraw at any time, without giving a reason, without my legal rights being affected:	☐
I understand that relevant sections of the anonymised data collected during the study may be looked at by responsible individuals from The University of Nottingham and that sections of anonymised data might be used in publications:	☐
I agree to take part in the study:	☐

Name: _____. Date: _____.

Signed: _____.

Laird
Smart Technology. Delivered.

3080-500 SilverTek Fabric
Silver Plated Stretch Nylon Knit



SILVER PLATED STRETCH FABRIC WITH ANTI-TARNISH COATING

Laird's SilverTek is a unique fabric designed for todays Smart Textile applications. This fabric may be suited for use in on-body medical sensors, antimicrobial wound care, performance monitoring clothing for sports and military applications, and consumer wearable electronics.

FEATURES RoHS

- RoHS/REACH compliant
- Halogen-free per IEC-61249-2-21 standard
- Surface resistivity of < 2 Ω/□ (nominal)

MARKETS

- Specialty
- Medical
- Military
- Performance Sportswear
- Wearable electronics

PHYSICAL PROPERTIES

Item	Unit	Value	Advantage
Substrate	78% Nylon / 22% Spandex		Stretchable, Conformable
Metal Plating	99% Pure Silver		Antimicrobial, Hypoallergenic
Fabric Weight (nominal)	oz/yd² (g/m²)	4.0 (136)	Light Weight
Thickness (nominal)	inch (mm)	0.018 (0.45)	Flexible
Temperature Range	°C	-40° to 90°	

ELECTRICAL PROPERTIES

Item	Unit	Value
Surface Resistivity (ASTM F390)	ohms/square	< 2.0

MECHANICAL PROPERTIES

Item	Unit	Value[fi]
Elongation*, MD (ASTM D4964 mod)	(%)	>250

*(@ 3 lbf / inch width)

USA: +1.866.928.8181
Europe: +49.0.8031.2460.0
Asia: +86.755.2714.1166

www.lairdtech.com

EMI-DS-FOF-3080-500 0214

Any information furnished by Laird Technologies, Inc. and its agents is believed to be accurate and reliable. All specifications are subject to change without notice. Responsibility for the use and application of Laird Technologies materials rests with the end user, since Laird Technologies and its agents cannot be aware of all potential uses. Laird Technologies makes no warranties as to the fitness, merchantability or suitability of any Laird Technologies materials or products for any specific or general uses. Laird Technologies shall not be liable for incidental or consequential damages of any kind. All Laird Technologies products are sold pursuant to the Laird Technologies' Terms and Conditions of sale in effect from time to time, a copy of which will be furnished upon request. © Copyright 2013 Laird Technologies, Inc. All Rights Reserved. Laird, Laird Technologies, the Laird Technologies Logo, and other marks are trade marks or registered trade marks of Laird Technologies, Inc. or an affiliate company thereof. Other product or service names may be the property of third parties. Nothing herein provides a license under any Laird Technologies or any third party intellectual property rights.

CMA 2011190656S 有效期至2014年12月22日

ilac-MRA

CNAS 检 测 CNAS L1446

深圳市医疗器械检测中心

检 验 报 告

NICPBP 中国药检

报 告 编 号：WY20140189

检 品 名 称：SilverTek Fabric

供样/ 报验单位：Laird Technologies (Shenzhen) Ltd.

检 验 目 的：委托检验

签 发 日 期：2014-05-30

Technical Application Guide

PN# 1150902130

Shieldex® Medtex P130

- **Purpose: Antibacterial fabric for general use**
- **Description: Silver (Ag) plated knitted fabric**
- **Raw Material: 78% Nylon + 22% Elastomer**
- **Plating: 99% pure silver**
- **Stretch: DS (double stretch direction –warp—weft)**
- **Temperature Range: -30°C to 90°C / -22°F to 194°F**
- **Total Thickness: 0.018" (0.44mm) ± 10%**
- **Abrasion Resistance: 10,000 cycles**
- **Weight: 135 g/m^2 ± 10%**
- **Roll Widths: 52" (132cm) ± 2"**
- **Master Roll Lengths: Average 30 Lm / 32.5 Lyd**



PRODUCT APPLICATION EXAMPLES

⇒ Base material for antibacterial products
⇒ Base material for fungicidal products
⇒ Base material for mattress/pillow covers for allergen protection
⇒ Medical clothes
⇒ Compression wrap
⇒ Base material for wound dressing

Accreditations:
RoHS: Compliant
Reach: Compliant
Acc. ISO 9001:2000
Oeko-tex Standard 100

V Technical Textiles, Inc
4502 State Rt. 31
Palmyra, NY 14522
Phone: 315-597-1674
Fax: 315-597-6687
Web: www.vtechtextiles.com
Email: whoge@rochester.twcbc.com

V Technical Textiles Inc.
A Woman's Owned Small Business

NWBOC WBE Certified
NWBOC EDWOSB Certified

Statex Productions & Vertriebs GmbH
Kleiner Ort 11 28357
Bremen Germany
Tel: +49 421 275047/8,
Fax: +49 421 273643
info@statex.de

HOHENSTEIN

Certificate

17.8.9.0045

According to the report n° 17.8.5.0632 dated on 23 October 2017 and report n° 17.8.5.0681 dated on 20 November 2017, we confirm that the below mentioned item was tested at the Hohenstein Laboratories GmbH & Co. KG and is awarded with the certificate confirming

Biological Safety

The following listed biocompatibility tests were carried out according to the appropriate standards and were successfully passed:

- No cell damaging effect in the Cytotoxicity Test according to DIN EN ISO 10993-5

Sample: Shieldex® Med-Tex P130; Colour: silver
Shieldex® Silver Jersey Modal; Colour: lightgrey-melange
Shieldex® Technik-Tex P130+B; Colour: silver
Shieldex® 235/36 dtex 2ply HC+B; Colour: lightgrey-melange
Shieldex® Silitex P130; Colour: black/silver
Shieldex® 78/18 dtex Z-turns+B; Colour: silver

Company: Statex Produktions & Vertriebs GmbH
Kleiner Ort 11
D-28357 Bremen

The certificate is valid until 30 November 2019

Schloss Hohenstein · D-74357 Boennigheim, 23 November 2017

Chief Executive Officer

Dr. Timo Hammer

Hohenstein Laboratories · Schloss Hohenstein ·

CERTIFICATE

OEKO-TEX® Zertifizierungsstelle GmbH

Kaiserstraße 39 · 60329 Frankfurt am Main

The company

Statex Produktions & Vertriebs GmbH

Kleiner Ort 11

28357 Bremen, GERMANY

is granted authorisation according to Oeko-Tex® Standard 100 to use the Oeko-Tex® mark, based on our **test report 15.0.61348**

CONFIDENCE IN TEXTILES

Tested for harmful substances

according to Oeko-Tex® Standard 100

A03-0143 **Hohenstein**

for the following articles:

Shieldex®-yarns and Shieldex®- fabrics made of metallized/silvered fibers (polyamide, polyamide/elastane, polyamide/modal, cotton/polyamide/elastane, polyester/polyamide, white and coloured), partly finished with tarnish protection, produced with fibres accepted by OEKO-TEX® having biological properties and produced by using OEKO-TEX® Standard 100 certified materials.

The results of the inspection made according to Oeko-Tex® Standard 100, **product class I** have shown that the above mentioned goods meet the human-ecological requirements of the standard presently established for baby articles.

The certified articles fulfil the requirements of Annex XVII of REACH (incl. the use of azo-dyes, nickel, etc.) as well as the American requirement regarding total content of lead in children's articles (CPSIA; with the exception of accessories made from glass).

The holder of the certificate, who has issued a conformity declaration according to ISO 17050-1, is under an obligation to use the Oeko-Tex® mark only in conjunction with products that conform with the sample initially tested. The conformity is verified by audits.

This authorisation is valid until 31.05.2016

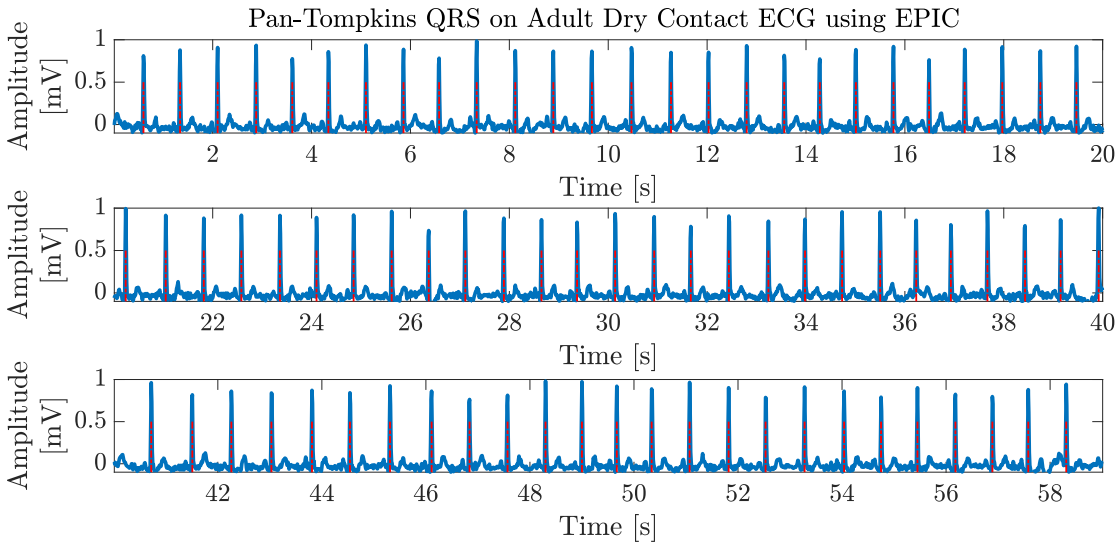
Frankfurt am Main, 08.06.2015

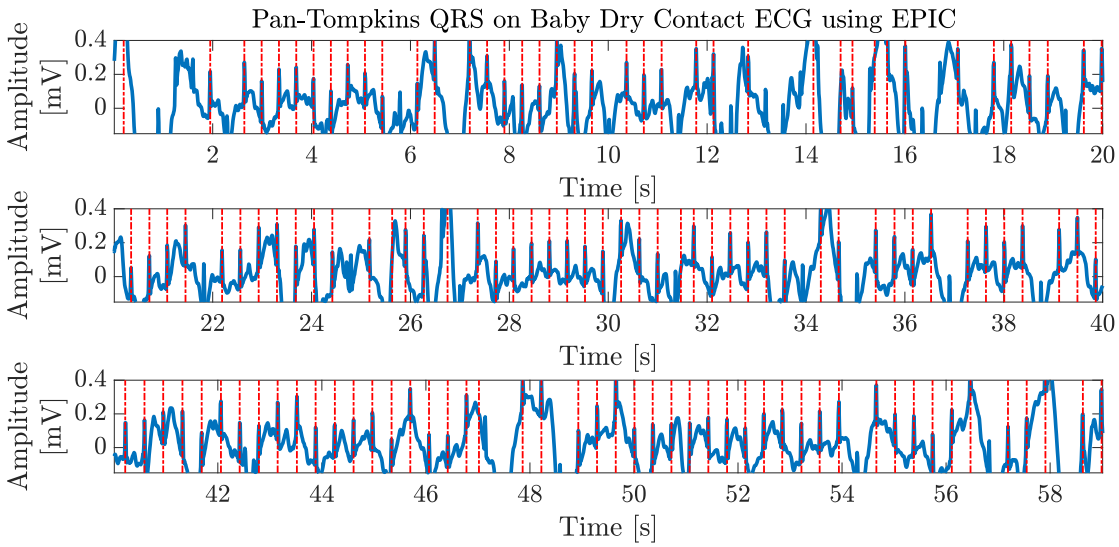
Oeko-Tex Zertifizierungsstelle GmbH
Kaiserstr. 39 60329 Frankfurt a.M.
Tel. +49 (0) 69-400 34 08-0, Fax: 400 34 08 299
e-mail: info@zertifizierung-oekotex.com

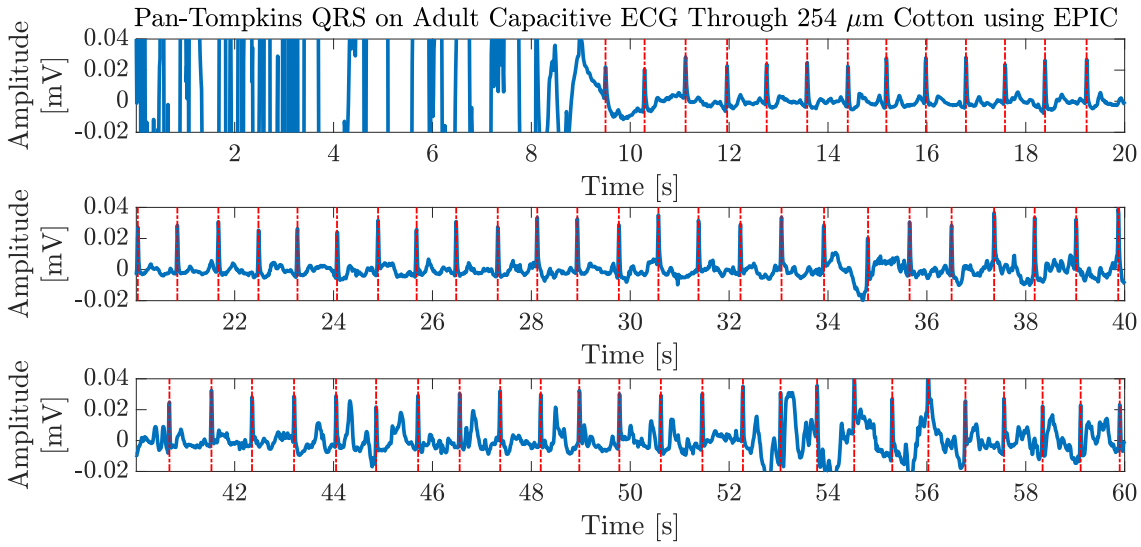
Jutta Knels
Geschäftsführung

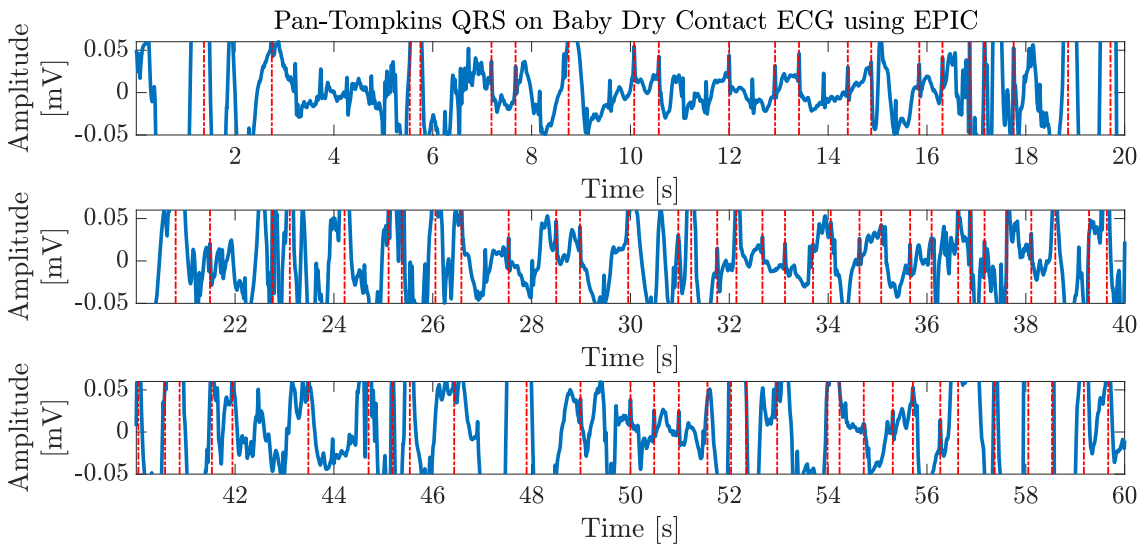
Appendix B

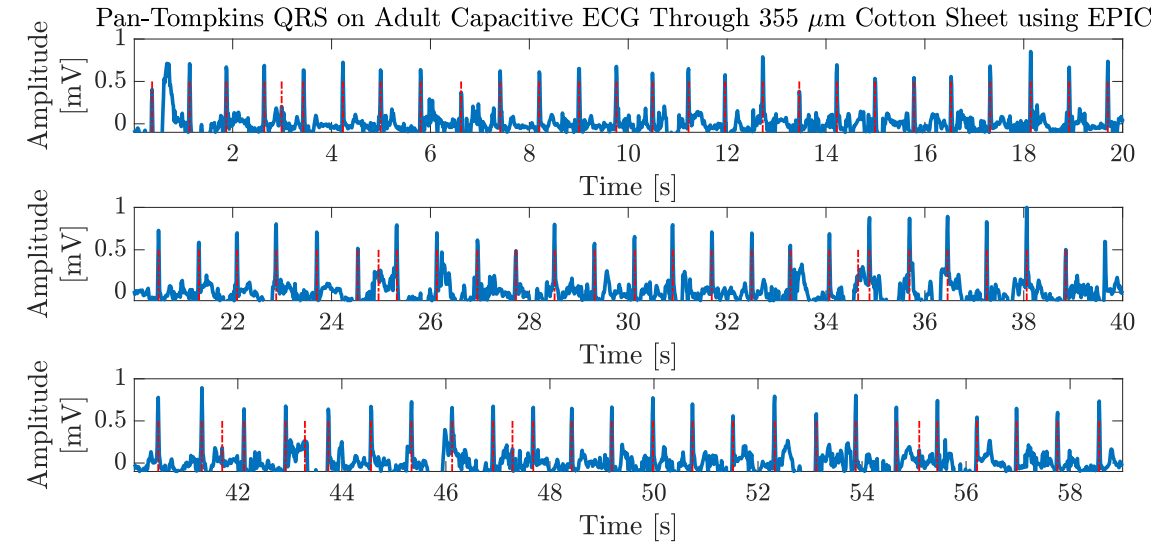
EPIC Sensors Recordings

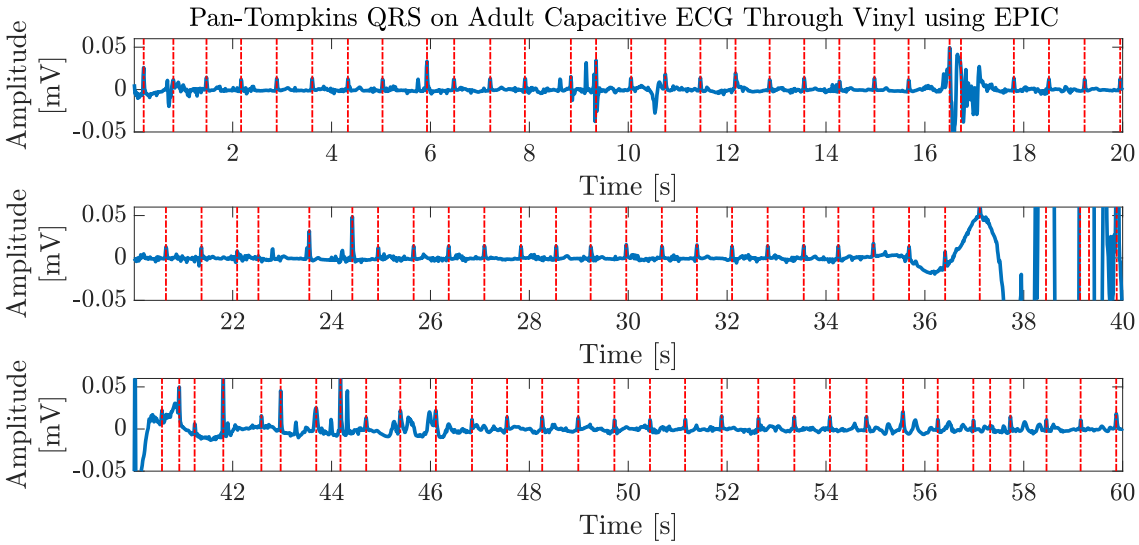





Pan-Tompkins QRS on Adult Capacitive ECG Through 254 μm Cotton using EPIC
Amplitude [mV]
0.04
0.02
0
-0.02
2 4 6 8 10 12 14 16 18 20
Time [s]
22 24 26 28 30 32 34 36 38 40
42 44 46 48 50 52 54 56 58 60


Pan-Tompkins QRS on Baby Dry Contact ECG using EPIC
Amplitude [mV]
0.05
0
-0.05
2 4 6 8 10 12 14 16 18 20
Time [s]
22 24 26 28 30 32 34 36 38 40
42 44 46 48 50 52 54 56 58 60


Pan-Tompkins QRS on Adult Capacitive ECG Through 355 μm Cotton Sheet using EPIC
Amplitude [mV]
Time [s]


Pan-Tompkins QRS on Adult Capacitive ECG Through Vinyl using EPIC
Amplitude [mV]
Time [s]

Appendix C

Fabric Sensors Recordings

